TESLA REPORT NO. 94-17
UPDATE NOV. 1995

A STUDY OF PRESSURES, TEMPERATURES AND LIQUID LEVELS IN THE 2 KELVIN REFRIGERATION CIRCUIT OF A 1830 m TESLA SUBUNIT UNDER DIFFERENT CONDITIONS AND SYSTEM CONFIGURATIONS.

by
G. Horlitz

DESY/Hamburg/Germany

TABLE OF CONTENTS

1. INTRODUCTION

An international study group is presently investigating the conditions for realizing a superconducting 2 x 250 GeV e^+e^- linear accelerator (fig. 1). The system, being composed of a series of high frequency resonators (cavities), fabricated of high purity niobium, has to be operated at a temperature of approx. 2 K. A nominal refrigeration power of ca. 51 KW at 2 K, 37 KW at 4.5 K and 314 KW at 40/80 K is required. The cooling power has to be distributed over a distance of more than 30 km. By means of a numerical simulation model, liquid/vapor/gas flow aspects in the 2 K circuits are calculated and discussed for different circuit combinations. A lower temperature option is discussed as well.
Only the 2 K distribution system, excluding the refrigerator, the cold compressors and the main heat exchanger, is part of this investigation. Some data about the 4.5 K and the 40/80 K systems are added in Appendix 2 for information.

2. GENERAL LAYOUT

The structure of the system has been described several times [1], [2] in different modifications. Principal features as agreed at present are:

2.1 THE CAVITIES

In our terminology a cavity includes a 9 cell resonator (the basic RF-element) together with its cylindrical helium container (fig. 2).

2.2 THE MODULES

Eight cavities are combined, together with a correction quadrupole (the latter to be operated at 4.5 K), in a common cryostat module of 12.2 m length (fig. 3). All cold supply- and return lines are included as well (fig. 4).

2.3 THE STRINGS

A string is a series of 12 modules. Each string is alimented through an individual JT-valve with a helium stream of liquid/vapor in equilibrium, containing sufficient liquid to remove all heat load of the string by complete evaporation of the liquid.
Only vapor escapes from the end of the string (fig. 5, detail A). Including supply- and endbox, the string length amounts to 148 m.

2.4 THE SUBUNITS

A series of 12 strings, supplied from one refrigeration station of sufficient power is called a subunit. The cryogenic length of this unit, including a 54 m long connection to the refrigerator, is 1830 m (fig. 5). The refrigeration power required (including 50% contingency) amounts to 4800W at 2 K, 3500W at 4.5 K and 30000W at a non-isothermal level between 40 K and 80 K.

2.5 THE TOTAL SYSTEM

On the basis of acceleration gradients of 25 MV/m, and considering gradient free spaces between the active parts of the structure, a total of 16 identical subunits is required for particle energies of 2 x 250 GeV. So, the total length of the machine including an option of

100 m warm beam tube between adjacent subunits and a 2 km interaction region between the two half linacs amounts to about 32 km (fig. 6).

2.6 GEOMETRY

To begin with, the helium flow to be investigated occurs entirely in the return tube of circular shape with diameter d_{tub} = 0.3 m (a marginal parasitic liquid flow through the cooldown/warm up capillaries (fig. 5) can be neglected). We asume the tube to be exactly horizontally orientated. Its total length is composed as follows:
The length of one cavity (including one bellow of length LB) is LC (fig. 7, detail A).

Every module consists of 8 cavities, 1 quadrupole of length LQ and a free end for insertions, length LX.

With

LC = 1.3848 m
LB = 0.1086 m
LQ = 0.8302 m - LB = 0.7216 m*
LX = 0.4 m

* (In the technical drawings, the bellow between the last cavity of the module and the quadrupole is part of the quadrupole and its length is contained in LQ. In order to conserve uniform cavity lengths we leave this bellow at the cavity)

The total length of a module amounts to (fig. 7):

(1) $$LMOD = 8 * LC + LQ + LX$$

LMOD = 12.2 m

Taking into account the lengths of a supply box (LSA = 0.8 m) and an end box (LSE = 0.8 m) the string length (fig. 5, detail A) is

(2) $$LSTR = 12 * LMOD + LSA + LSE$$

LSTR = 148 m

A subunit contains 12 strings. Since the last string has to be connected to the refrigerator at a distance L0 (fig. 5) we obtain, with L0 = 54 m

(3) $$LUN = 12 * LSTR + L0$$

LUN = 1830 m

Remark:

For practical reasons, the longitudinal intervals for calculation have been shifted to coincide with the space between two adjacend connections between cavity and return tube (fig.7, upper denotation; at the right hand side of the module the cryogenic longitudinal subdivision has been completed by

LC 1 = LC - LC0 - LB = 1.0312 m and LC2 = LQ + LX + LC0 = 1.4752 m). This shifts the thermodynamical longitudinal scale in respect to the mechanical scale (lower denotation) by the interval LCO (0.245 m) the distance of the vertical connection tube of the cavity from the end flange of the beam tube.

2.7 NOMENCLATURE

For numerical calculations we define longitudinal points on the x-axis:

L (NS, NM, NC)

where NS, NM, NC are the position numbers of strings within the subunit, of modules within strings and of cavities within modules respectively. The ranges of the numbers are

(4) $$1 \leq NS \leq NSM + 1$$

(5) $$0 \leq NM \leq NMM + 1$$

(6) $$0 \leq NC \leq NCM + 1$$

NSM = 12 number of identical strings
NS = 13 nominates the end connection to the refrigerator (L0)

NMM = 12 number of modules per string
NM = 0 nominates the supply box
NM = 13 nominates the end box

NCM = 8 number of cavities per module
NC = 9 nominates the quadrupole bypass

According to the remark at the end of the preceeding chapter, a position L (NS, NM, NC) is allocated to the end of the interval between the vertical connection tubes of cavities number NC and NC + 1, in the module number NM of string number NS (fig.7).
NC = 0 indicates the beginning of the first interval of a module.

Within this system, some positions must be identical:

(7) $$L(NS + 1,0,0) = L(NS,NMM + 1,1)$$

(8) $$L(NS,NM + 1,0) = L(NS,NM,NCM + 1)$$

(9) $$L(NS,1,0) = L(NS,0,1)$$

All parameters will be named by the triple of numbers indicating the positions along the x-axis, i.e. P (NS, NM, NC) is the pressure at the point L (NS, NM, NC) etc. For simplicity, the values in the supply tube need only single identification numbers:

The supply parameters are then

(10) $$P_S = PS(NSM + 1)$$

(11) $$T_S = TS(NSM + 1)$$

3. CRYOGENICS

3.1 GENERAL DESCRIPTION

As mentioned before, the cavities have to be operated at a maximum temperature of Tmax ≤ 2 K. In order to minimize heat loads to the system at this temperature level, all 2 K operated components will be surrounded by two systems of radiation shields, one at 4.5 K and a second one between 40 K and 80 K. At these temperature levels also all mechanical supports, electrical cables and RF-leads will be intercepted. The superconducting quadrupoles are cooled from the 4.5 K shield circuit. Higher order mode absorbers, installed in the quadrupoles will be cooled from the 40/80 K shield line.

Consequently the cryogenic supply and distribution system splits up into:

- the 2 K circuits
- the 4.5 K circuits
- the 40/80 K circuits
- a variable temperature cool down/warm up system
- the refrigerators with warm and cold compressor groups, turbines and heat exchangers
- He gas and liquid storage facilities.

In this paper only the 2 K circuits are considered more in detail.

The cryogenic scheme of one subunit is displayed in fig. 5. We assume, that at the supply end of each subunit there exists a refrigerator which provides a helium mass flow at temperatures of ~ 4.5 K and a pressure of about 5 bar. The flow rate is sufficiently high to cover all heat load requirements of the subunit:
The whole mass flow rate enters firstly the 4.5 K shield/quadrupole system at point 3. Having absorbed the heat load of this circuit it returns at point 5 with elevated temperature and a reduced pressure of ca. 3 bar. A fraction (ca. 50%) is liquefied into the bath cooler HX5.

After having passed the second loop in HX5 the remaining supercritical helium is further cooled in counterflow with returning evaporated gas (T ≈ 2 K) in a heat exchanger HX6. Provided, HX6 is sufficiently well designed, we obtain the following supply data for the helium entering the subunit 2 K system:

supply pressure: $P_S = 3.0$ bar
supply temperature: $T_S = 2.2$ K
(These values may be modified depending on the exact properties of the refrigerator).

3.2 THE 2 K DISTRIBUTION SYSTEM

Every cavity vessel is connected in its top region to a 0.3 m diameter helium return tube. The connection is performed by a vertical tube of 0.1 m length and 0.065 m diameter (figs. 2 + 3).

At the end of the modules the return tube bypasses the 4.5 K quadrupoles.
At the far end (in respect to the refrigerator position) of each string there is a supply box, the other end is terminated by an endbox. Between adjacent strings the end box of the preceeding string and the supply box of the next one will mechanically be one unit (fig. 5). Within that box the two different liquid levels will be separated by a liquid barrier. On the top of the box the vapor is passed through from one string to the next one (fig. 5, detail A).

From a supply line, being connected to the cold outlet of the heat exchanger HX6 and running parallel to the return line, cold pressurized helium will be expanded into the supply boxes through Joule-Thomson valves.
Within the return tube a liquid level l(x) (x = longitudinal coordinate) of some centimeters is maintained, while the tube liquid is connected with the cavity liquid through the vertical connection tubes (figs. 2 + 3).

All heat load from the cavities is transported to the return tube liquid by superfluidal heat conduction through the connection tubes. It has been shown, that the maximum tolerable heatflow density of about 1 Watt/cm² in the vertical tubes is not exceeded under all expected conditions [3].

In addition, a continuously distributed heat flow (mainly from the supports) enters the return tube as well. Both heat flows cause the liquid to evaporate. In order to maintain a steady state liquid level, a continuous flow of liquid has to be supplied into the tube. The vapor has to be removed with pressure gradients as low as possible. Liquid and vapor flow, pressure drops, temperatures and liquid levels along the return tube of one subunit will be investigated in the following chapters.

4. CALCULATIONS

As mentioned before, there will be continuous streams of liquid and vapor from the inlet (supply box) to the outlet (end box). In flow direction the massflow rates are decreasing for the liquid and increasing for the vapor. The liquid flow rate decays to zero at the end of each string. It is reestablished at the beginning of the next string through the JT-valves. The vapor flow is a sum of all helium, being evaporated in the preceeding strings and increases steadily over the whole subunit. Flow conditions of liquid and vapor, considering their mutual dependance in the tube, will be calculated.

4.1 PARAMETERS AND INPUT DATA

4.1.1 Temperatures and pressures

Supply data for the 2 K system are assumed as follows:

P_S = 3.0 bar
T_S = 2.2 K.

The desired maximum operation temperature at the hot end of the subunit is T_{max} = 2.0 K. (1.8 K problems will be discussed in chap. 8). The corresponding equilibrium vapor pressure (i.e. the expanded pressure at the JT-valve) amounts to P_{max} = 31.29 mbar.

4.1.2 Heat loads

Using data published in [4] we calculate heat loads for the components of a subunit as summarized in table 1. The first column gives the calculated estimates (nominal values), the second column the design values which contain a safety factor of 1.5.

Furthermore, the additional loads in the end- and supply boxes, the parallel running 2.2 K supply line and the end connections between the last string and the refrigerator have been taken into account.

Table 1: Heat load details

		nominal	design		entering mode
static load per cavity	QCS	0.335	0.503	W	pointwise
dynamic load per cavity*	QCD	2.325	3.488	W	pointwise
total load per cavity	QC	2.660	3.991	W	pointwise
load to return tube	DQRC	0.01	0.015	W/m	distributed
static load per module	QMS	2.80	4.21	W	
dynamic load per module*	QMD	18.60	27.90	W	
total load per module	QM	21.40	32.11	W	
load to supply- and end box	QC0	1.0	1.5	W	distributed
static load per string	QSTS	35.6	53.5	W	
dynamic load per string*	QSTD	223.2	334.8	W	
total load per string	QST	258.8	388.4	W	
load to 2.2 K supply line	DQS	0.05	0.075	W/m	distributed
load to 54 m end connection	DQR	0.05	0.075	W/m	distributed
static load per subunit	QSUBS	521.9	783.4	W	
dynamic load per subunit*	QSUBD	2678.4	4018.2	W	
total load per subunit	QTOT	3200.3	4801.6		

* The dynamic loads given in this table are the difference between total and static load. It represents the increase of load when HF-power is switched on. It should be considered, that in this case heat input by conduction is different from the static case due to the different temperature distributions in the components.

The heat load values of table 1 are related as follows:

(12a) $$QMS = NCM * QCS + LMOD * DQRC$$

(12b) $$QMD = NCM * QCD$$

(12) $$QM = QMS + QMD$$

(13a) $$QSTS = NMM * QMS + 2 * QC0 + (LSA + LSE) * DQRC$$

(13b) $$QSTD = NMM * QMD$$

(13) $$QST = QSTS + QSTD$$

(14a) $$QSUBS = NSM * QSTS + LUN * DQS + L0 * DQR$$

(14b) $$QSUBD = NSM * QSTD$$

(14) $$QTOT = QSUBS + QSUBD$$

4.2 MODEL ASSUMPTIONS

We introduce a rectangular system of coordinates (x; y; z) with x-axis in flow direction and y-axis in vertical direction.

The calculations have been performed with the following assumptions:

4.2.1 In the whole tube volume, the temperature T (x) is in saturation equilibrium with the local vapor pressure $P_d(x)$.

(15) $$T(x) = T_{sat}[P_d(x)]$$

Within a local cross section at fixed longitudinal position x, both liquid and gas temperatures are constant and equal to T_{sat} at the boundary between liquid and vapor.

(16) $$\left(\frac{\partial T}{\partial y}\right)_x = \left(\frac{\partial T}{\partial z}\right)_x = 0$$

4.2.2 In the vapor space the local pressure of the vapor is constant for fixed x.

(17) $$\left(\frac{\partial P_d}{\partial y}\right)_x = \left(\frac{\partial P_d}{\partial z}\right)_x = 0$$

The local liquid pressure $P_f(x)$ increases hydraulically with the vertical distance Δl from the surface

(18) $$P_f(x) = P_d(x) + \rho_f * g * \Delta l_y$$

(ρ_f = liquid density, g = 9.81 m/s²).

4.2.3 Vapor and liquid in the tube are completely separated. They occupy different fractions of the tube cross section depending on the local level height l(x) of the liquid. This assumption is based on two facts:

4.2.3.1 Due to the great ratio of densities of liquid and vapor

(19) $$\frac{\rho_f}{\rho_d} \geq 150$$

the existance of liquid droplets in the vapor is very unprobable at flow speeds occuring in the tube.

4.2.3.2 The production of bubbles within the superfluidal He II would require heat flow densities much higher than expected even under maximum heat load conditions. Evaporation occurs only at the boundary surface between liquid and vapor.

4.2.4 The pressure drops of vapor and liquid can be calculated independently with usual flow formalism. Flow areas and circumferences can be calculated geometrically from the tube diameter d_{tub} and the liquid level l(x) (see Appendix A1); and flow rates for vapor and liquid will be calculated as shown in the next chapters.

4.2.5 A difference in flow dependent pressure gradients in liquid and vapor is compensated by a level gradient in the liquid.

4.2.6 Longitudinal heat transport within the liquid is entirely performed by internal heat conduction in He II. Enthalpy transport by liquid motion can be neglected (maximum expected liquid flow speed in x-direction < 0.1 m/s, compared with velocity of second sound of ~ 20 m/s).

4.2.7 The return tube axis follows an equipotential line of gravitation

(20) $$\frac{dy_{ax}}{dx} = 0$$

(Deviations from this condition will be discussed in chapter 9.2).

4.2.8 The model is a stationary one. Both transient and inertia effects are neglected. Superfluidal film creep effects are negligible compared with bulk mass flow rates.

5. EQUATIONS

5.1 THE PRESSURE DROPS

We consider a short section of the return tube of length Δx between points 1 and 2 (fig. 8). At point 1 a total massflow $\dot{m}_c$ penetrates the total area

(21) $$A_{tot} = 0.25 * \pi * d_{tub}^2$$

$\dot{m}_c$ is splitted into a liquid flow $\dot{m}_{f1}$ and a vapor flow $\dot{m}_{d1}$. Within one string, $\dot{m}_c$ remains constant while $\dot{m}_d$ and $\dot{m}_f$ may change their values:

(22) $$\dot{m}_c = \dot{m}_{f1} + \dot{m}_{d1} = \dot{m}_{f2} + \dot{m}_{d2}$$

The local ratio

(23) $$q(x) = \frac{\dot{m}_d(x)}{\dot{m}_c(x)}$$

which is called the "quality" is variable with x (at the end of each string, q becomes q = 1). The vapor pressure is $P = P_1$ and the temperature is the saturation temperature $T_1 = T_{sat}(P_1)$. With h_{f1} and h_{d1} as saturation enthalpies of liquid and vapor, the total specific enthalpy of the mass flow is

(24) $$h_{c1} = (\dot{m}_{d1} * h_{d1} + \dot{m}_{f1} * h_{f1}) / \dot{m}_c$$

According to chapter 4.2.3 the vapor will occupy a large section A_d in the upper region of the tube cross section, the liquid collects in the remaining lower area

(25) $$A_f = A_{tot} - A_d$$

For a given liquid level l (x) and the tube diameter d_{tub} both areas and the wetted peripheries U_d and U_f can be calculated geometrically (see appendix 1).

In the following equations the suffix 'f' is to be taken for liquid and 'd' for vapor respectively. Inserting these data, we obtain the flow speeds

(26) $$v_{d,f1} = \dot{m}_{d,f1} / (A_{d,f1} * \rho_{d,f1})$$

the Reynolds numbers

(27) $$\mathrm{Re}_{d,f1} = \frac{4 * \dot{m}_{d,f1}}{(\eta_{d,f1} * U_{d,f1})}$$

the hydraulic diameters

(28) $$d_{d,f_{hy}} = \frac{4 * A_{d,f1}}{U_{d,f1}}$$

the pressure drops

(29) $$\Delta P_{d,f} = 0.5 * \psi_{d,f} * \rho_{d,f} * v_{d,f}^2 * \Delta x / d_{d,f_{hy}}$$

and the final pressure

(30) $$P_{d,f}(x + \Delta x) = P_{d,f}(x) - \Delta P_{d,f}$$

For Re < 2300 we use the expression for the laminar friction parameter with correction factor 1.5 for noncircular cross section [5] (in fact, laminary flow does occur only in extremely rare cases in the liquid).

(31) $$\psi_{d,f} = \psi_{lam} = 96/\mathrm{Re}_{d,f}$$

and for Re > 2300 the Colebrook formula [5]

(32) $$\frac{1}{\sqrt{\psi_{d,f}}} = -\log\left(\frac{2.51}{\mathrm{Re}_{d,f}\sqrt{\psi_{d,f}}} + \frac{k}{3.71 * d_{d,f_{hy}}}\right)$$

(k [m] = surface roughness)

Equation 32 can be solved iteratively.

5.2 THE LIQUID LEVEL

Generally, the two dynamic pressure drops for vapor (ΔP_d) and liquid (ΔP_f) are different. Let us first assume that liquid and vapor are in separate tubes with flow areas A_f and A_d respectively. At both ends in a distance of Δx the tubes are connected by vertical pipes (fig. 9).

Leaving the liquid at rest we maintain a gas flow which causes a pressure drop ΔP_d between the points 1 and 2. At the liquid/vapor boundaries in points 1 and 2, both vapor and liquid pressure must be equal.

(33a) $$P_{d1} = P_{f1}$$

(33b) $$P_{d2} = P_{f2}$$

Due to the pressure drop ΔP_d we have

(33c) $$P_{d2} = P_{d1} - \Delta P_d$$

As long as the liquid remains at rest, no horizontal static pressure gradient in the liquid is possible (fig. 9a). In order to satisfy simultaneously equs. 33 a; b and c, a level difference Δl between points 1 and 2 is required so that

(33d) $$\rho_f * g * \Delta l = \Delta P_d$$

(ρ_f = density of liquid; g = acceleration of gravity)

The liquid pressure at the surface in point 2 is then (fig. 9a)

(33e) $$P_{f2} = P_{f1} - \rho_f * g * \Delta l$$

If also the liquid does flow, we have to consider the pressure drop ΔP_f in the liquid as well and we obtain with different Δl^*

(33f) $$P_{f2}^{*} = P_{f1} - \Delta P_f - \rho_f * g * \Delta l^{*}$$

Renaming $P^*_{f2} \rightarrow P_{f2}$ and $\Delta l^* \rightarrow \Delta l$ and using (33a) and (33b) we get

(33g) $$P_{d2} = P_{d1} - \Delta P_f - \rho_f * g * \Delta l$$

and finally

(33h) $$\rho_f * g * \Delta l = P_{d1} - P_{d2} - \Delta P_f$$

or, with equ. 33 c

(34) $$\Delta l = (\Delta P_d - \Delta P_f)/(\rho_f * g)$$

If the pressure drop ΔP_d in the vapor is larger than the pressure drop in the liquid then Δl is positive, the level increases in flow direction (fig. 9b) and vice versa (fig. 9c).

For infinitsimal short distances Δx we can eliminate the separation wall between liquid and vapor and dividing by Δx, we obtain within one single two phase tube

(35) $$\frac{dl}{dx} = \left(\frac{dp_d}{dx} - \frac{dp_f}{dx}\right)/(\rho_f * g)$$

for the level gradient in the tube.

Numerical calculations will use the preceeding equ. 34 which finally gives the new value

(36) $$l(x + \Delta x) = l(x) + \Delta l$$

5.3 ENERGY CONSERVATION LAW

The new pressure and level in point 2 gives a new set of data T_2 (P_{d2}), A_{d2}, A_{f2} and consequently a change of flow speeds. This has to be considered under the aspect of energy conservation.

The total energy flow through point 1 is

$$\dot{W}_1 = \dot{m}_{f1}*(h_{f1} + 0.5* v_{f1}^2)+ \dot{m}_{d1}*(\dot{h}_{d1}+ 0.5* v_{d1}^2) \tag{37}$$

and through point 2

$$\dot{W}_2 = \dot{m}_{f2}*(h_{f2} + 0.5* v_{f2}^2)+ \dot{m}_{d2}*(\dot{h}_{d2}+ 0.5* v_{d2}^2) \tag{38}$$

$h_{f1,2}$ and $h_{d1,2}$ are the specific enthalpies for liquid and vapor respectively.

We define a specific energy density, referred to the total tube cross section A_{tot}: $w = \frac{\dot{W}}{\dot{m}_c}$

and, for energy conservation we must write

$$w_1 = \frac{\dot{W}_1}{\dot{m}_c} = \frac{\dot{W}_2}{\dot{m}_c} = w_2 \tag{39}$$

Introducing equs. (37) and (38) into 39, we obtain

$$\begin{aligned}(\dot{m}_{f1}* h_{f1} + \dot{m}_{d1}* h_{d1})/\dot{m}_c + 0.5*(\dot{m}_{f1}* v_{f1}^2 + \dot{m}_{d1}* v_{d1}^2)/\dot{m}_c \\ =(\dot{m}_{f2}* h_{f2} + \dot{m}_{d2}* h_{d2})/\dot{m}_c + 0.5*(\dot{m}_{f2}* v^2{}_{f2} + \dot{m}_{d2}* v_{d2}^2)/\dot{m}_c\end{aligned} \tag{40}$$

which can be rewritten, together with equ. 24

$$\begin{aligned}h_{c1} + 0.5*(\dot{m}_{f1}* v_{f1}^2 + \dot{m}_{d1}* v_{d1}^2)/\dot{m}_c \\ = h_{c2} + 0.5*(\dot{m}_{f2}* v_{f2}^2 + \dot{m}_{d2}* v_{d2}^2)/\dot{m}_c\end{aligned} \tag{41}$$

The left hand side of equ. 41 represents w_1, the right hand side w_2, which leads to

$$w_2 = w_1 = h_{c2} + 0.5*(\dot{m}_{f2}* v_{f2}^2 + \dot{m}_{d2}* v_{d2}^2)/\dot{m}_c \tag{42}$$

We can express the flow rates by

(43) $$\dot{m}_{d2} = q_2 * \dot{m}_c$$

(44) $$\dot{m}_{f2} = (1 - q_2) * \dot{m}_c$$

and the enthalpy

(45) $$h_{c2} = w_1 - 0.5 * [q_2 * v_{d2}^2 + (1 - q_2) * v_{f2}^2]$$

A subroutine out of HEPAK [6] which returns ρ_{2f}, ρ_{2d}, q_2 as a function of h_{c2} and P_{d2} can be used to find values of q_2, v_{d2}, v_{f2} by variation of h_{c2} at given w_1, which satisfy equ. 45.

5.4 THE HEAT INPUT

The preceeding equations do not yet consider the heat input. The heat flow QC from the cavities enters pointwise at the points L (NS, NM, NC), if
NC ≤ NCM - 1 and 1 ≤ NM ≤ NMM. With negligible loss of accuracy, we introduce the distributed heat load also at discrete points: The distance between two main points
L (NS, NM, NC) and L (NS, NM, NC +1) is subdivided into N0C intervals of length

(46) $$\Delta x = [L(NS,NM,NC+1) - L(NS,NM,NC)]/N0C$$

and at the end of every interval an amount of

(47) $$QR = DQRC * \Delta x$$

enters the return tube.

The cavity heat load QC at point 1 of the first interval of every cavity enters at constant pressure. It does not change the saturation temperature, but there is a change of enthalpy, q-value, flow rates and flow speeds of gas and vapor and finally of the energy.
Adding QC to the energy, we obtain

(48) $$w_1' = w_1 + QC/\dot{m}_c$$

and

(49) $$h_{c1}' = w_1' - 0.5 * [q_1' * v_{d1}'^2 + (1 - q_1') * v_{f1}'^2]$$

from which we derive a modified data set h'_{c1}, ρ'_{f1}, ρ'_{d1}, q'_1, $\dot{m}_{f1}$, $\dot{m}_{d2}$, v_{f2}, v_{d2}, as described in chapter 5.3.

At the end of each interval Δx, we add the distributed heat flow QR of this section.

(50) $$w_2' = w_2 + QR/\dot{m}_c$$

Replacing in equ. 49 all parameters with suffix '1' by values with suffix '2' we obtain the values h'_{c2}, ρ'_{f2}, ρ'_{d2}, q'_2, m'_{f2}, m'_2, v'_{f22}, v'_{d2} for mass flow rates, enthalpies, flow speeds of vapor and liquid at the end of the interval which are transferred to the next interval.

5.5 LONGITUDINAL HEAT FLOW

The longitudinal temperature gradient $\frac{dT}{dx}$ causes a longitudinal heat flow QL in the liquid. According to the theory of He II [7], the heat flow density is

(51) $$dQ_{HeII} = [\frac{1}{f(T,P)} * \frac{dT}{dx}]^{1/3}$$

The heat conductivity function $[f(T,p)]^{-1}$ has been taken from a subroutine of the program HEPAK [6].

With

(52) $$\frac{dT}{dx} = (T_2 - T_1)/\Delta x$$

we obtain a longitudinal heat flow

(53) $$QL = A_f * dQ_{HeII}$$

A_f is the mean value between A_{f1} and A_{f2}. Generally, $\frac{dT}{dx}$ and consequently QL varies with x. The difference of the longitudinal heat flow between point 2 and point 1

(54) $$\Delta QL = QL(x + \Delta x) - QL(x)$$

leaves the interval and does not contribute to evaporation within this interval. Consequently, equ. 50 has to be modified into

(55) $$w_2' = w_2 + (QR - \Delta QL)/\dot{m}_c$$

Within the accuracy being obtainable in the calculation, we assign the QL value, obtained from the temperature difference between point 1 and 2, to the end point 2 (fig.8). Consequently it is not yet known at the beginning of the calculation in point 1. To overcome this difficulty, a first iteration step has to set ΔQL = 0 and taking all relevant values from point 1. It will be followed by a second iteration taking mean values of mass flow rates, densities, liquid levels and flow areas between point 1 and point 2. Only in the second run ΔQL can be introduced.

6. EXECUTION

For practical reasons, the numerical calculations have been started at the cold end of the 2 K - heat exchanger HX 6. Consequently, all equations of the preceeding chapter have to be used in opposite direction: from given values in points 2 the values in the points 1 have to be calculated.

6.1 THE SUPPLY LINE

The absorbtion of the total heat load QTOT requires a mass flow of

(56) $$\dot{m}_0 = QTOT/(h_0 - h_{end})$$

h_0 is the enthalpy of the supercritical helium in point 2 a (fig. 5). It is given by the fixed supply data P_S and T_S

(57) $$h_0 = h(P_S, T_S)$$

h_{end} is the enthalpy of the returning gas in point 8a (fig. 5). Both pressure and temperature at the end depend on the required maximum temperature, the local distribution of heat loads and the pressure drops in the system.

Starting with a reasonable assumption for P_{end}, $T_{end} \approx T_{sat}(P_{end})$ gives a first approximation for the total mass flow rate in the supply line.

(58) $$MP(NSM + 1) = MP(NSM) = \dot{m}_0$$

At the positions of the JT-valves of every string, the flow in the supply line is reduced by MPS (NS), the required mass flow rate of string number NS:

(59) $$MP(NS - 1) = MP(NS) - MPS(NS)$$

Assuming a uniform distribution of mass flow to the strings, we start with

(60) $$MPS(NS) = \dot{m}_0/NSM$$

Introducing the heat load of the supply line DQS, we calculate the distribution of temperature and pressure within the supply tube. In a second approximation we will have to use the calculated values of MPS (NS), which are not exactly equal.

6.2 THE END CONNECTION

The end box of string number NSM is connected to the heat exchanger HX 6 by a 54 m long additional end of the return tube (we neglect the buffer reservoir at the end of this line).

If the system is in equilibrium, the flow rate coming out of this string must be equal to $\dot{m}_0$ and the quality of the saturated helium in the end box of the last string (number NSM) must

be 1. The gas arriving at HX 6 is overheated by the parasitic heat load DQR of the end connection tube .

Starting with a fixed end pressure P_{end}, the end temperature must be varied this way, that, regarding pressure drop and heat load in the connection tube, the saturation condition in the last end box is satisfied.

6.3 THE STRINGS

Starting from the end box in point (NS, NMM + 1, 1) after all steps of calculation through the string we obtain the values in the supply box.

(61) $$MPD(NS,0,0)= \dot{m}_{d1}$$

(62) $$MPF(NS,0,0)= \dot{m}_{f1}$$

(63) $$MPC(NS,0,0)= \dot{m}_{c}$$

The liquid mass flow rate $\dot{m}_{f1}$ must be produced by expansion of helium from the supply line through the JT-valve.

The enthalpy in the supply line at this point is, according to our definitions,

(64) $$h_S(NS-1)= h[P_S(NS-1), T_S(NS-1)]$$

An expansion to the vapor pressure P_{d1} in the supply box results in a two phase mixture with quality q.

In order to obtain the required liquid flow rate $\dot{m}_{f1}$, we need a mass flow rate into the string of

(65) $$MPS(NS)= \dot{m}_{f1}/(1-q)$$

Due to the variations of data both in the supply line and return line, MPS (NS) is different for all strings.

The vapor being produced by the expansion amounts to

(66) $$\dot{m}_{d,\exp} = q * MPS(NS)$$

and the mass flow, coming from the preceeding string which is pure vapor at this point must be

(67) $$MPC(NS-1)= MPC(NS)- \dot{m}_{d,\exp}$$

6.4 THE SUBUNIT

Calculation through all strings gives maximum pressure and temperature in the supply box of the first string. Furthermore, the exact value for the total mass flow supply rate must be

$$\dot{m}_S = \sum_{1}^{NSM} MPS(NS) \tag{68}$$

If

$$\dot{m}_S \neq \dot{m}_0 \tag{69}$$

the calculation has to be repeated, setting

$$\dot{m}_0 = \dot{m}_S \tag{70}$$

Furthermore, if the end value of the temperature is too high or too low, the calculation has to be repeated as well, using an improved end value p_{end}.

7. RESULTS AND COMMENTS

7.1 FLOW CONDITIONS IN THE SUPPLY TUBE

As explained in the preceeding chapters, the helium enters the supply tube at the refrigerator side of the subunit and flows in a direction of decreasing x-coordinate. In Dia. 1 one can see (subdiagram A) the mass flow rate decreasing from the input rate to zero in discrete steps at every string supply. Heat loads at design value, nominal value and static value are considered.

The pressure drop is displayed in the subdiagram B. The pressure gradient decreases from right to left because of the decreasing mass flow rate.

The temperature (subdiagram C) increases as consequence of the parasitic heat load DQS. The temperature gradient grows with decreasing mass flow rate. The approximate coincidence between curves a and b is due to the fact that the safety factor 1.5 is applied simultaneously both to the total heat load (which increases the mass flow rate) and the parasitic heat load of the supply line (see table 1).

7.2 FLOW CONDITIONS IN THE RETURN TUBE.

7.2.1 Pressures and Temperatures

Dia. 2 represents vapor, pressure and temperature in the return tube along a subunit. In order to establish the required maximum temperature of 2 K the refrigerator has to maintain lower temperatures and pressures at the outlet (right hand) end of the subunit, depending on the actual total heat load.
The temperature increase after the end of the last string for x > 1756 m is due to the overheating of the gas by the heat load of the end connection.

The liquid hydrostatic pressure has been calculated for the upper part of the cavity (point A, fig.7). A minimum overpressure of more than 1.5 mbar above saturation pressure provides

sufficient safety against bubble formation within the expected range of operation. The variations of the liquid pressure are due to liquid level variations (DIA 2, section C).

7.2.2 Liquid level

As mentioned in chapter 5.2, a longitudinal liquid level gradient is required in order to maintain a steady state liquid flow through the return tube. The value of the level at the end of each string is not determined by the equations of chapter 5.2. It is a free parameter.

With $l \approx 0$ at the end of each string (the consequence of higher levels will be discussed later), the longitudinal level distribution has been calculated for the different heat loads (DIA 3).

7.2.3 Flow rates, velocities and Reynolds numbers for vapor and liquid.

The longitudinal distribution of mass flow rate, flow speed and Reynolds numbers is represented in Dia. 4 for vapor and in Dia. 5 for the liquid. Both vapor and liquid velocities are low enough to justify the assumptions of chapter 4.2.

7.2.4 Liquid level at higher end values.

In 7.2.2 the liquid level at the end of each string was maintained at $l_{end} \cong 0$. The level distribution at higher end levels is quite different, as can be seen in Dia. 6 (nominal heat load) and Dia. 7 (design heat load). For comparison, both diagrams contain calculations for end levels $l_{end} \approx 0$ cm (curves I); 3 cm (curves II) and 5 cm (curves III).

As pointed out in chapter 5.2 (equ. 35), the level gradient is expected to be

$$\frac{dl}{dx} < 0 \qquad \text{for} \qquad \left|\frac{\partial p_d}{\partial x}\right| < \left|\frac{\partial p_f}{\partial x}\right| \tag{71}$$

and vice versa.

The gradients in vapor and liquid are displayed in sections B, C and D (figs. 6 and 7). In fact, a comparison with the level profiles in section A confirms the statements of equ. 71:

At the higher flow rate in the design case and for larger end levels (curves II and III in Dia. 7), we observe a change of sign of the level gradients within each string. The explanation is that both liquid flow areas (as function of the liquid level) and liquid mass flow rates change with different laws along the x-axis. Since the liquid pressure gradient depends in nonlinear way from both parameters, one finds a behavior as displayed in the diagrams.

It has to be investigated, whether these level profiles at higher flow rates and/or higher end levels will cause instabilities or not. At the moment it is recommendable to avoid instable situations by running the system at end levels close to zero.

7.2.5 Longitudinal heat flow

Using equations 51, 52 and 53 in chapter 5.5, the longitudinal heat flow in the liquid has been calculated for different level profiles and heat loads (DIA 8). For low levels (section A), the heat flow decreases in all strings with decreasing liquid levels.

the distorted string. The heater can be controlled by the end level. In that case the load conditions of the refrigerator remain unchanged.

The change of pressure drop (section A, curves 'c') is only a second order one because the overall mass flow rate remains constant, only the longitudinal distribution changes.

The level profiles are displayed in curves 'c'. The rapid decay of the level at the end (sections B + C, curves 'c') is due to the fact that a large fraction of the total liquid mass flow is evaporated locally in the end box.

7.2.6.3 Leaving the mass flow rate in the string constant at reduced heatload.

If neither the mass flow rate is changed nor a heater is activated, an excess of liquid is produced equivalent to the difference in the liquid flow rates before and after the failure occurs. The system runs out of balance and an overproduction of liquid will increase the liquid being stored in the string. The increased total mass of liquid is indicated by an increase of the end level. This is displayed in the sections A + B of Dia. 10 and 12. The time required for reaching a certain end level is plotted in section C of Dia. 10 and 12. The difference in time scale between failure in the middle or the end string is due to the fact, that the pressure gradient at the end is higher than in the middle. Consequently the end level increases faster if the failure occurs in the last strings.

The results show, that the response time for level and flow rate controls seems to be not very critical.

8. LOWER TEMPERATURES (1.8 K ≤ T ≤ 2.0 K)

In order to minimize the HF-losses of the cavities, it may be desirable to reduce the operating temperature furthermore to about 1.8 K. Although the change in T_{max} amounts only to 0.2 K = 10%, the consequences for the refrigeration system are not negligible.

DIA 13 represents pressure and temperature profiles which have been calculated for different outlet pressures. For obtaining 1.8 K at the hot end for the design case, the outlet pressure has to be reduced to about 6 mbar, compared with 27 mbar at T_{max} = 2.0 K. Under nominal load conditions, the outlet pressure has to be reduced from 29.5 mbar to 12.8 mbar (DIA 14).

In DIA 15, pressure (section A); Temperature (section B); Gas density (section C) and gas flow speed are displayed for the end of the return line at HX 6 as function of the required maximum temperature T_{max}. Reason for the drastic decrease of the required outlet pressure is, at fixed return tube diameter, the decrease of gas density (see equs. 26, and 29, chapter 5.1).

These reduced outlet pressures have drastical consequences, mainly for the cold compressors and the heat exchangers, especially HX6:

8.1 HEAT EXCHANGERS:

As displayed in DIA 15, section C, the vapor density is reduced by almost a factor 5 between 2 K and 1.8 K maximum subunit temperature. Consequently, in order to keep pressure losses in HX6 sufficiently low, this heat exchanger requires very large flow areas which will blow up the dimensions into sizes hardly to be realized.

8.2 COLD COMPRESSORS:

8.2.1 Number of compression stages

For the low suction pressures, the compression ratio to be reached with 4 compressor stages is not sufficient. Even for nominal heat load operation, at least 5 stages will be required. Still more stages will be necessary to reach 6 mbar for the design case.

8.2.2 Size of cold compressors

The large specific gas volume, especially at the inlet of the first stage, would require compressor wheel sizes which exceed the present state of the art by farthest (for comparison, the largest cold compressors being built and operated up to now are the CEBAF machines with suction pressures of about 30 mbar, flow rates of 0.220 kg/s having wheel diameters in the first stage of the order of almost 0.5 m). It might be necessary to subdivide the massflow rate to several parallel compressor stages.

8.2.3 Energy consumption

The refrigerators have to provide refrigeration at the lowest temperature level. The outlet temperatures corresponding to the pressures in the end box of the last string reduce from 1.958 to 1.593 K in the design case and from 1.983 to 1.739 in the nominal case (Tab. 3a).

Provided, the machine efficiencies remain constant (a very optimistic assumption), only the change in Carnot's efficiency would increase the requirement for primary energy from 817 W/W to 1004 W/W for design load and from 806 W/W to 920 W/W for nominal load (The primary power input values in the last lines of tables 3a, 3b and 3c are based on a conversion factor of 800 W/W at 2.0 K minimum temperature).

8.3 CONSEQUENCES

Having in mind the preceeding results and conclusions, it appears extremely unrealistic, to realize 1.8 K under maximum load conditions within a system as presently proposed.
It was designed for a safe operation at T_{max} = 2.0 K, and the range of operation can be seen in DIA 16, criterion I.

An acceptable compromise might be to design the system for 1.8 K not at the highest temperature but for the minimum temperature at the cold end of the system. This would require an outlet pressure of about 16 mbar to be realized with 5 compressor stages. Compressors for these operating conditions may be available in the near future. The possible operation range can be seen in DIA 16, criterion II. It would allow maximum temperatures of ca. 1.88 K at design load and 1.84 K under nominal conditions.

Another possibility has been investigated in addition: DIA 17 represents flow data to be obtained if the return tube diameter is increased from 0.3 m to 0.4127 m. It requires an outlet pressure of 15 mbar and remains below 1.8 K within the whole range of operation.

8.4 FINAL REMARKS

Any step to temperatures lower than 2 K, even in the case of nominal heat loads, requires an enormous effort and is an increased challenge for the system. The decision for this step

should be very well justified by sufficiently high advantages for the technique of the accelerator.

9. ALTERNATIVE CIRCUITS

9.1 ONE JT-VALVE PER UNIT

It seems to be possible to inject the whole massflow rate for every subunit through one single JT-valve at the far end of the unit (fig. 10). The number of strings is reduced to one with 144 modules. There is only one supply box at the far end and an end box at the refrigerator side. Consequently, the total length of a subunit reduces from 1830 m to 1812,4 m. The number of JT-valves, control circuits and heaters is reduced to one.

DIA 18 and 19 show the main flow parameters in the supply tube and the return tube, DIA 20 represents the liquid level profiles under different conditions. Pressures, temperatures and liquid level as well as massflow rates (DIA 21) and longitudinal heat flow (DIA 22) occur much smoother (DIA 23 to 26).

The influence of power failures is observable mainly at the end, independently on the location of occurence. The time constants are of the same order of magnitude as in the case of the twelve JT-valve system.

A disadvantage is the high amount of stored liquid helium in the return tube. The high liquid massflow rate immediately after the injection requires a large flow area for the liquid which can be realized only by a high level in the tube (DIA 20). A comparison of stored helium masses in the two systems, is given in Tab. 2.

Table 2.

Helium stored in different sections of a TESLA unit at design load

Circuit section	A [kg]	B [kg]
Liquid in the return tube	257.9	1625.4
Vapor in the return tube	95.7	85.8
Gas in the end connection	2.7	2.6
Liquid in the cavaties	4153.8	4121.5
subcooled He in the supply tube	678.9	673.2
Total 2 K Helium mass	5189.0	6508.5

A = 12 JT-valve version
B = 1 JT-valve version

9.2 NON HORIZONTAL SYSTEMS

Depending on the final location of the TESLA site, it may be very difficult to obey the condition of horizontality. The influence of an inclined return tube has been investigated and results (which are not yet complete) are presented in DIA 27 for inclination angles of $\alpha = 0.0$ and $\pm$ 1 mrad:

At a negative inclination angle of α = - 1 mrad (section B), there seems to be no serious problem. The liquid flows, as naturally expected, downhill and consequently, only a lower level gradient is necessary in the tube (the level has mainly to provide the desired flow area). There may occur some difficulties for restarting the system after a stop, because without heat load, all remaining liquid will collect at the lower end of the subunit. It must probably be evaporated by an electrical heater.

For positive inclination the situation is completely different: since the liquid has problems to flow uphill, the lowest section has first to be filled with liquid before a steady state flow can start (DIA 27, section C). Consequently, a large amount of helium will be collected in the tube. For comparison, the helium masses for positive, zero and negative inclination are remarked in the diagrams.
The results seem to indicate that there will be no serious problems for constant negative inclination; positive angles can be avoided by reversing the flow directions. But, considering fig. 6, the layout with two adjacent refrigerators in one cryo hall requires flow rates in alternative directions for adjacent subunits (fig. 11), i.e. half of the units have the wrong inclination angle.

Some first ideas to overcome this problem are in discussion. They will have to be investigated in the future from both technical and economical aspects:

9.2.1 Change of refrigerator positions:

For constant tunnel inclination, the refrigerators have to be placed always at the highest ends of the subunits. This would require twice as much cryogenic halls with half the distance between them (fig. 12). There will be only 1 refrigerator per hall. This solution will increase the costs of civil engineering and also increase the problems for finding sites above ground for the halls.

9.2.2 Stepwise approximation of the angle

It seems to be possible to leave the return tube horizontal over the distance of 1 string, the next string is lowered by an amount of

(72) $$\Delta y = \alpha * LSTR$$

(α = inclination angle, LSTR = string length).

The cavities can be mounted in a straight line which follows the tunnel axis (fig. 13). This arrangement requires different modules with variing lengths of the connection tubes. The difference in connection tube length of the first and last module of a string has to be Δy.

If α is too large, Δy will also grow. In this case it may be necessary to reduce the length of the strings (with the disadvantage, that the number of JT-valves will increase).

9.2.3 Separation of vapor and liquid flow

All cavities are connected to the return tube by vertical tubes of the same length. All tubes are interconnected by a longitudinal tube of moderate diameter which is completely filled with liquid. The liquid level will increase into the vertical connections but at no point in the system liquid will go into the gas return tube. With no liquid movement, all liquid levels will

be at the same horizontal level, the motion of the liquid will require level differences and gas pressure gradients as described in the preceeding chapters.

For every string, individual supply and end boxes are required. Again, the vertical position of the boxes has to be matched to the tunnel inclination (fig. 14).

In order to keep the length of the vertical connection tubes below a tolerable maximum (long connection tubes require large diameter cryostats, see fig. 4), the string length has to be reduced for larger inclination angles. For $\alpha \cong 16$ mrad, it may happen that the string length has to be reduced to the module length, i.e. every single module has to be supplied by its own JT-valve. Inclination angles larger than about 15 mrad may require a forced flow, one phase cooling system.

A system like this seems to be adaptable to different tunnel inclinations. A separate parallel tube has already been realized in the TTF cryostats. The difference is, that for TESLA there is no vapor flow in the liquid tube. The liquid tube diameter can be reduced without safety risk because of the short longitudinal distance between the vertical exhaust tubes from every cavity.

A disadvantage may be the fact that the surface for evaporation is limited to the connection tube cross section, compared with the large surface areas being available in the return tube. Furthermore, it should be mentioned that shorter string lengths also require a redesign of the warm up/ cool down system. The longitudinal interconnection of the cavaties has to be interrupted at the string ends in order to avoid an overfilling of the sections at the lowest position.

10. SUMMARY AND CONCLUSIONS

A selection of the most important results of the preceeding chapters has been summarized in Tables 3a and b. In the first table we find original design cases and extension to 1.8 K, in the second one all cases with deviating hardware.
In the last two lines, M_2 represents the total mass of helium being contained in the 2 K respectively 1.8 K circuits, including cavities, 2 K supply line and return tube.

$W_{in,2}$ is the primary power, required for 2 K (1.8 K) cooling only. On the basis of a specific primary energy factor at 2.0 K of 800 W/W, $W_{in,2}$ has been calculated for the individual minimum temperatures T_{min}, taking into account only the change of Carnot's efficiency with the temperature.

The temperature T_{min} is the equilibrium temperature in the end box of the last string. P_{out} is the outlet pressure in point 8a (fig. 5).

Table 3a: Summary of important results for original design

A/ B/ C static/ nominal/ design heat load; T_{max} = 2.0 K

D/ E nominal/ design heat load; T_{min} = 1.8 K

F/ G nominal/ design heat load; T_{max} = 1.8 K

	A	B	C	D	E	F	G	
QM	2.8	21.4	32.1	21.4	32.1	21.4	32.1	Watt
QTOT	522	3200	4802	3200	4802	3200	4802	Watt
$\dot{m}_0$	0.026	0.160	0.242	0.167	0.250	0.169	0.261	kg/s
T_{max}	2.000	2.000	2.000	1.844	1.887	1.800	1.800	K
T_{min}	1.999	1.983	1.958	1.800	1.800	1.739	1.593	K
P_{max}	31.27	31.32	31.28	19.08	22.03	16.38	16.36	mbar
P_{out}	31.22	29.60	27.25	16.11	15.82	12.82	5.92	mbar
M_2	4992	5157	5188	5102	5143	5088	5108	kg
$W_{in,2}$	0.418	2.582	3.924	2.844	4.268	2.944	4.823	MWatt

Table 3b Summary of inportant results for alternative designs

H design heat load; T_{max} = 1.8 K (enlarged return tube diameter; d_{tube} = 0.4127 m)

I/ J nominal/ design heat load; T_{max} = 2.0 K (1 JT-valve-system)

K design heat load; T_{max} = 2.0 K (inclined return tube; α = - 1.0 mrad)

L design heat load; T_{max}= 2.0 K (inclined return tube; α = + 1.0 mrad)

	H	I	J	K	L	
QM	32.1	21.4	32.1	32.1	32.1	Watt
QTOT	4802	3177	4767	4802	4802	Watt
$\dot{m}_0$	02.51	0.159	0.241	0.242	0.243	kg/s
T_{max}	1.800	2.000	2.000	2.000	2.000	K
T_{min}	1.778	1.978	1.944	1.959	1.934	K
P_{max}	16.40	31.32	31.31	31.32	31.26	mbar
P_{out}	15.00	29.14	26.10	27.35	25.22	mbar
M_2	5243	6383	6508	5073	7821	kg
$W_{in,2}$	4.321	2.570	3.923	3.922	3.973	MWatt

Operating conditions under many aspects for a TESLA cooling system as proposed at present have been investigated. Simulating calculations of steady state behaviour at a maximum cavity operation temperature of T_{max} = 2 K in a horizontal system do not indicate any

problems. Dynamic simulation programs, including transient states will have to investigate the system more in detail.

It has been shown that extensions of the system either in direction of lower temperatures or to inclined flow tubes may cause more problems and/or higher costs. These cases will have to be investigated more in detail as well.

REFERENCES

[1] G. Horlitz, T. Peterson, D. Trines, "A 2 Kelvin Helium II Distributed Cooling System for the 2 x 250 Gev e^+e^- Linear Collider TESLA"
Proc. 15, Intern. Cryog. Eng. Conf., Genova, 1994, p. 131

[2] G. Horlitz, T. Peterson, D. Trines, "The TESLA 500 Cryogenic System Layout", Proc. 16. Intern. Cryog. Eng. Conf., Columbus/Ohio, 1995, to be published

[3] T. Peterson, "Notes about the Limits of Heat Transport from a TESLA Helium Vessel with a Nearly Closed Saturated Bath of Helium II", TESLA Report No. 94-18, 1994

[4] D. A. Edwards (Editor), "TESLA Test Facility LINAC-Design Report", TESLA Report No. 95-01, 1995, p. 228

[5] H. Brauer, "Grundlagen der Einphasen- und Mehrphasenströmungen", Verlag Sauerländer AG, Aarau (Schweiz), 1971, p. 31/p. 94 and p. 40

[6] V. Arp, R.D. Mccarty and B.A. Hands, PC-Program "HEPAK, Thermodynamic Properties of HELIUM.....", Version 3.01, Copyright by Cryodata Company, P.O. Box 558, Niwot, CO 80544

[7] S. W. Van Sciver, "Helium Cryogenics", Plenum Press, New York, 1986, p. 152

APPENDIX:

A1: FLOW AREAS AND CIRCUMFERENCES

We consider the circular cross section of the return tube with radius $r = 0.5\ d_{tube}$. The lower part of the tube is filled with liquid up to a level hight l (fig. 15). The liquid boundary s (straight line A $\rightarrow$ B) subdivides the cross section A_{tot} into the lower liquid fraction A_f and the upper vapor fraction A_d.

The liquid periphery is the sum of the chord s and the arc ACB. The gas periphery is s plus arc ADB.
Flow areas and peripheries can be calculated as follows (fig. 16):

(A1.1) $$(\frac{s}{2})^2+(r-l)^2=r^2$$

(A1.2) $$s = 2*\sqrt{2*r*l-l^2}$$

(A1.3) $$\varphi^{[rad]} = 2*\arcsin\frac{s}{2*r}$$

(A1.4) $$A_f = 0.5*[r^2*\varphi - s*(r-h)]$$

(A1.5) $$A_{tot} = \pi*r^2$$

(A1.6) $$A_d = A_{tot} - A_f$$

For the peripheries the calculation is neither straight forward nor evident. Geometrically, the circumferences would be:

(A1.7) $$U_{f,a=}r*\varphi + s$$

(A1.8) $$U_{d,a=}(2*\pi-\varphi)*r + s$$

This would be true, if s would be a solid wall. In the theory of gas/liquid flow, at the walls the speed of the fluid is zero, because due to adhesive forces between fluids and walls, an outer, very thin layer of the liquid is fixed to the wall which is at rest. So steel boundaries both of vapor and liquid, contribute completely to the wetted peripheries.

Along the liquid/gas boundary, the situation is different.

A plausibility consideration leads to the assumption, that the liquid does only see a "wall of gas" with negligible density. There is nothing to adhere to. We neglect the contribution of the chord s to the wetted diameter of the liquid.

On the other hand, the vapor is in touch with the liquid, the density of which we consider as infinite compared with that of the vapor. We assume, that it contributes to the wetted circumference of the vapor like a solid wall.

Under these assumptions, we choose for the pressure calculations

(A1.9) $$U_{f=}r*\varphi$$

(A1.10) $$U_{d=}(2*\pi-\varphi)*r + s$$

2: COMPLETE HEAT LOAD INFORMATION

Although this paper investigates only the 2 K circuits, for general information a summary of all heat loads, which has been published recently [2], is added in table A2.1 and for the primary energy comsumption in table A2.2.

Table A2.1

TESLA heat loads

(n = normally expected values; d = design values; stat = HF-power off; dyn = HF-power on)

Temperature	2 K		4.5 K		40/80 K		
	stat	total	stat	total	stat	total	W
Module n	2.8	21.4	13.9	16.0	76.8	136.0	W
d	4.2	32.1	20.9	24.0	115.2	204.0	W
String n	35.64	258.8	166.8	192.0	921.6	1632.0	W
d	53.51	388.4	250.2	288.0	1382.4	2448.0	W
Subunit n	521.9	3200	2007	2309	11070	19595	W
d	783.4	4802	3011	3500	16605	30000	W
TESLA n	8350	51204	32112	37000	177120	313500	W
d	12534	76825	48168	56000	265680	480000	W

Table A2.2

TESLA ambient temperature electrical power input at design heat load [MWatt]

Temperature		2 K		4.5 K		40/80 K		Σ input	
		stat	total	stat	total	stat	total	stat	dyn
Subunit	n	0.42	2.58	0.5	0.58	0.28	0.49	1.2	3.7
	d	0.63	3.92	0.75	0.88	0.42	0.75	1.8	5.6
TESLA	n	6.7	41.3	8.0	9.3	4.4	7.8	19.1	58.4
	d	10.1	62.7	12.0	14.0	6.6	12.0	28.7	88.7

A3: REDUCED DYNAMIC LOAD

When this report was almost ready, a new information came to the author: It is envisaged to reduce the number of HF-power pulses by a factor of 2. This would mean, the dynamic load is cut to one half of the amount being considered in the preceeding chapters. The reduced loads are summarized in Tab. A3.1

In order to delay the edition of this report not any more, only two diagrams could be added being calculated for this new case: DIA 28 (pressure and temperature profile for T_{max} = 2 K) and DIA 29 (comparison of pressure and temperature profiles for T_{max} = 2 K, T_{max} = 1.8 K and T_{min} = 1.8 K).

Tables A3.2 and A3.3 summarize the heat loads for all temperatures and the total primary energy requirements for the reduced HF-pulse rate case.

Table A3.1 Heat load details at reduced HF-pulse rate

		nominal	design		entering mode
static load per cavity	QCS	0.335	0.503	W	pointwise
dynamic load per cavity*	QCD	1.1625	1.744	W	pointwise
total load per cavity	QC	1.4975	2.247	W	pointwise
load to return tube	DQRC	0.01	0.015	W/m	distributed
static load per module	QMS	2.80	4.21	W	
dynamic load per module*	QMD	9.30	13.95	W	
total load per module	QM	12.10	18.16	W	
load to supply- and end box	QC0	1.00	1.50	W	distributed
static load per string		35.64	53.51	W	
dynamic load per string*		111.60	167.42	W	
total load per string	QST	147.24	220.93	W	
load to 2.2 K supply line	DQS	0.05	0.075	W/m	distributed
load to 54 m connection	DQR	0.05	0.075	W/m	distributed
static load per subunit		521.9	783.4	W	
dynamic load per subunit*		1339.2	2006.9	W	
total load per subunit	QTOT	1861	2790	W	

Table A3.2 Summary of important results for heat loads at reduced HF pulse rate

M/ N nominal/design reduced heat load; T_{max}= 2.0 K

O/ P nominal/design reduced heat load; T_{max} = 1.8 K

	M	N	O	P	
QM	12.1	18.2	12.1	18.2	Watt
QTOT	1861	2793	1861	2793	Watt
$\dot{m}_0$	0.093	0.140	0.097	0.147	kg/s
T_{max}	2.000	2.000	1.800	1.800	K
T_{min}	1.995	1.987	1.782	1.756	K
P_{max}	31.32	31.31	16.41	16.39	mbar
P_{out}	30.75	30.00	15.28	13.73	mbar
M_2	5106	5139	5048	5074	kg
$W_{in\,2}$	1.493	2.249	1.671	2.545	MWatt

Table A3.3 TESLA heat loads at reduced HF-pulse rate

(n = normally expected values; d = design values; stat = HF-power off; dyn = HF-power on)

Temperature	2 K		4.5 K		40/80 K		
	stat	total	stat	total	stat	total	W
Module n	2.8	12.1	13.9	15.0	76.8	106.4	W
d	4.2	18.2	20.9	22.4	115.2	159.6	W
String n	35.64	147.2	166.8	179.4	921.6	1276.8	W
d	53.51	220.9	250.2	269.1	1382.4	1915.2	W
Subunit n	521.9	1861	2007	2158	11070	15333	W
d	783.4	2790	3011	3256	16605	23303	W
TESLA n	8350	29776	32112	34528	177120	245378	W
d	12534	44640	48168	52096	265680	372840	W

Table A3.4 TESLA ambient temperature electrical power input at reduced HF-pulse rate in MWatt

Temperature		2 K		4.5 K		40/80 K		Σ input	
		stat	total	stat	total	stat	total	stat	total
Subunit	n	0.42	1.49	0.50	0.54	0.28	0.38	1.2	2.41
	d	0.63	2.25	0.75	0.81	0.42	0.58	1.8	3.64
TESLA	n	6.7	23.8	8.0	8.6	4.4	6.1	19.1	38.5
	d	10.1	36.0	12.0	13.0	6.6	9.3	28.7	58.3

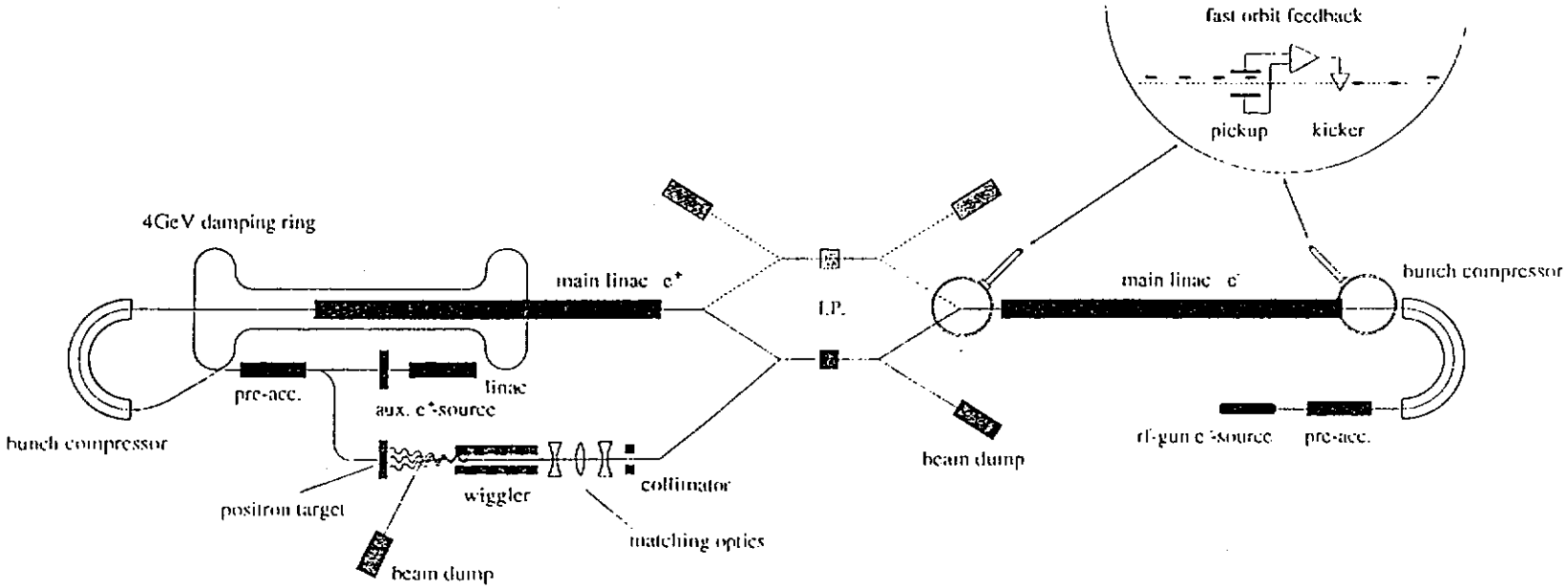

Fig. 1 TESLA General Layout

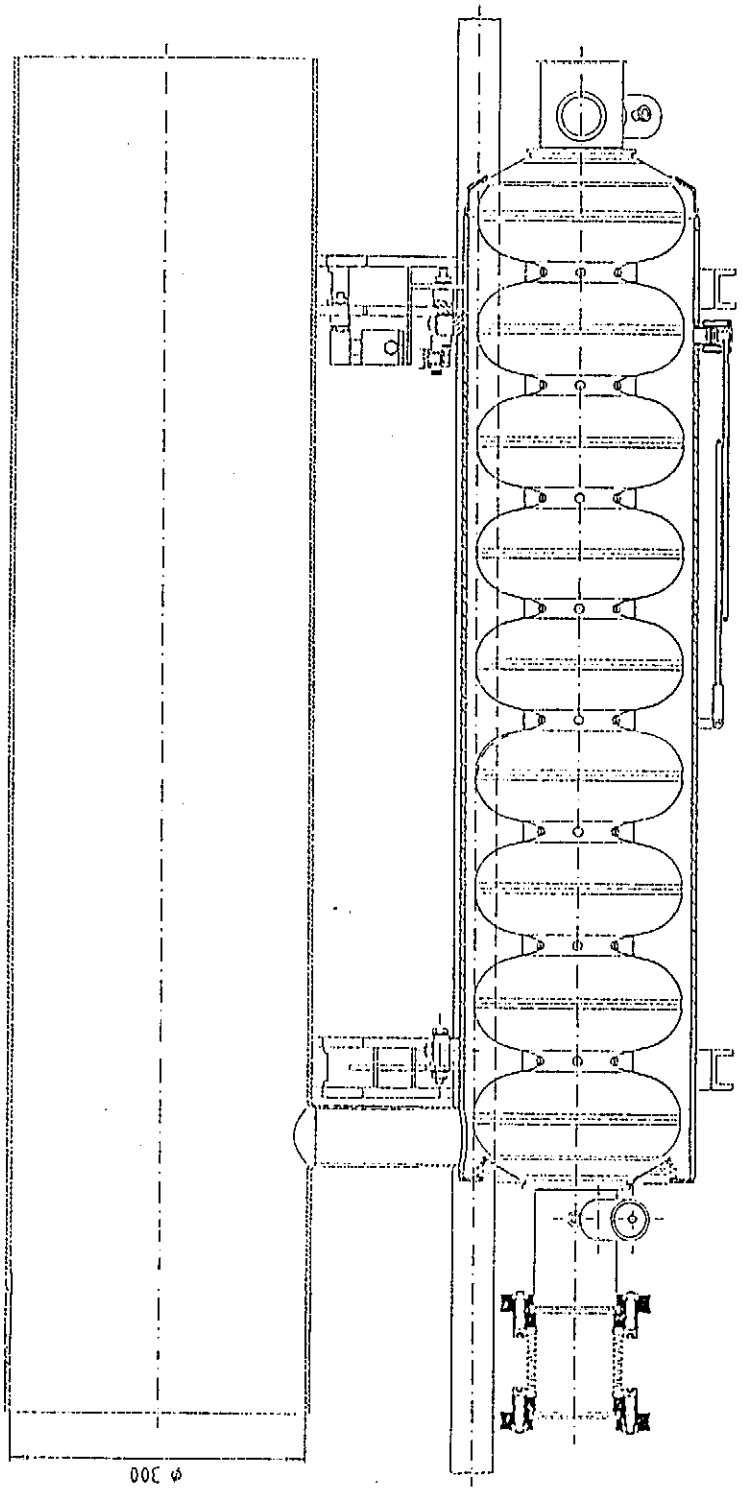

Fig. 2 TESLA Cavity and Vapor Return Tube

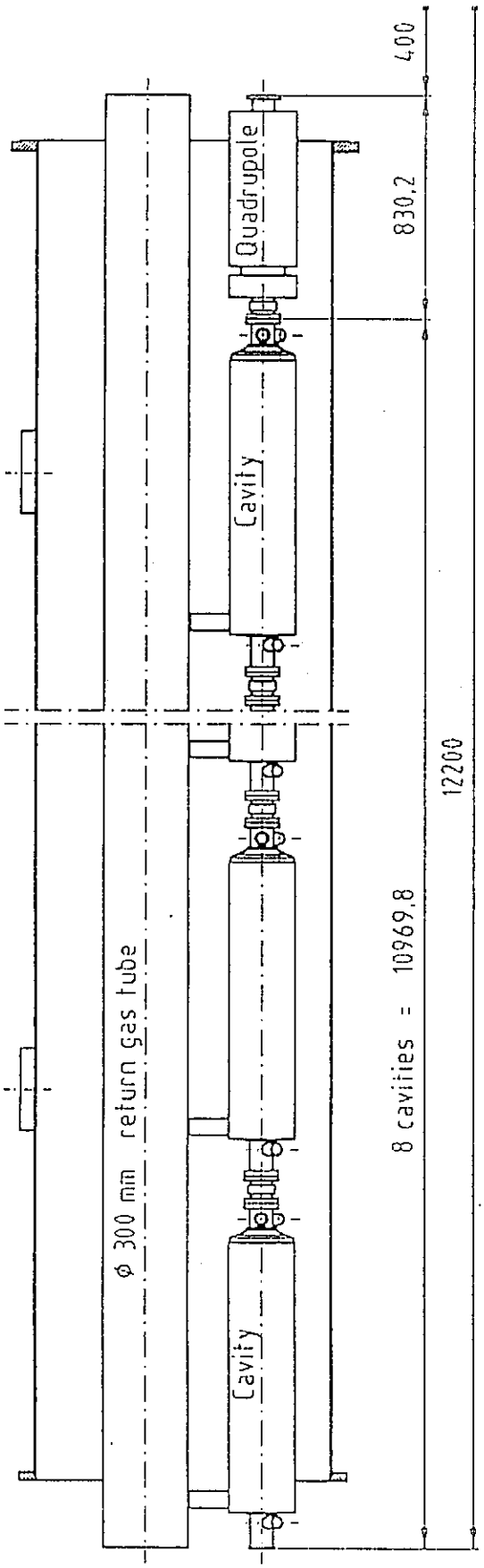

Fig. 3 TESLA Module

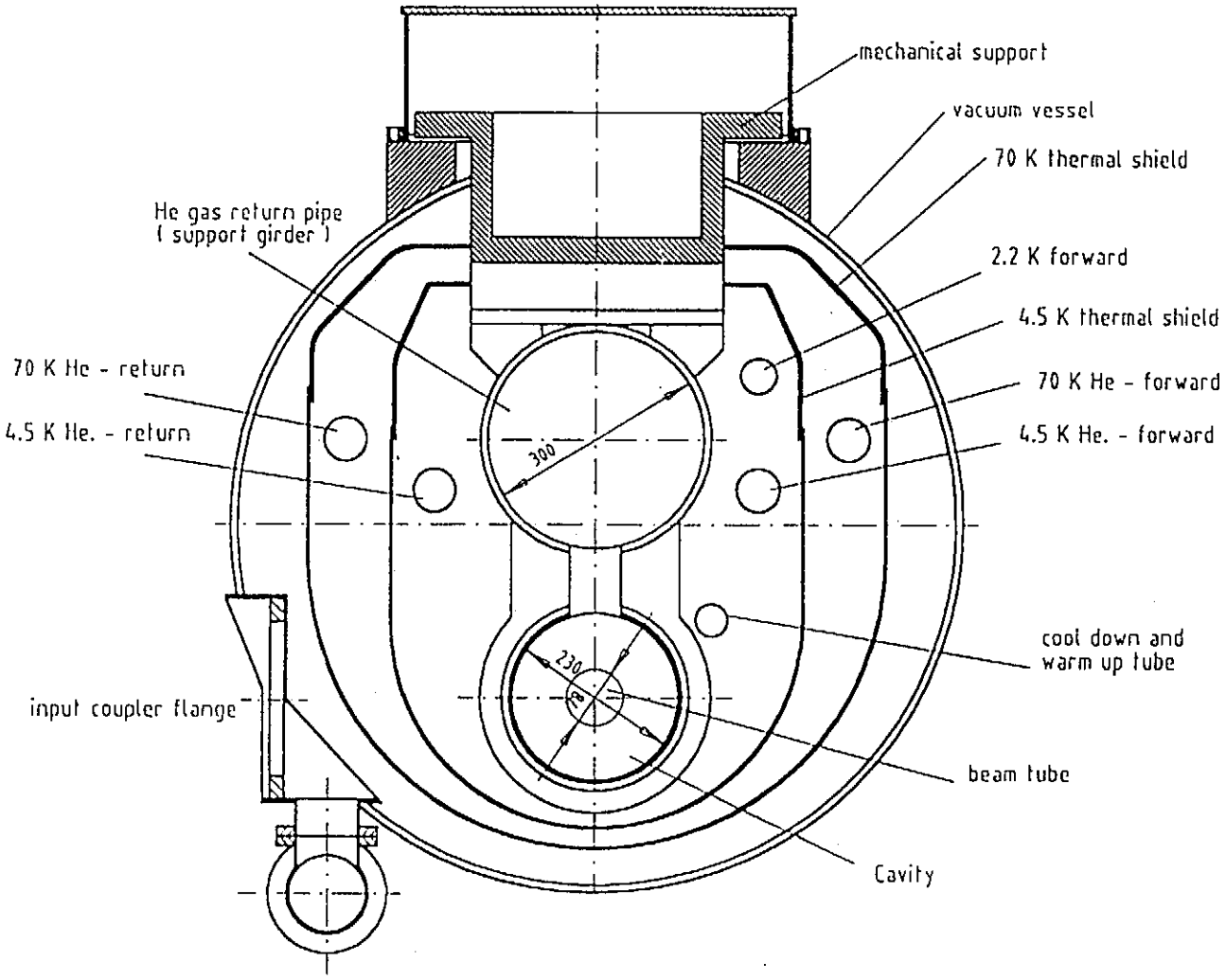

Fig. 4 TESLA Cryostat Cross Section

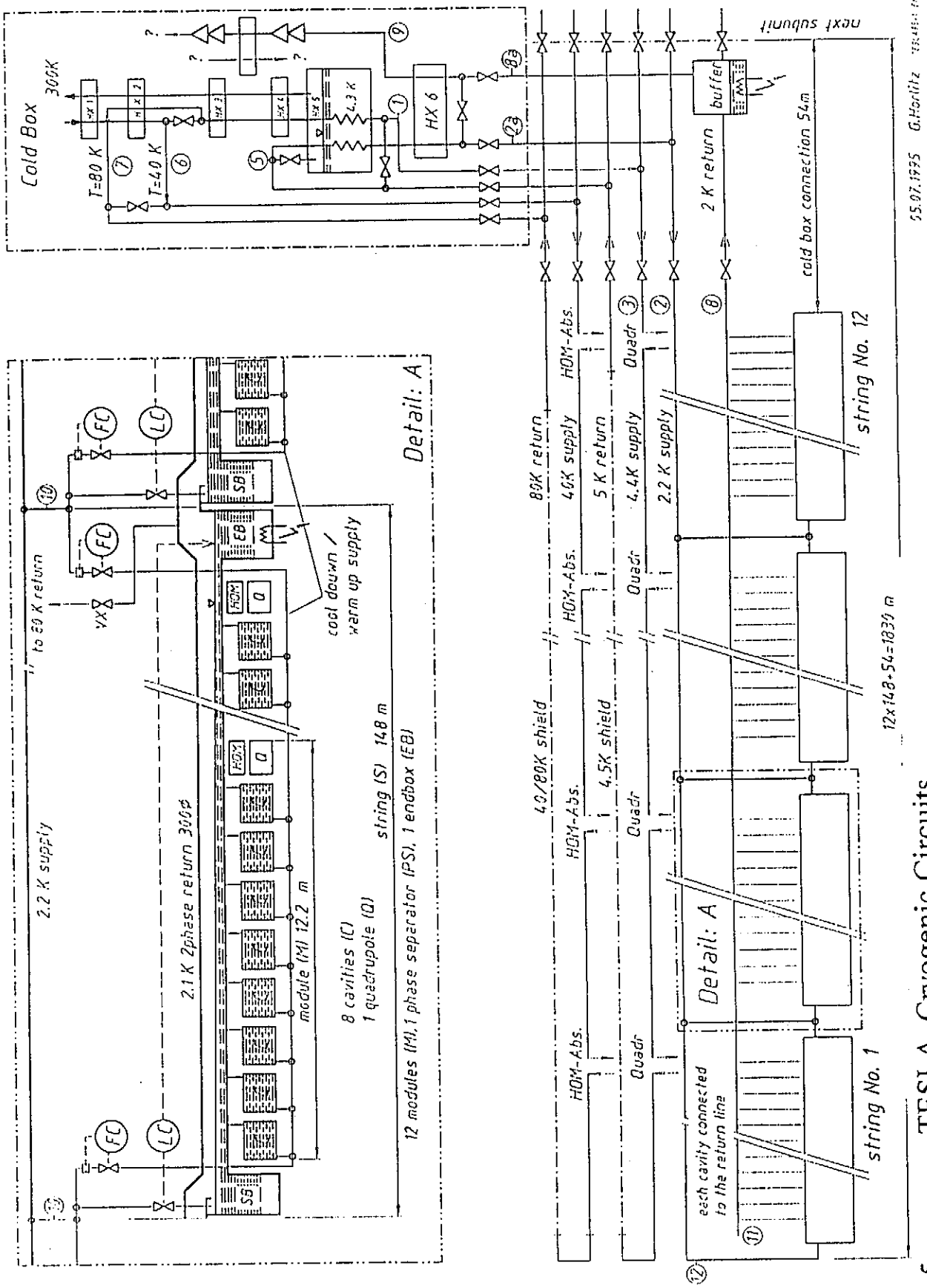

Fig. 5 TESLA Cryogenic Circuits
(version with one JT-valve for each string)

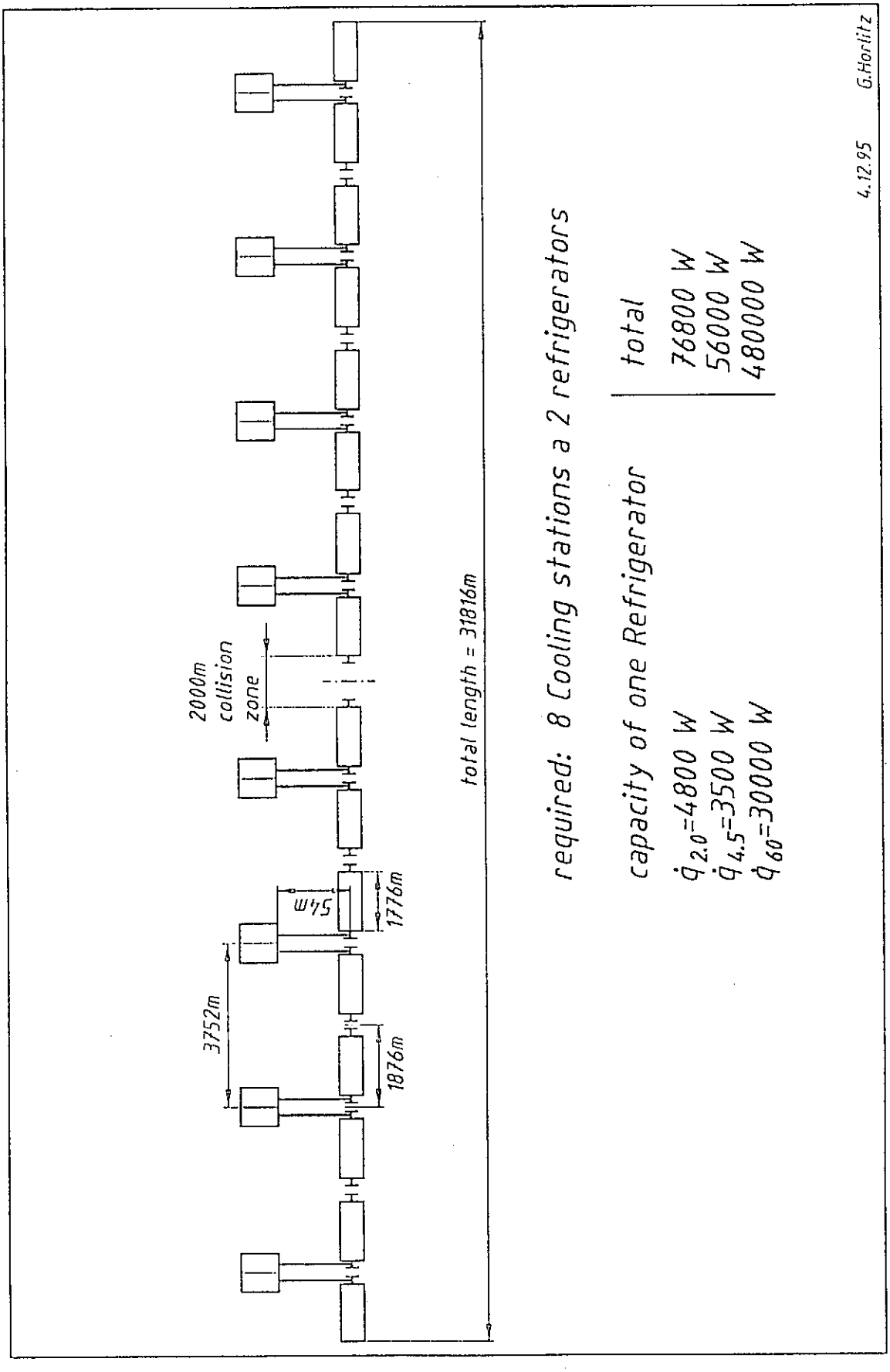

Fig. 6 TESLA Cryogenic System
(General layout and subdivisions)

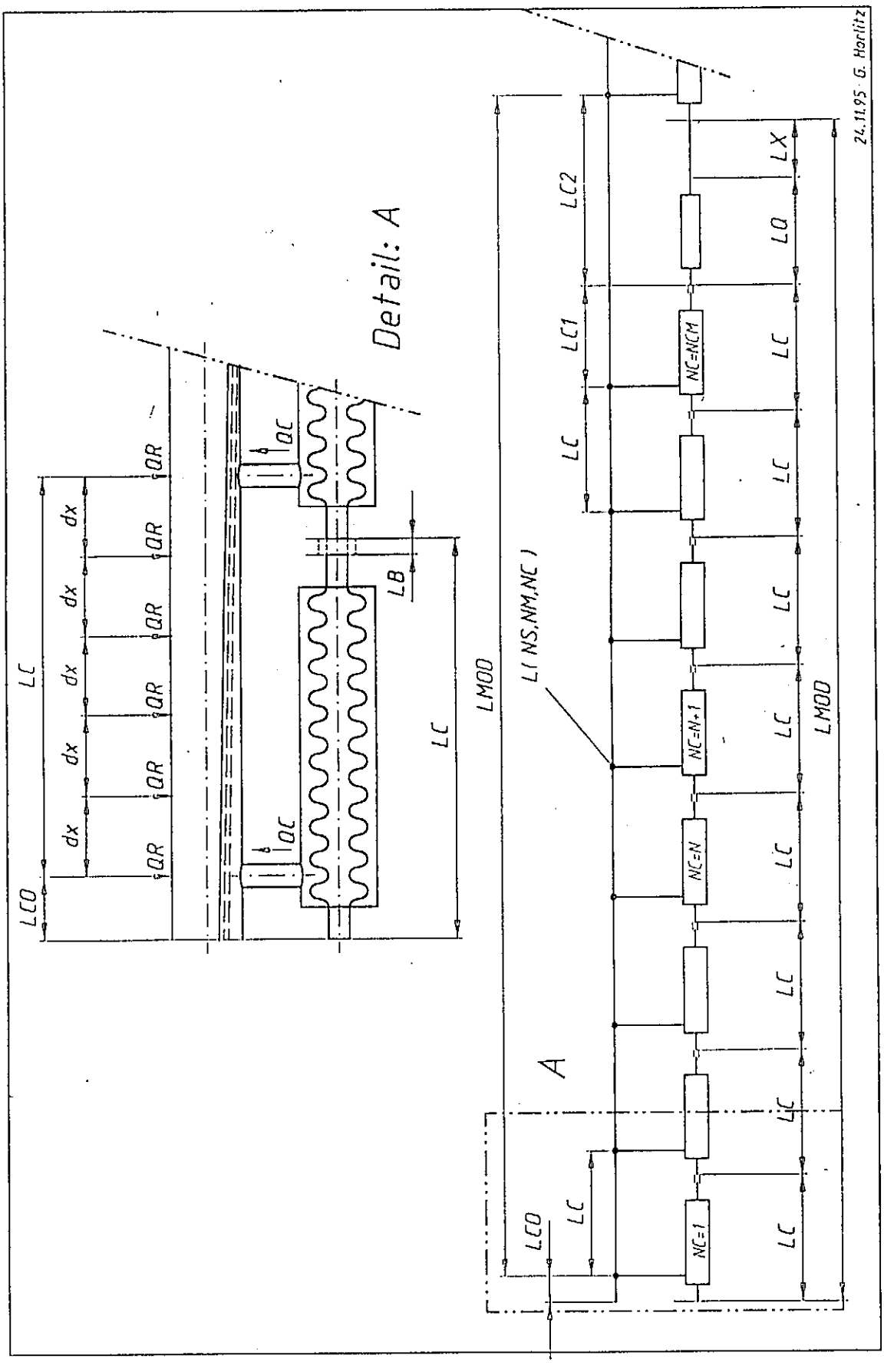

Fig. 7 TESLA Module Geometry

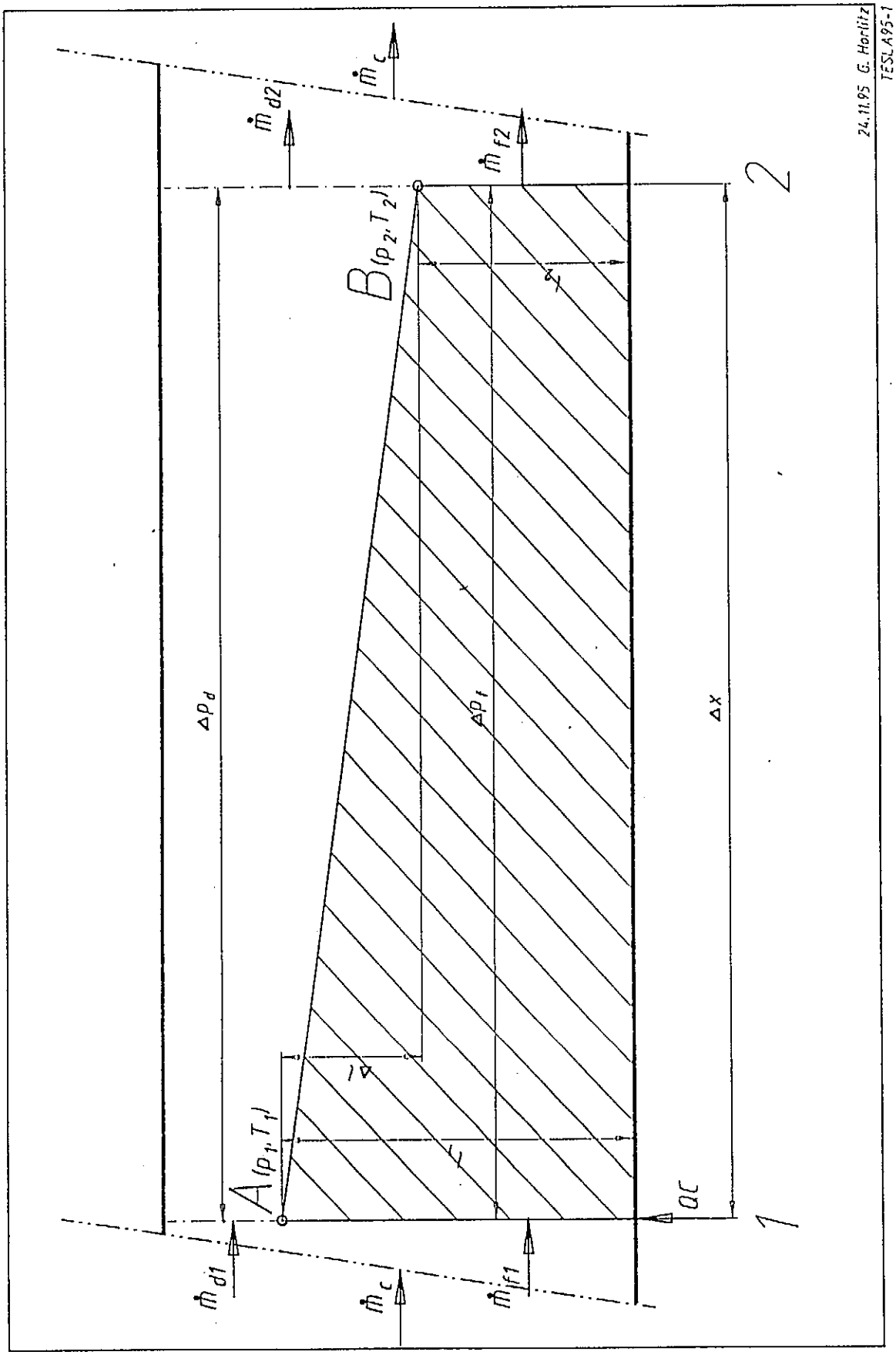

Fig. 8 Element of Length Δx of the TESLA Return Tube

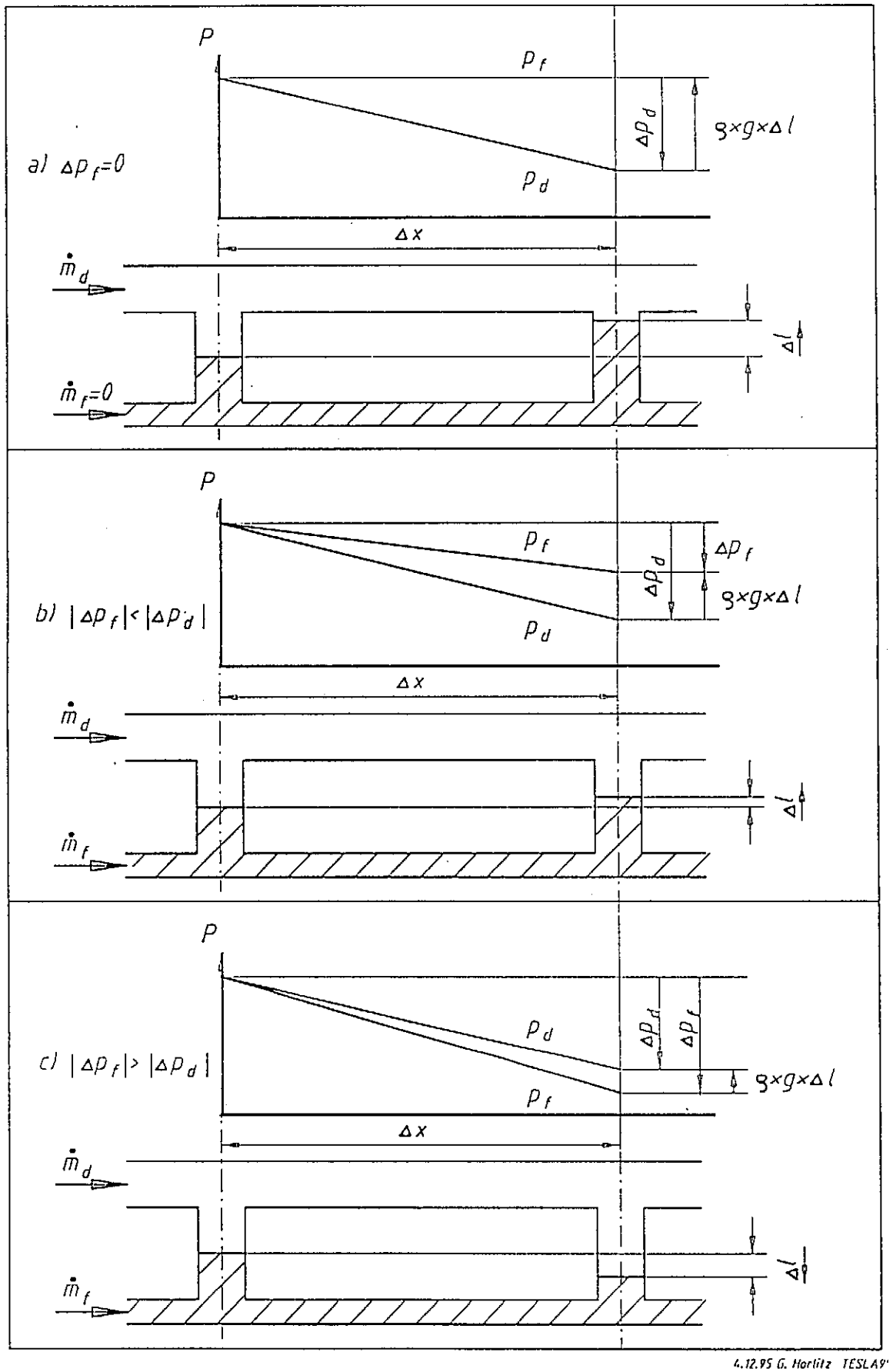

Fig. 9 Liquid Levels at different Pressure Drops in Vapor and Liquid

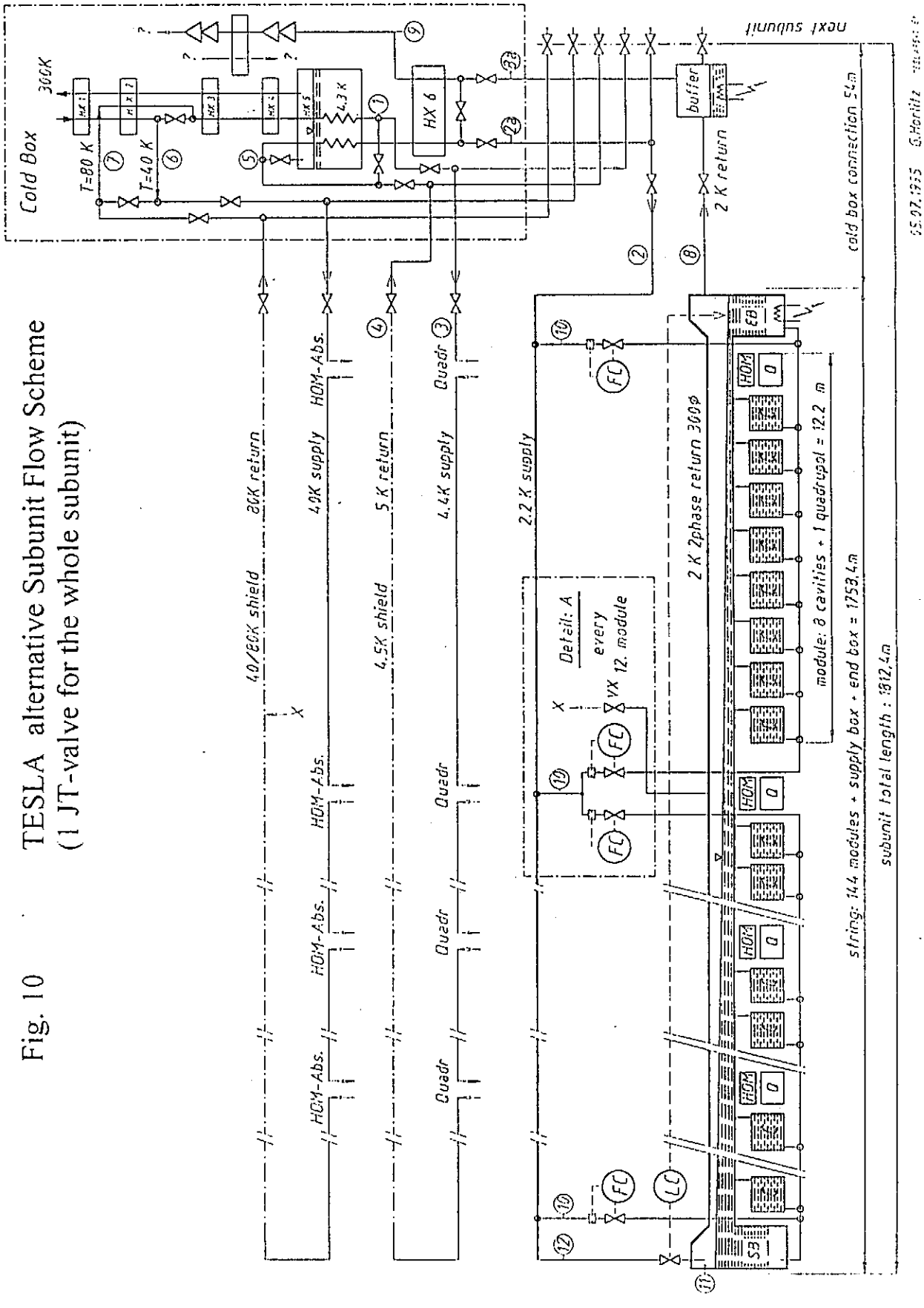

Fig. 10 TESLA alternative Subunit Flow Scheme
(1 JT-valve for the whole subunit)

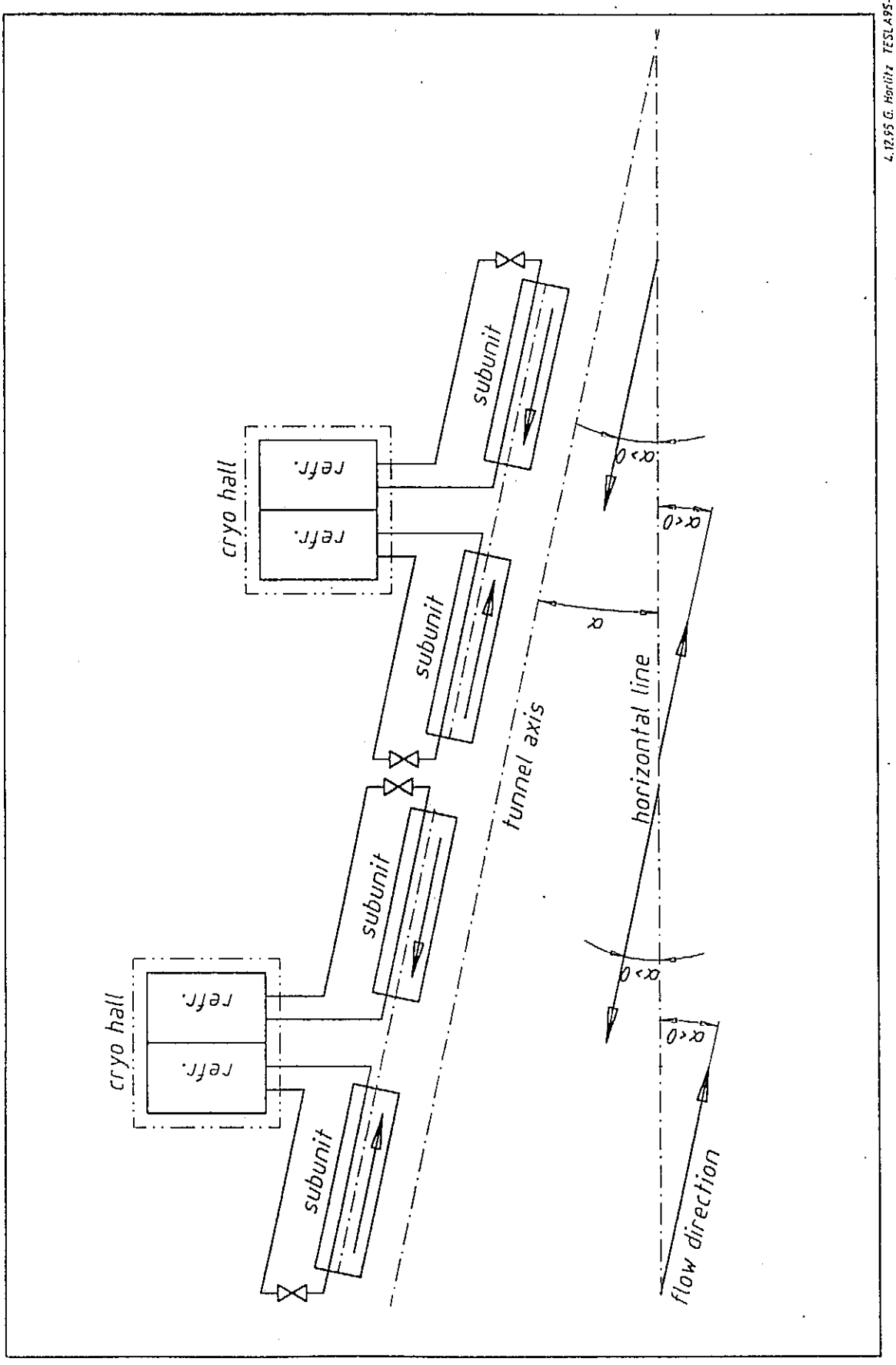

Fig. 11 Flow problems in a nonhorizontal Tunnel

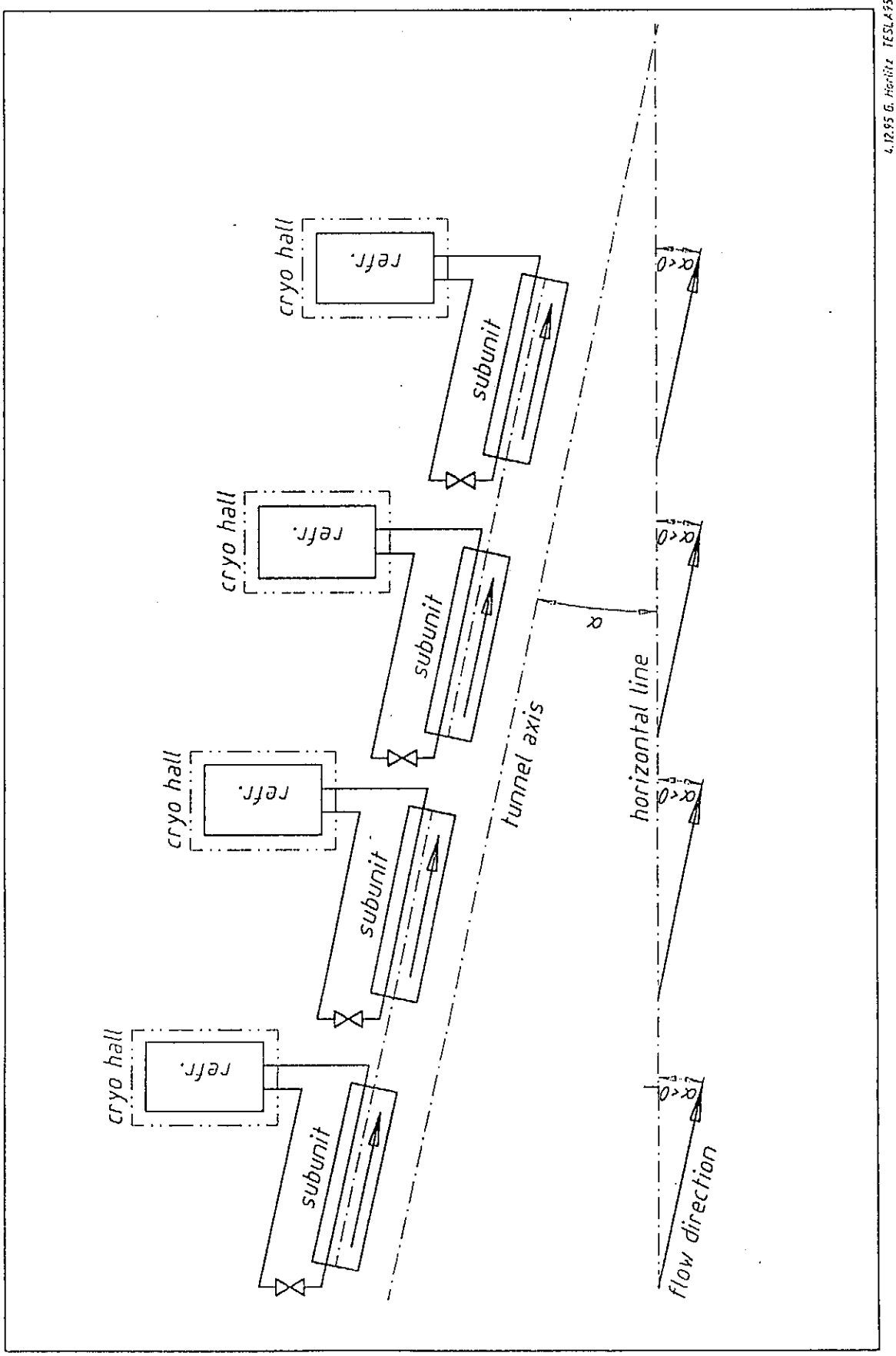

Fig. 12 Adaption to nonhorizontal Geometry 1

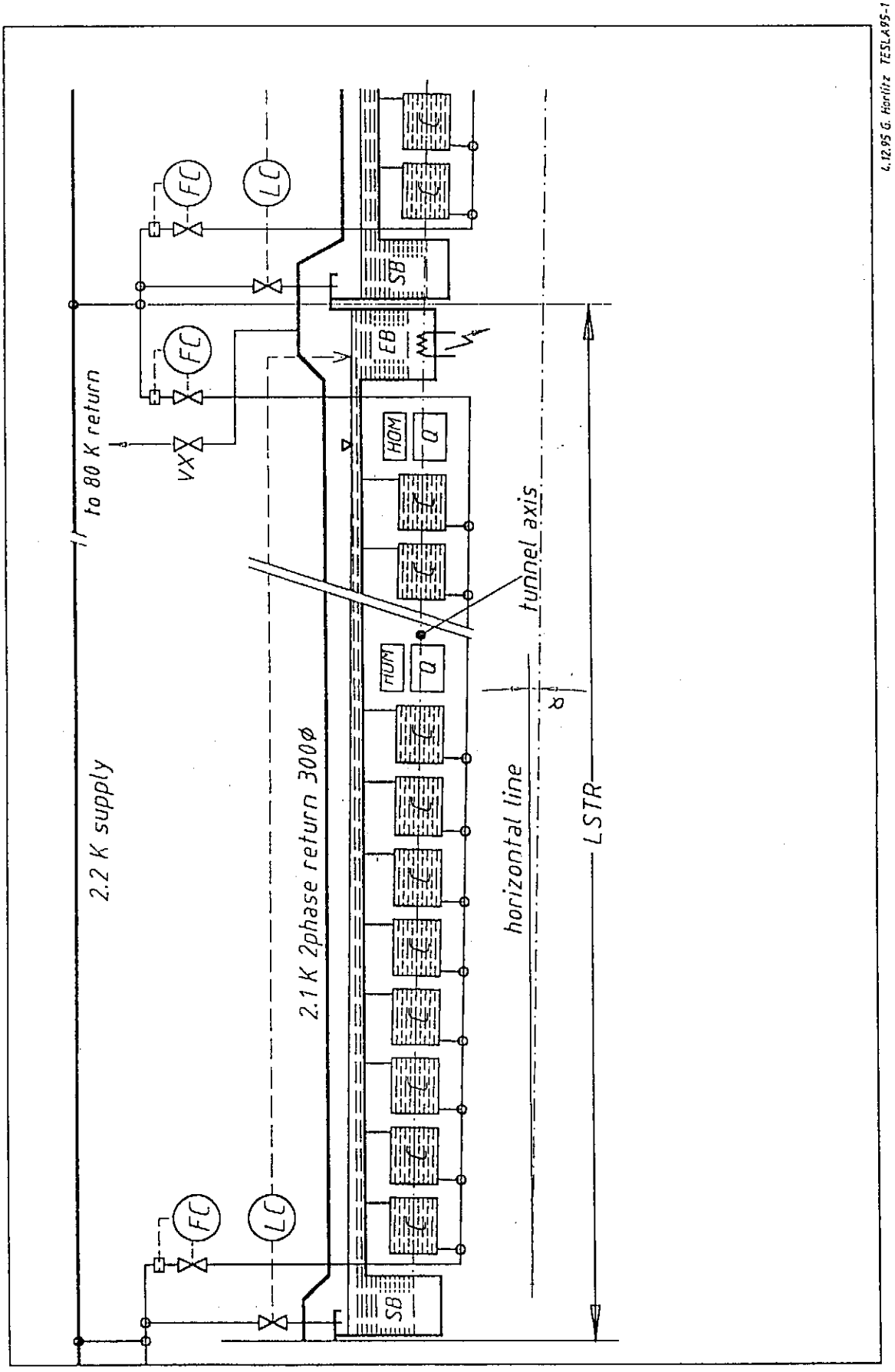

Fig. 13 Adaption to nonhorizontal Geometry II

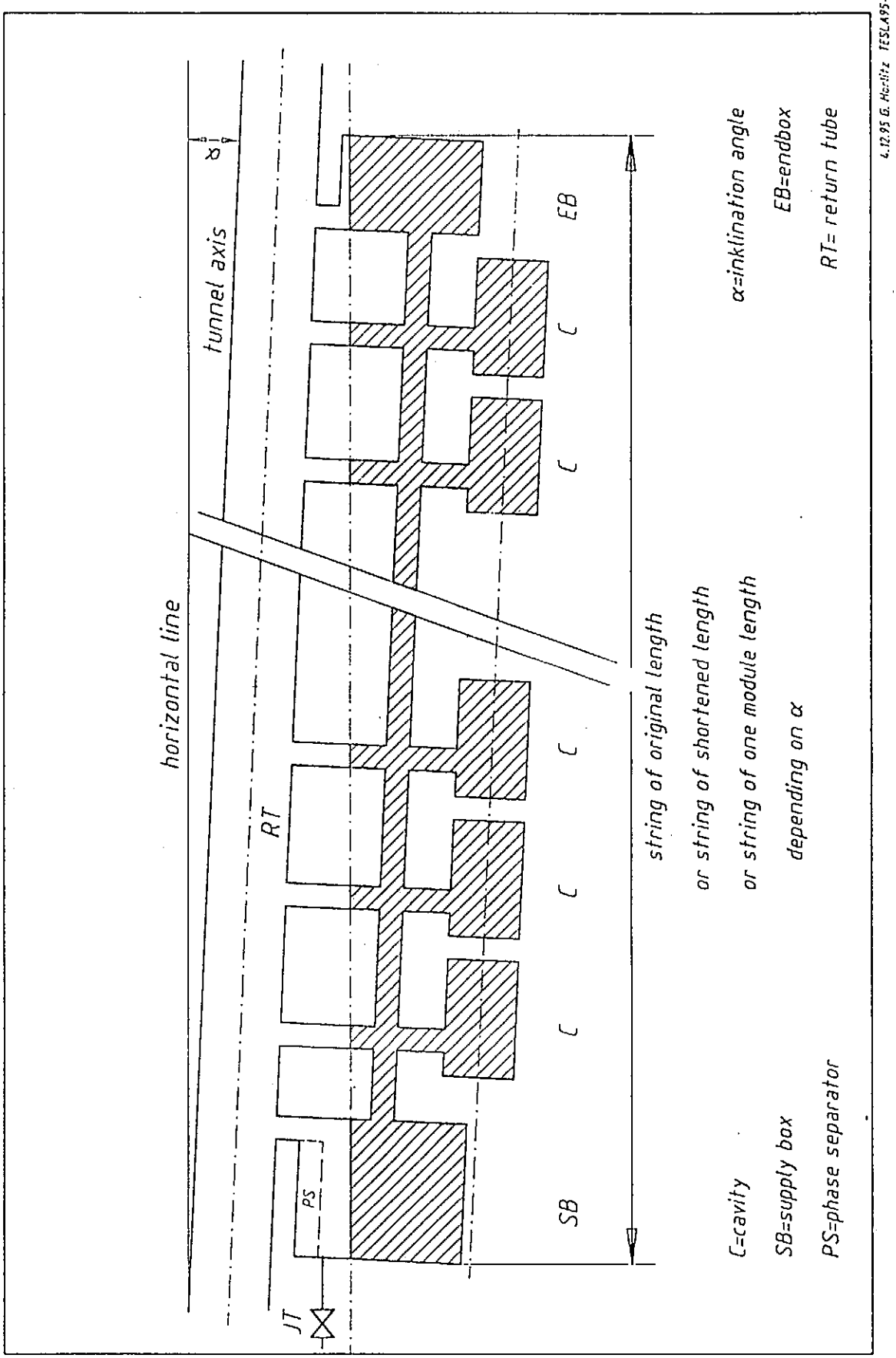

Fig. 14 Adaption to nonhorizontal Geometry III

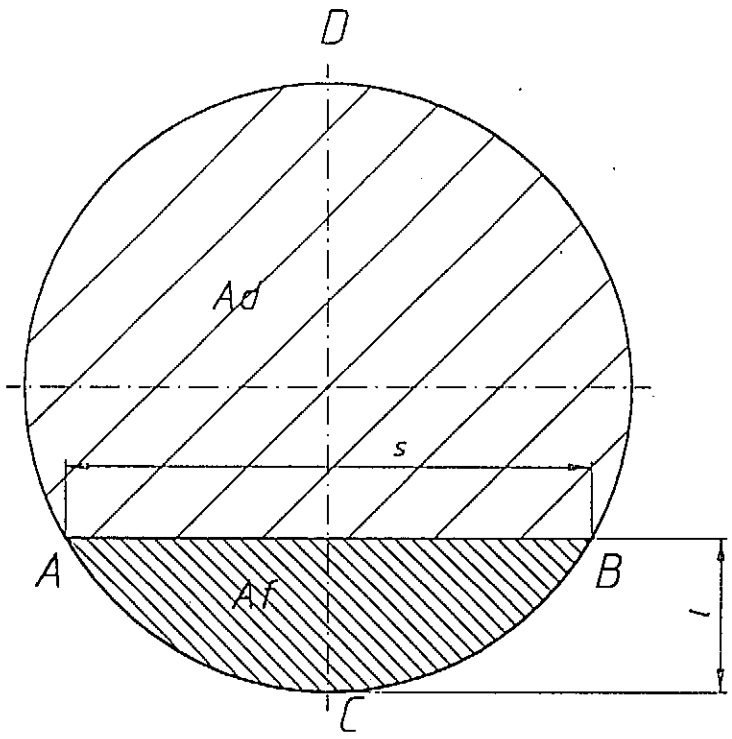

Fig. 15 Liquid/Vapor Areas in the Return Tube

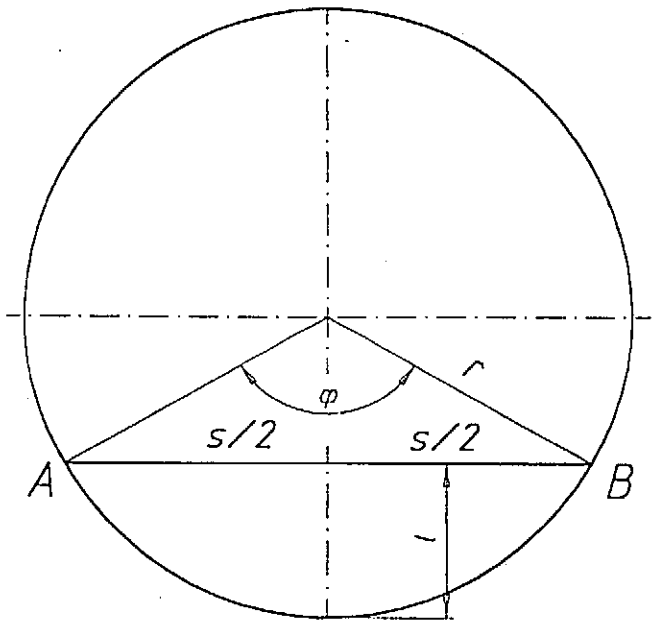

4.12.95 G. Horlitz TESLA9

Fig. 16 Flow Areas and Circumferences in the Return Tube

Dia.1

DIA1.XLS
G.HORLITZ
30.11.1995

FLOW DATA IN THE SUPPLY TUBE OF A 1830 m TESLA SUBUNIT

heat loads: 'a' 32.1 (design); 'b' 21.4 (nominal); 'c' 2.8 (static) W/module

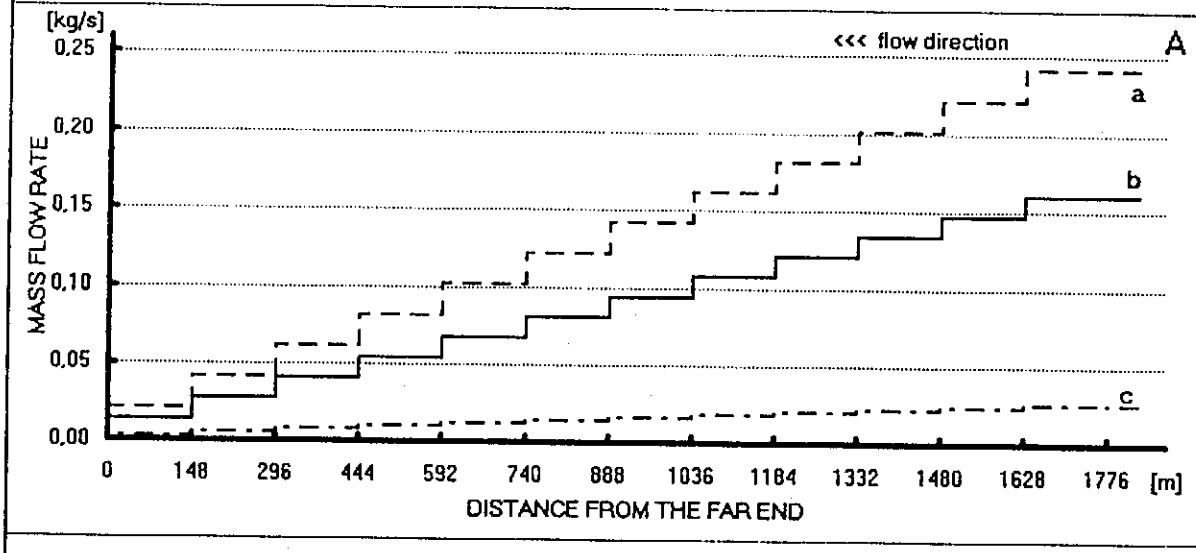

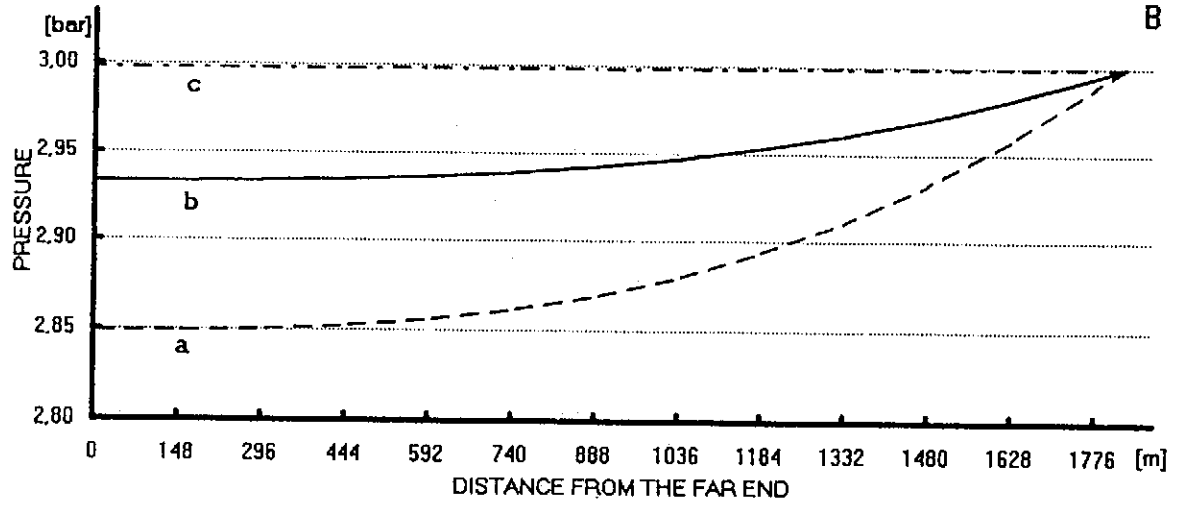

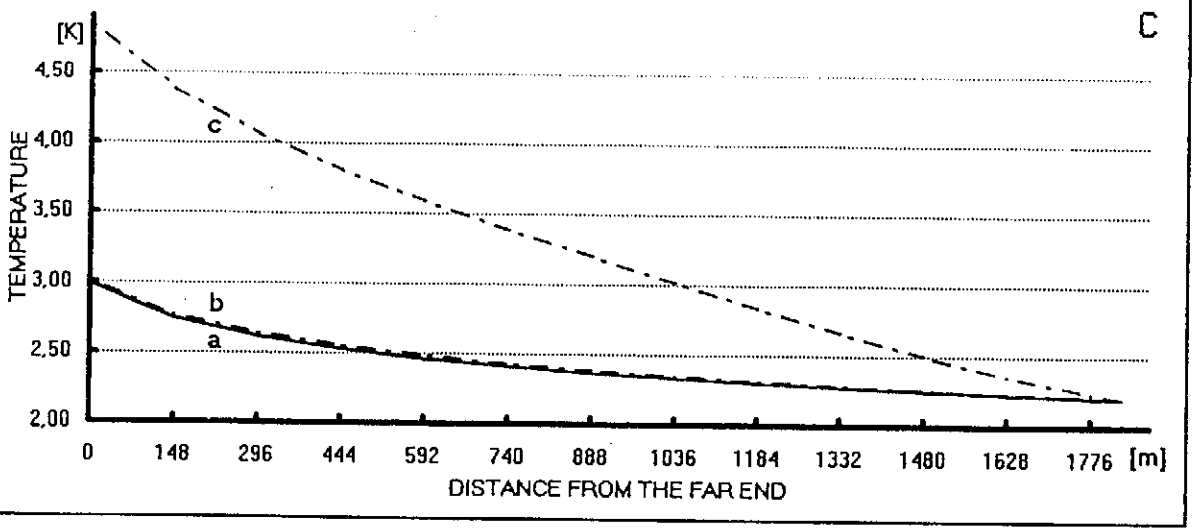

Dia. 2

DIA2.XLS
G.HORLITZ
30.11.1995

PRESSURES AND TEMPERATURES IN THE RETURN TUBE OF A 1830 m TESLA SUBUNIT

heat loads: 'a' 32.1 (design): 'b' 21.4 (nominal): 'c' 2.8 (static) W/module

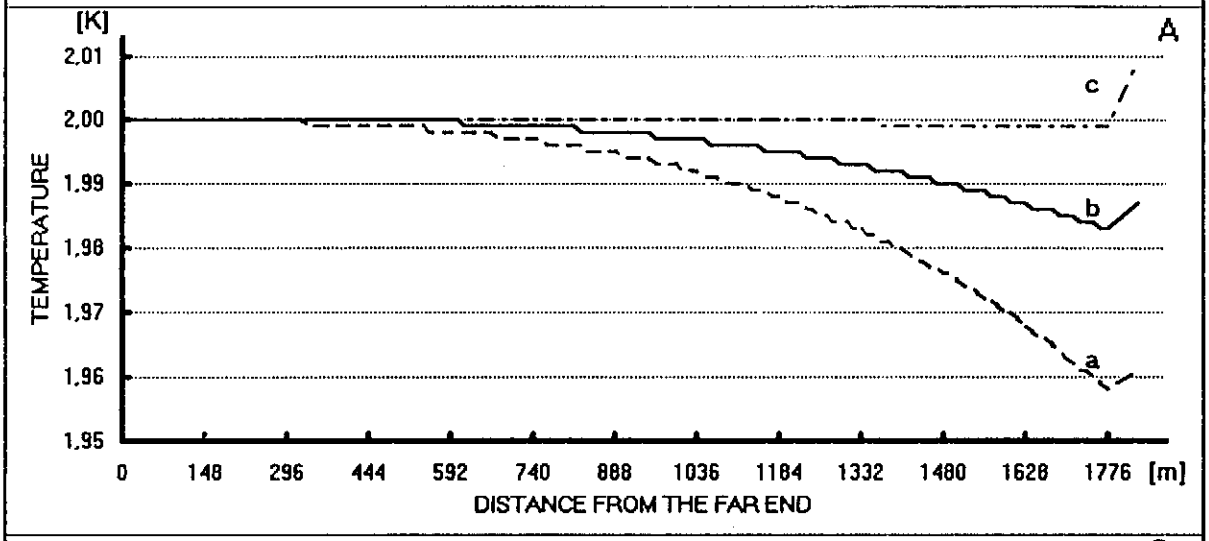

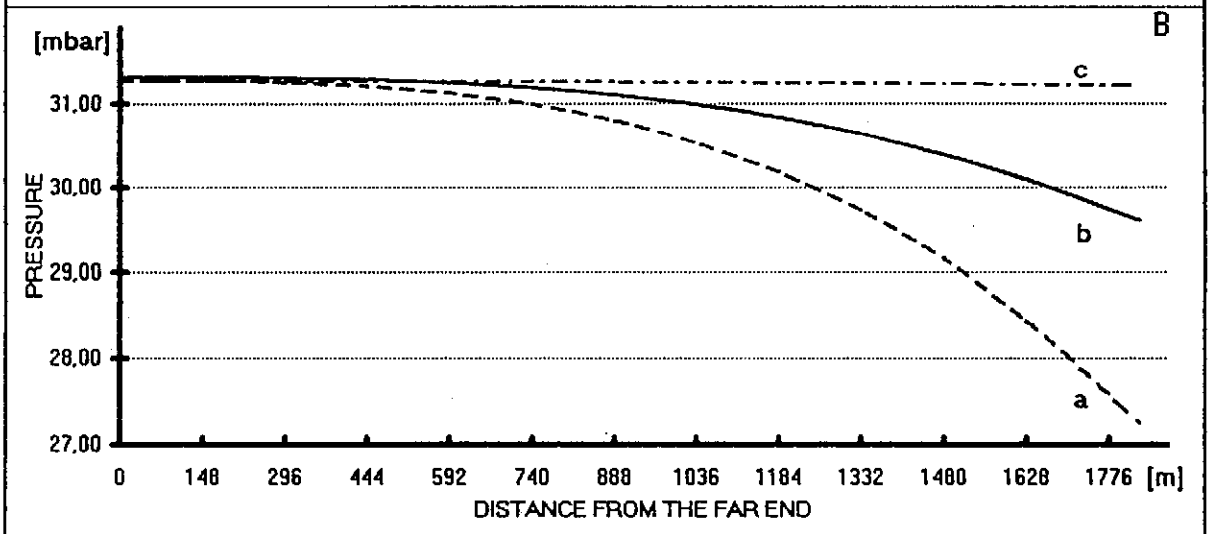

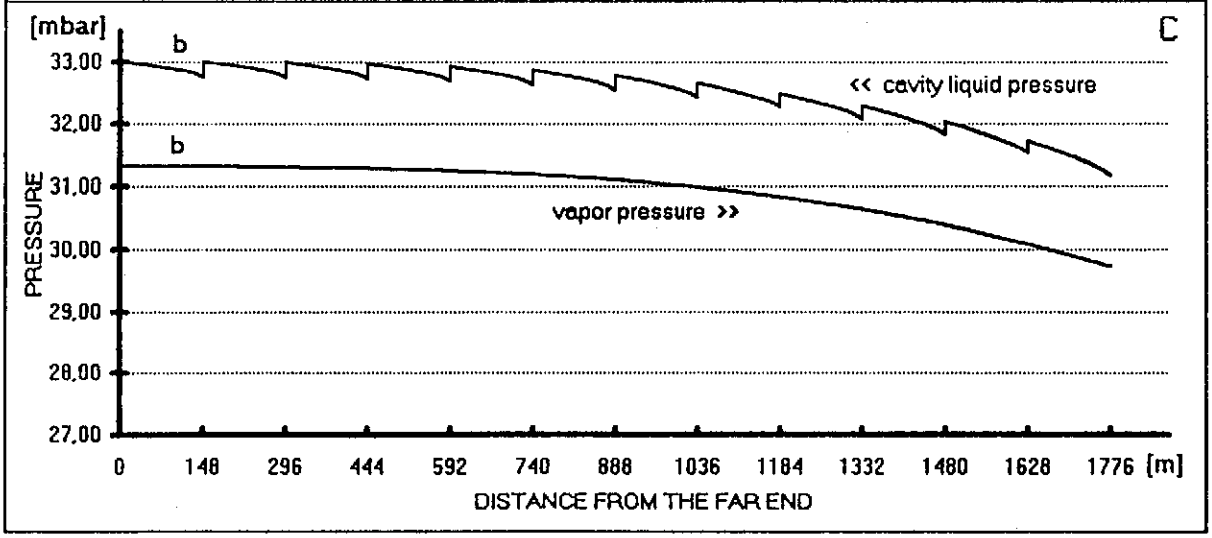

Dia. 3

DIA3XLS
G.HORLITZ
30.11.1995

LIQUID LEVELS IN THE RETURN TUBE OF A 1830 m TESLA SUBUNIT

heat loads: 'a' 32.1 (design); 'b' 21.4 (nominal); 'c' 2.8 (static) W/module

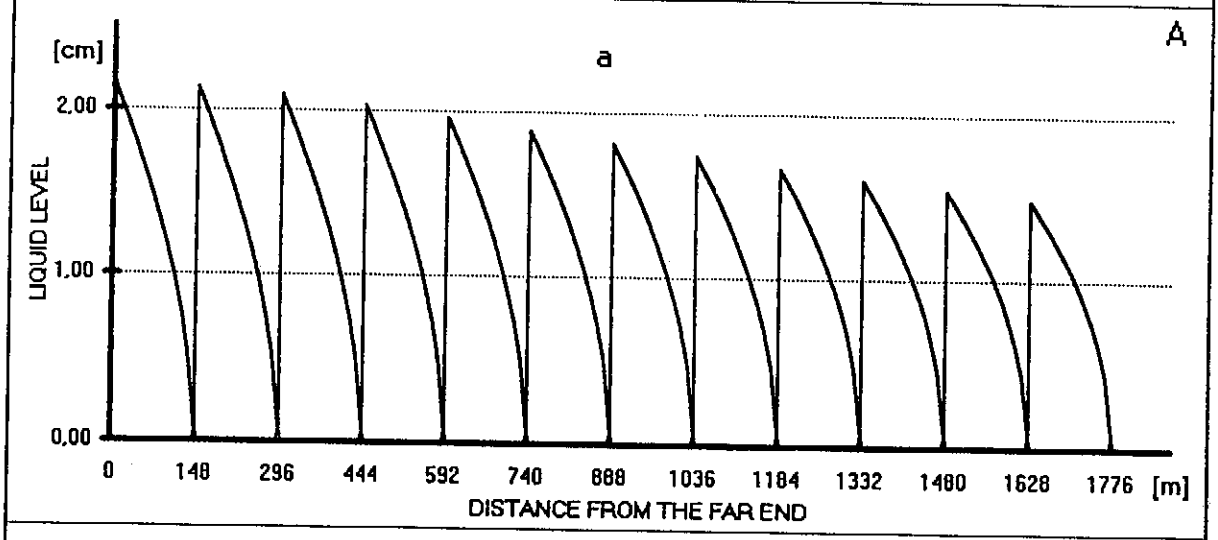

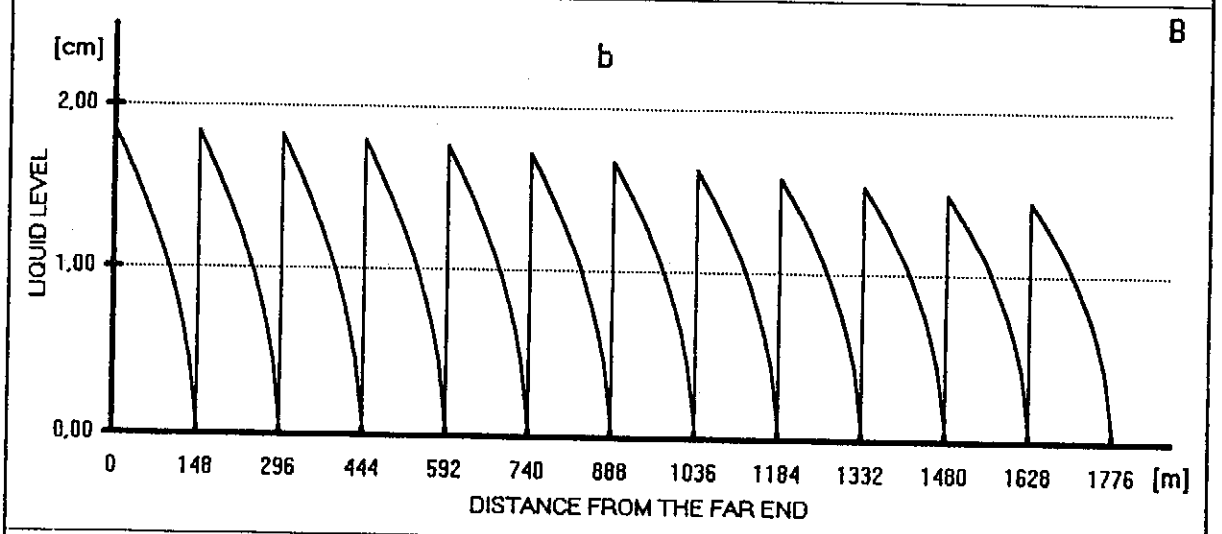

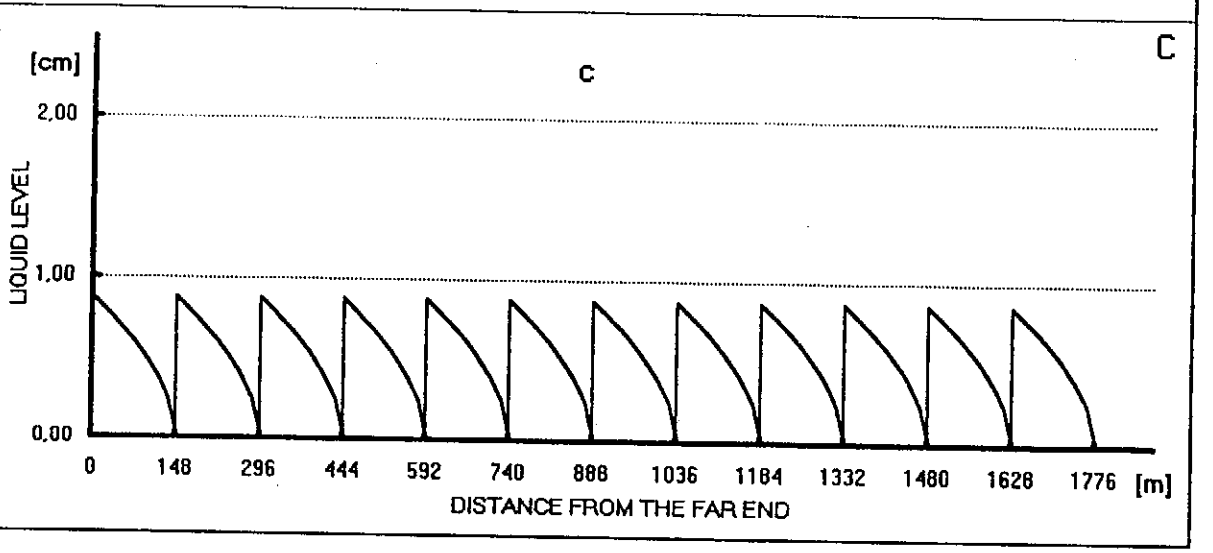

Dia. 4

DIA4.XLS
G.HORLITZ
30.11.1995

VAPOR FLOW DATA IN THE RETURN TUBE OF A 1830 m TESLA SUBUNIT

heat loads: 'a' 32.1 (design); 'b' 21.4 (nominal); 'c' 2.8 (static) W/module

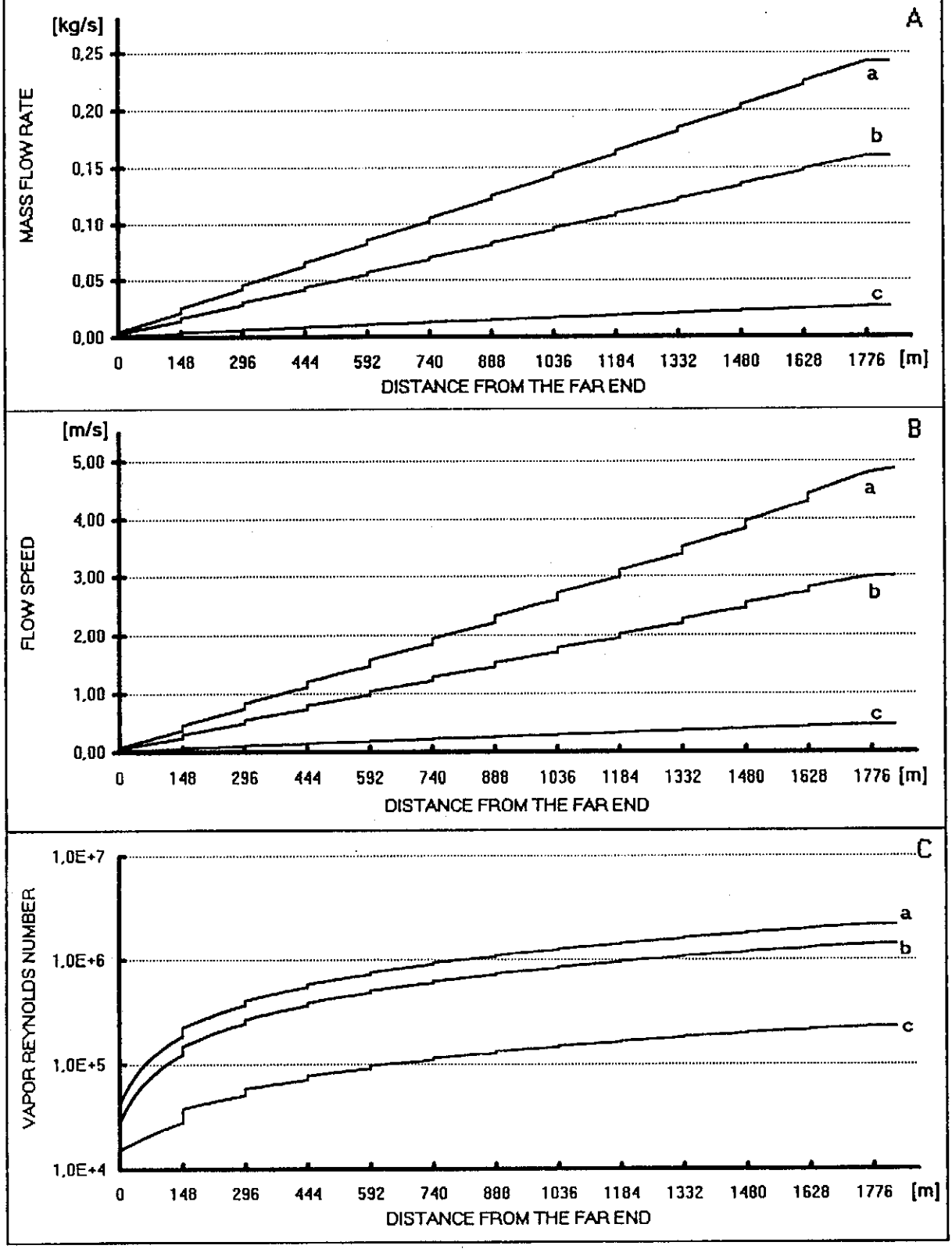

Dia. 5

DIAS.XLS
G.HORLITZ
30.11.1995

LIQUID FLOW DATA IN THE RETURN TUBE OF A 1830 m TESLA SUBUNIT

heat loads: 'a' 32.1 (design); 'b' 21.4 (nominal); 'c' 2.8 (static) W/module

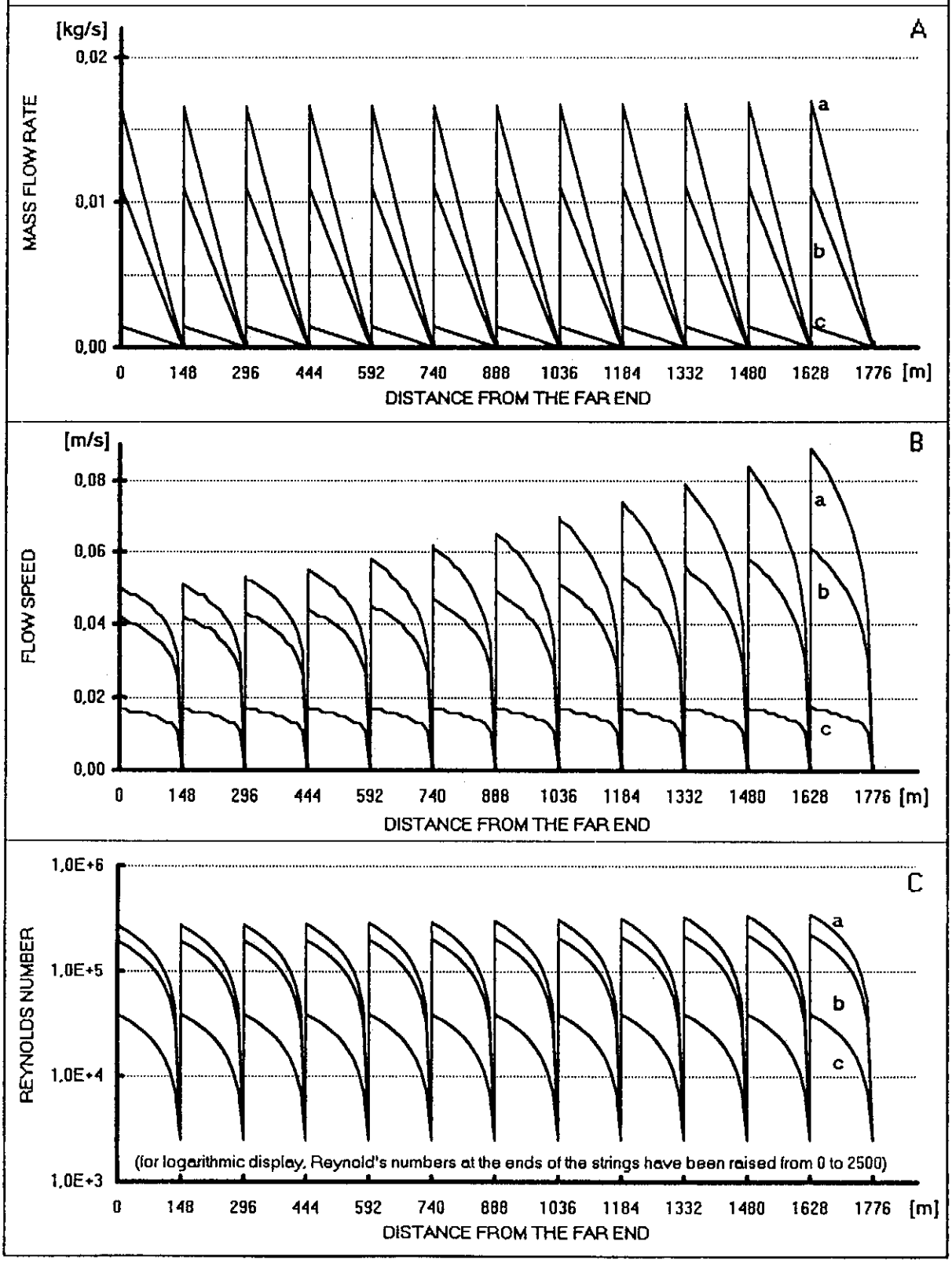

Dia. 6

DIA6.XLS
G.HORLITZ
30.11.1995

LIQUID LEVELS AND PRESSURE GRADIENTS IN THE RETURN TUBE OF A 1830 m TESLA SUBUNIT

heat load: 21.4 W/module

end levels : 'I': 0.0 cm; 'II': 3.0 cm; 'III' : 5.0 cm

pressure gradients : 'a' in the vapor; 'b' in the liquid

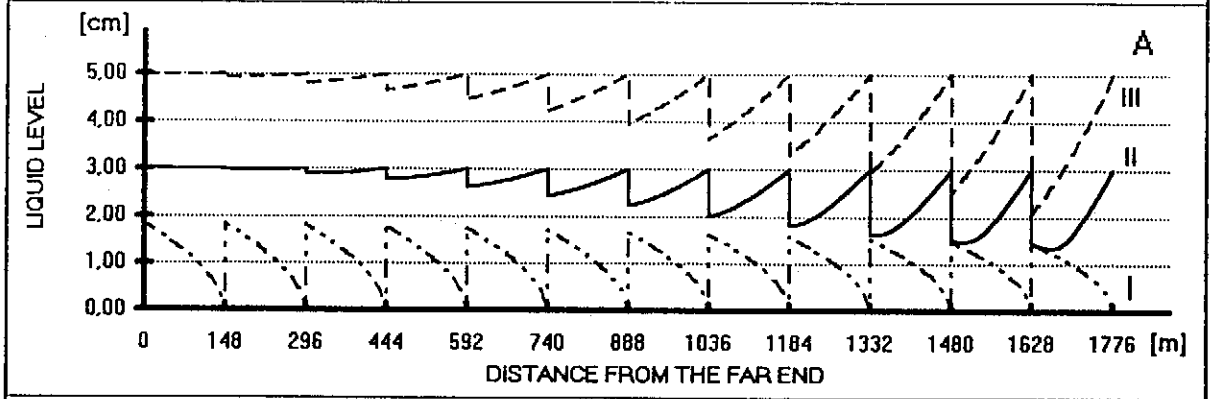

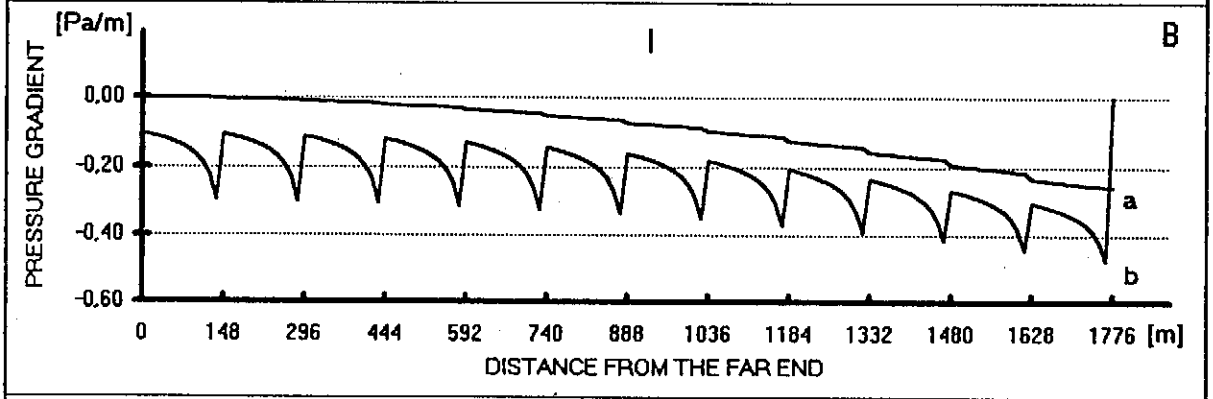

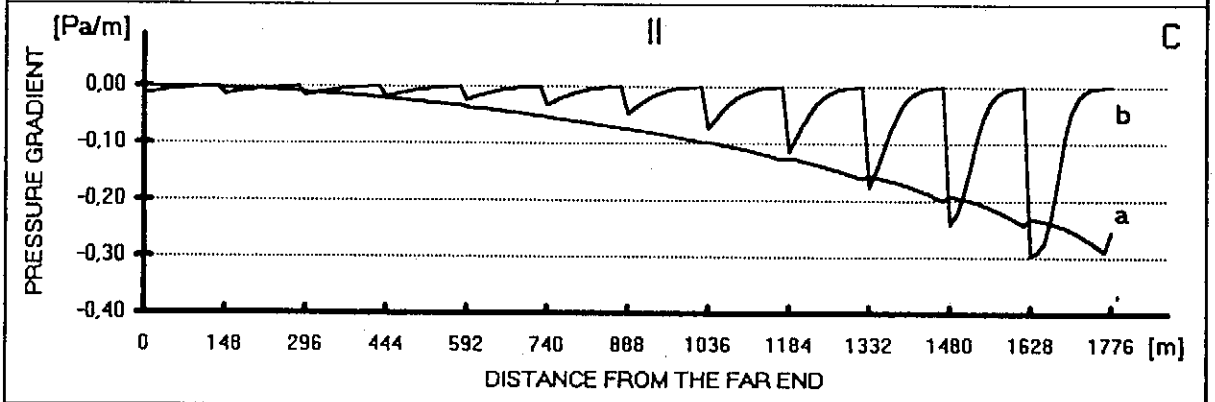

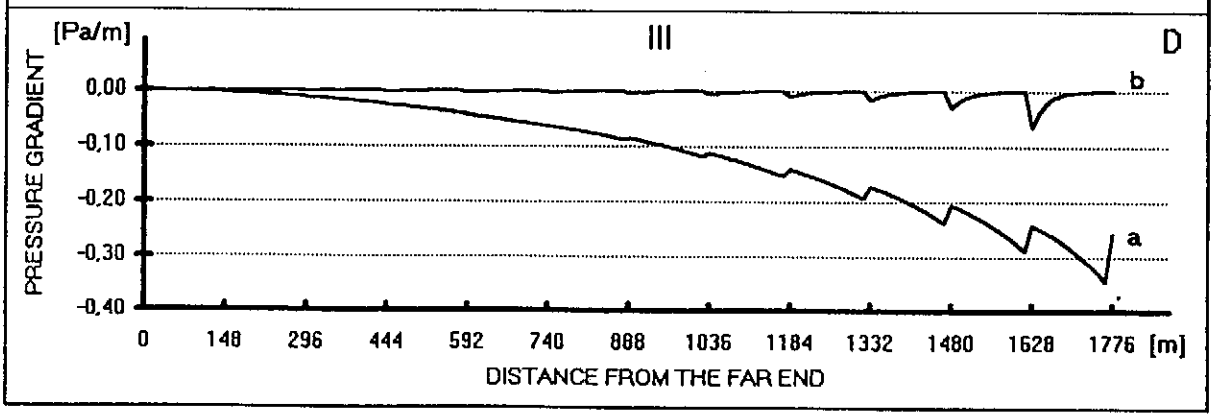

Dia. 7

DIA7.XLS
G.HORLITZ
30.11.1995

LIQUID LEVELS AND PRESSURE GRADIENTS IN THE RETURN TUBE OF A 1830 m TESLA SUBUNIT

heat load: 32.1 W/module

end levels : 'I': 0.0 cm; 'II': 3.0 cm; 'III' : 5.0 cm

pressure gradients : 'a' in the vapor; 'b' in the liquid

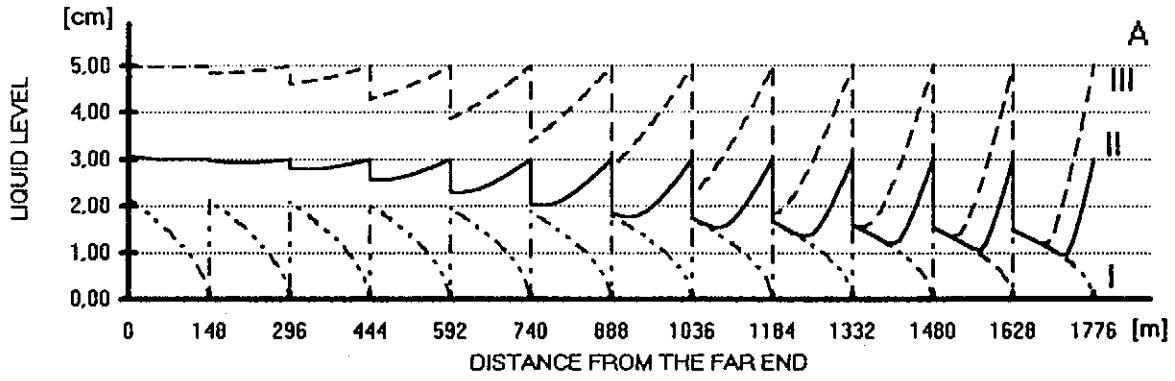

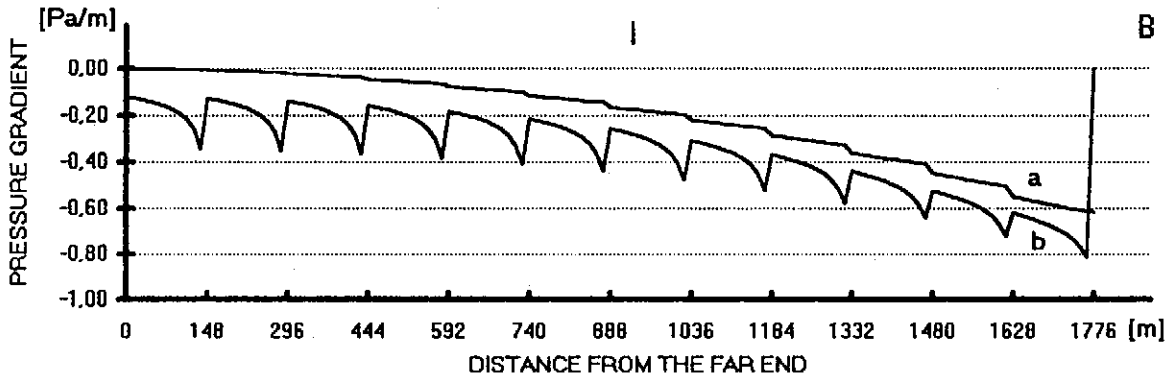

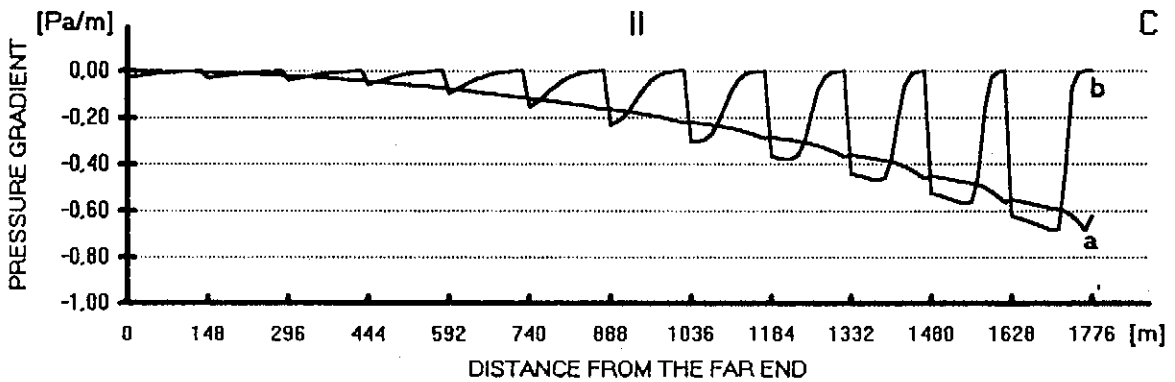

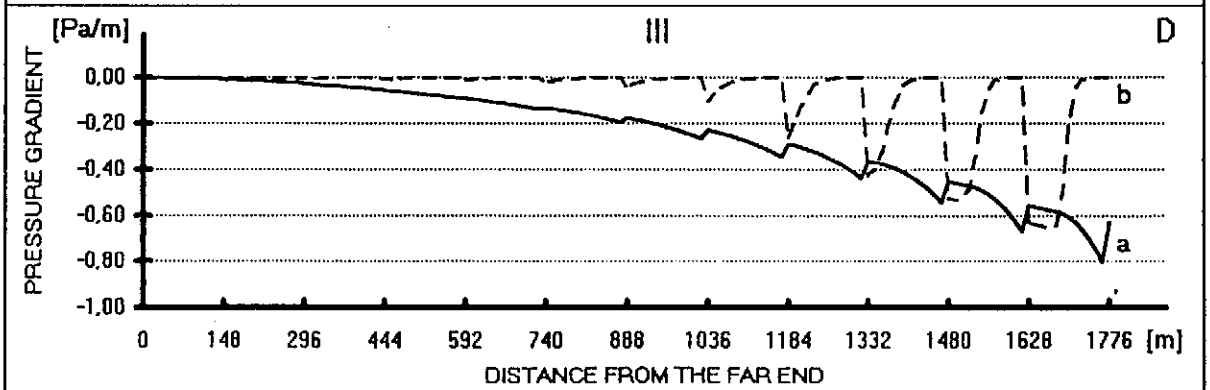

Dia. 8

DIA8.XLS
G.HOPLITZ
30.11.1995

LONGITUDINAL LIQUID HEAT FLOW IN THE RETURN TUBE OF A 1830 m TESLA SUBUNIT

heat loads: 'a': 32.1 (design); 'b' : 21.4 (nominal) W/module

end levels : 'A' : 0.0 cm 'B' : 3.0 cm 'c' : 5.0 cm

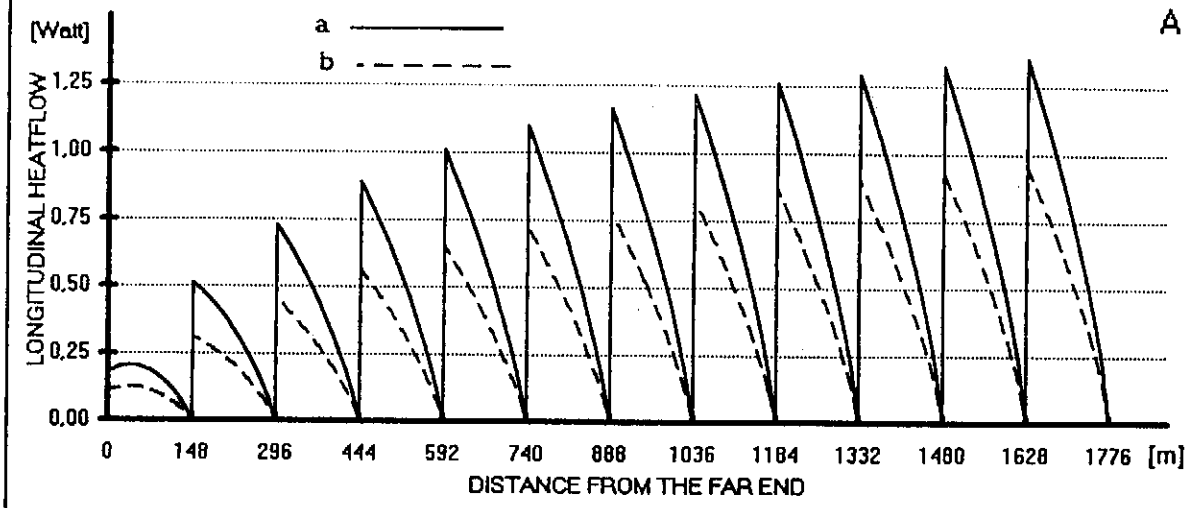

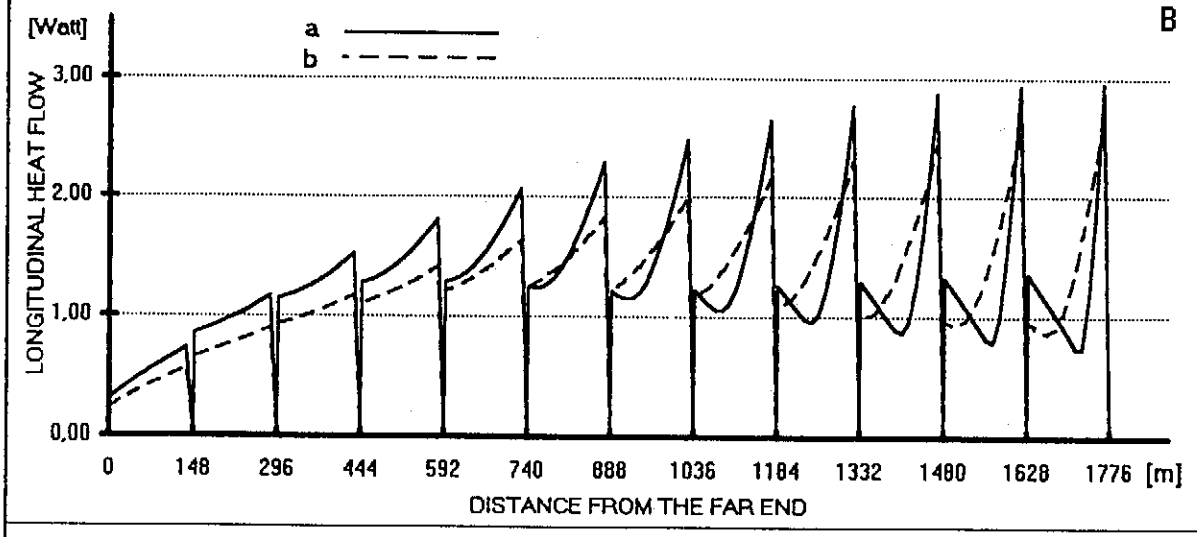

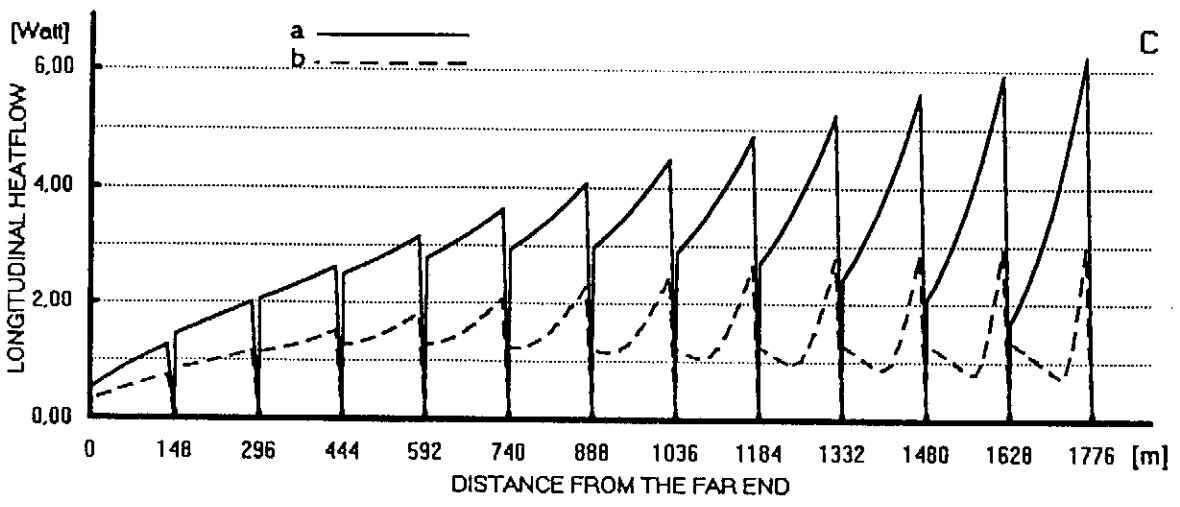

Dia. 9

DIA9.XLS
G.HORLITZ
30.11.1995

INFLUENCE OF HF- POWER FAILURES ON PRESSURE AND LIQUID LEVEL IN THE RETURN TUBE OF A 1830 m TESLA SUBUNIT

heat loads: 32.1 W/module (design)

'a' all modules normally powered

'b' HF-power off in string No 6, modules No. 5 to 8

'c' heat load reduction compensated by endbox heater

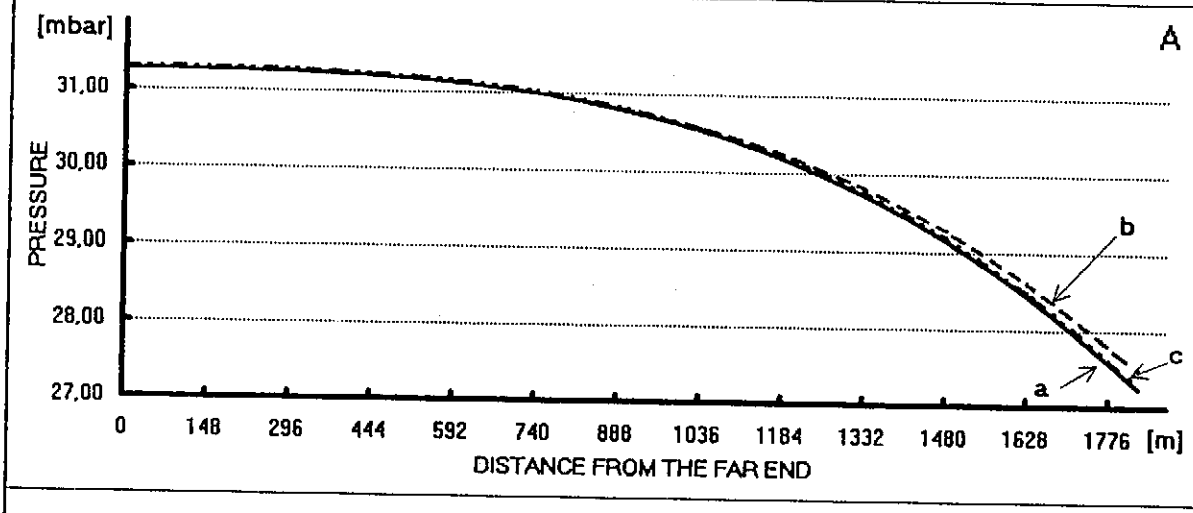

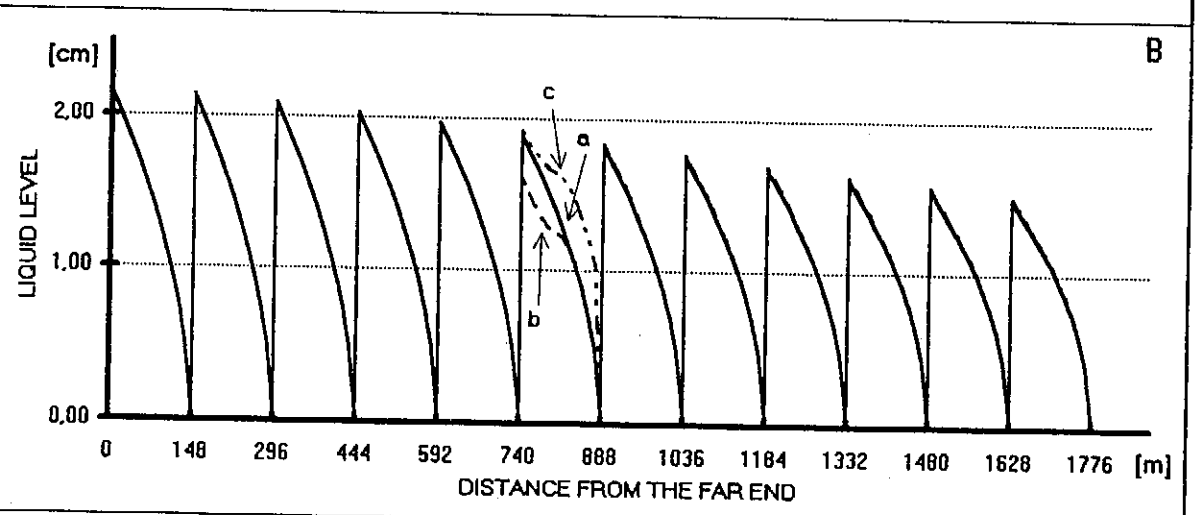

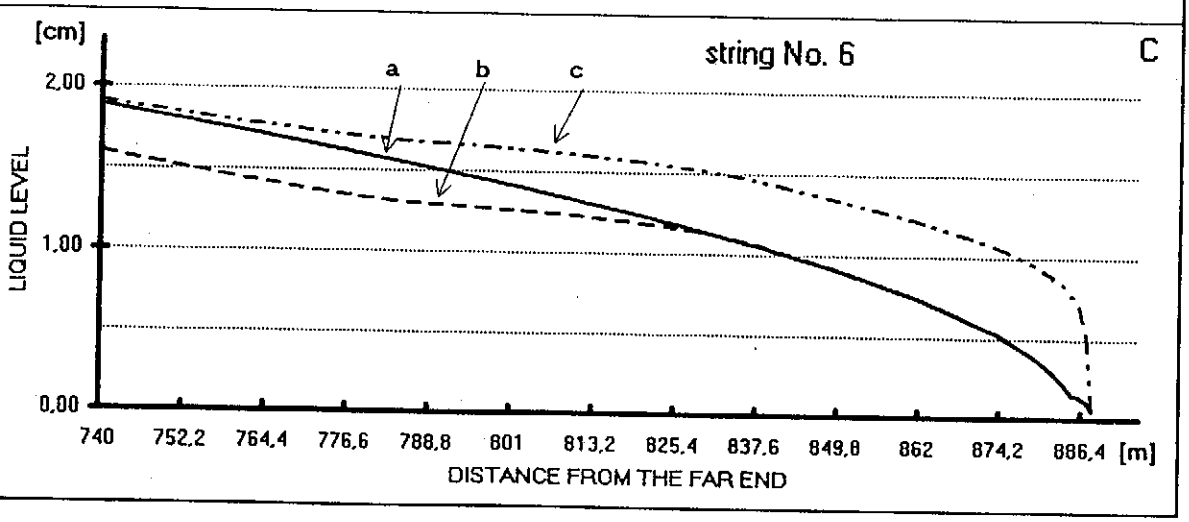

Dia. 10

CHANGE OF LIQUID LEVEL WITH TIME AFTER HF-POWER FAILURE

DIA10XLS
G.HORLITZ
30.11.1995

heat loads: 32.1 W/module (design)

a: all modules normally powered

other curves: HF-power off in string No 6, modules No. 5 to 8 at different times with unchanged flow rate as in 'a'

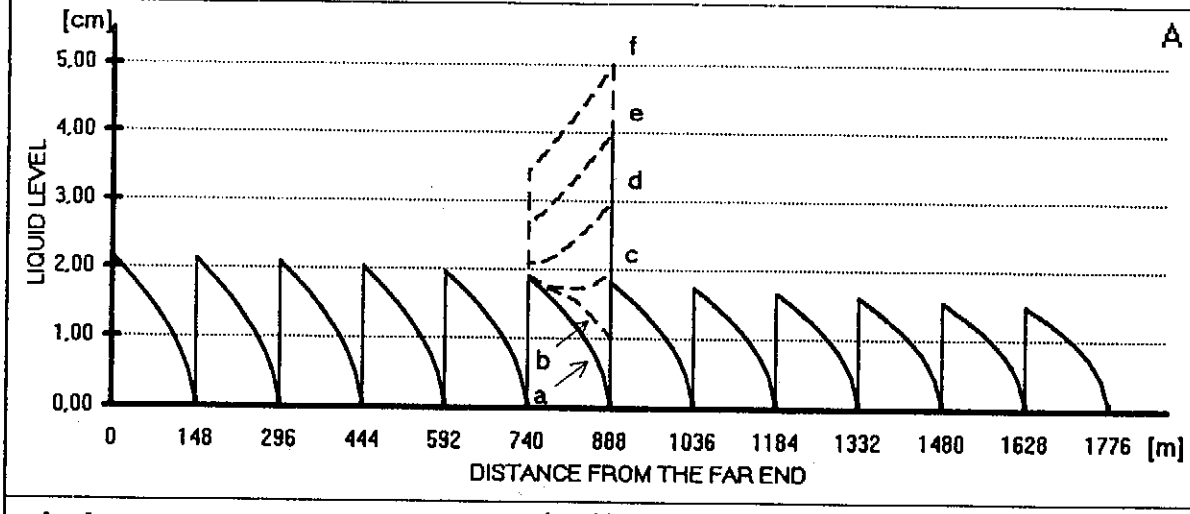

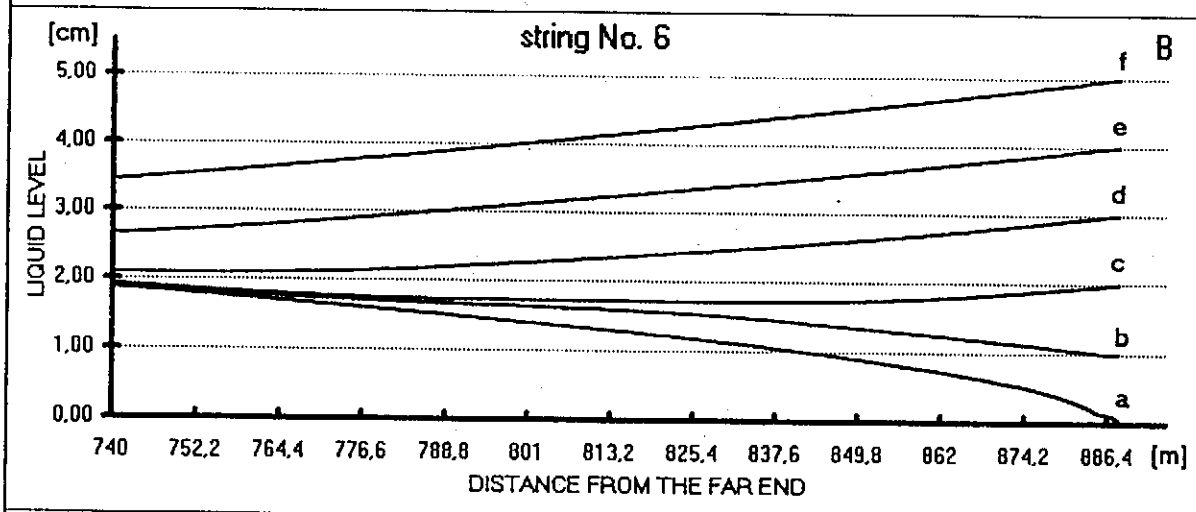

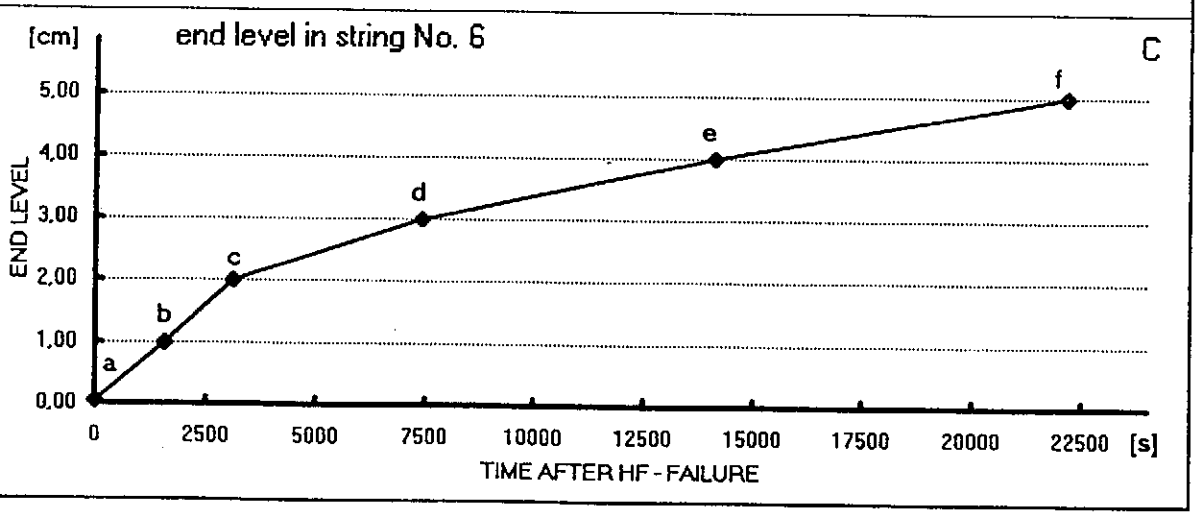

Dia. 11

DIA11XLS
G.HORLITZ
30.11.1995

INFLUENCE OF HF- POWER FAILURES ON PRESSURE AND LIQUID LEVEL IN THE RETURN TUBE OF A 1830 m TESLA SUBUNIT

heat loads: 32.1 W/module (design)

'a' all modules normally powered

'b' HF-power off in string No 12, modules No. 5 to 8

'c' heat load reduction compensated by endbox heater

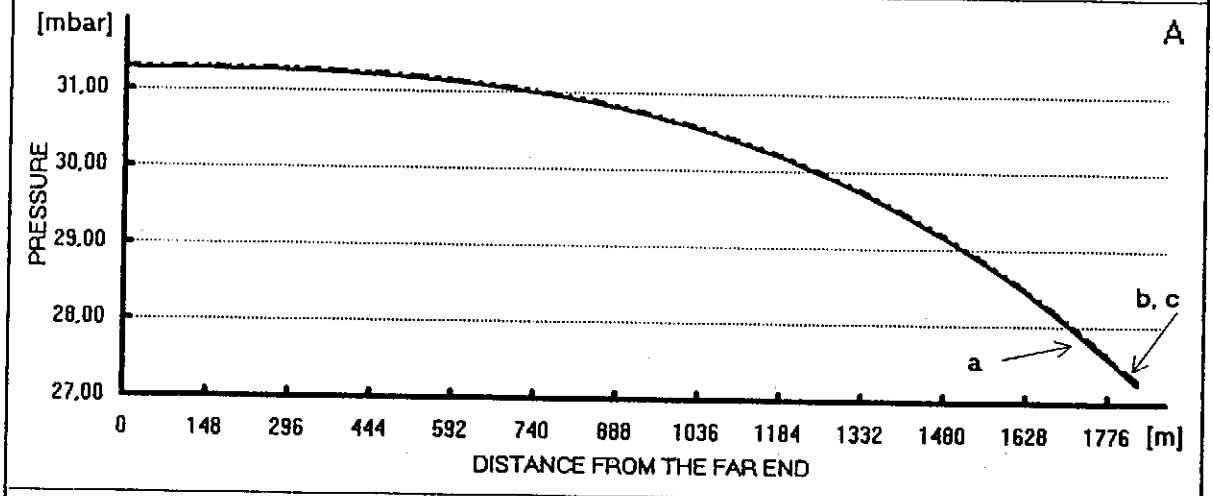

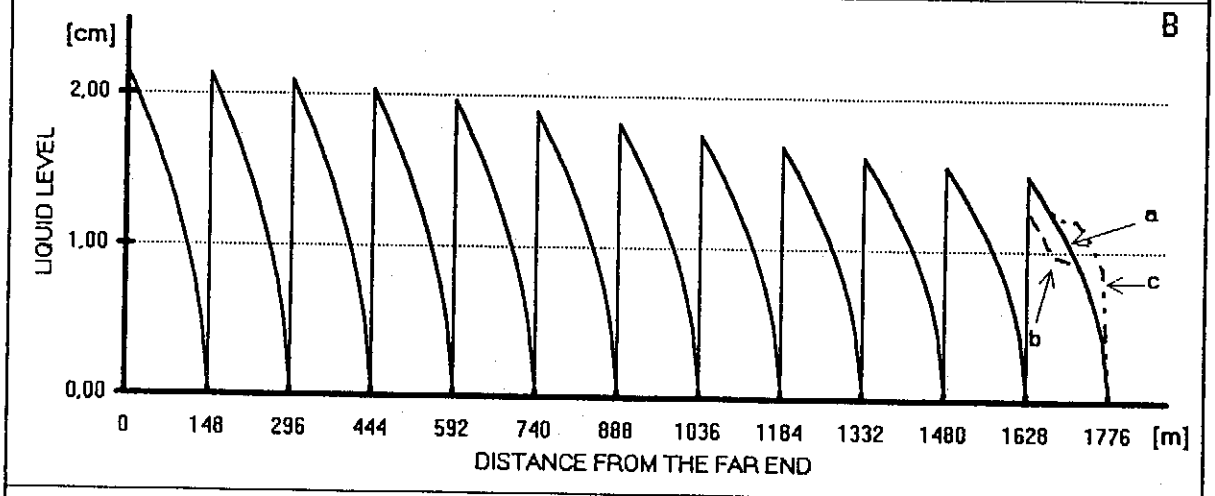

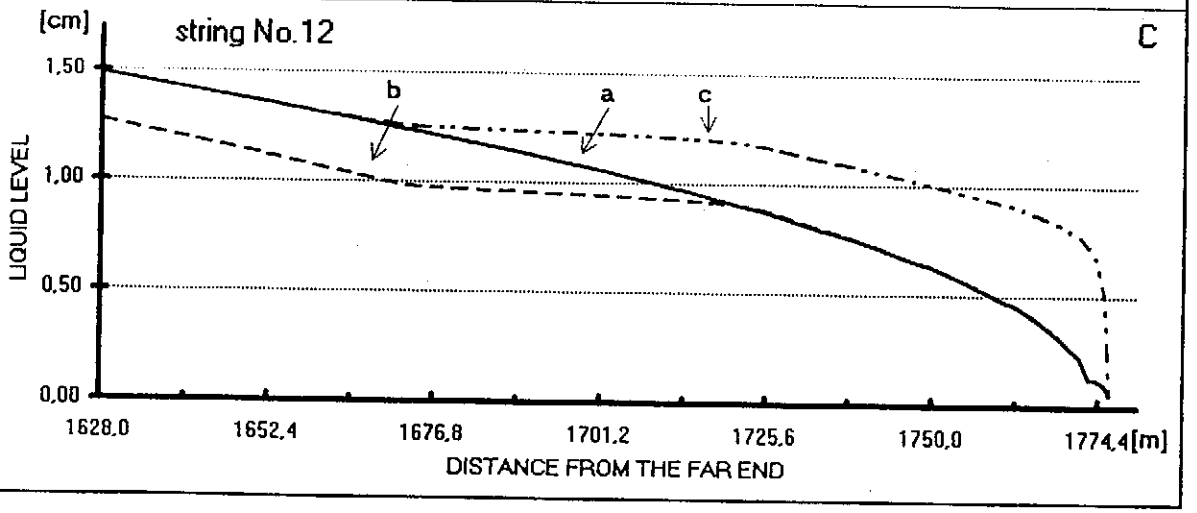

Dia. 12

DIA12XLS
G.HORLITZ
30.11.1995

CHANGE OF LIQUID LEVEL WITH TIME AFTER HF-POWER FAILURE

heat loads: 32.1 W/module (design)

a: all modules normally powered

other curves: HF-power off in string No 12, modules No. 5 to 8 at different times with unchanged flow rate as in 'a'

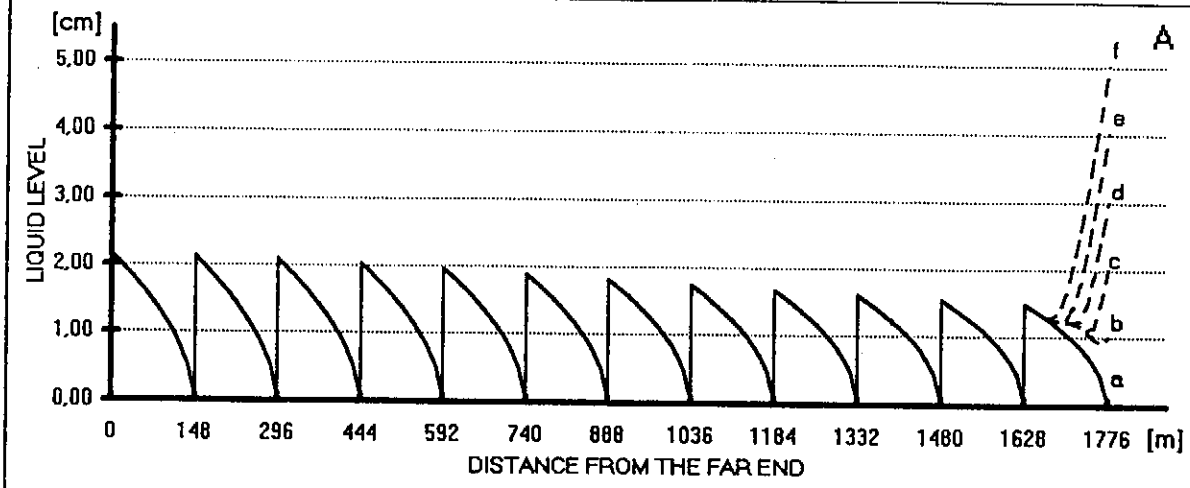

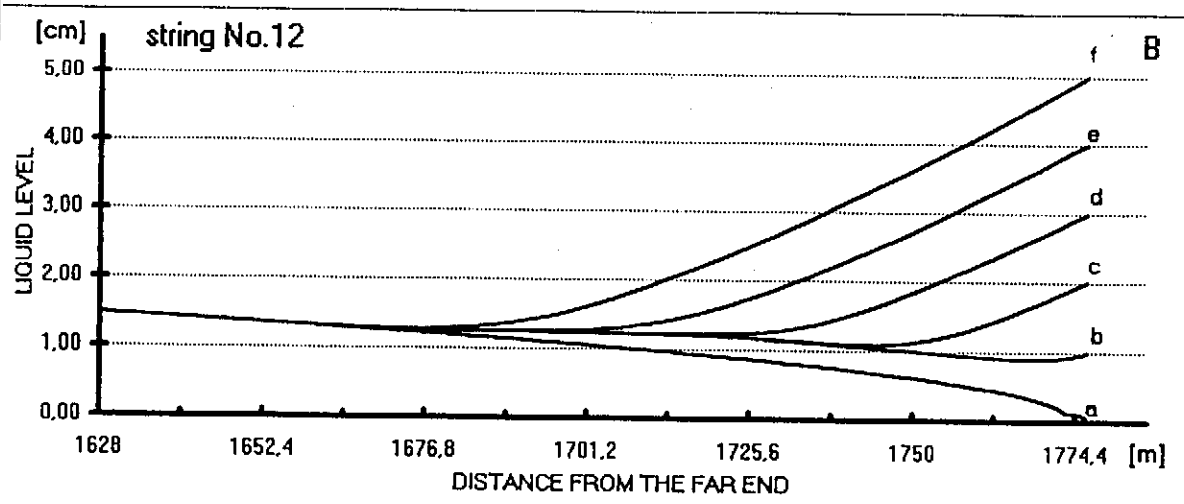

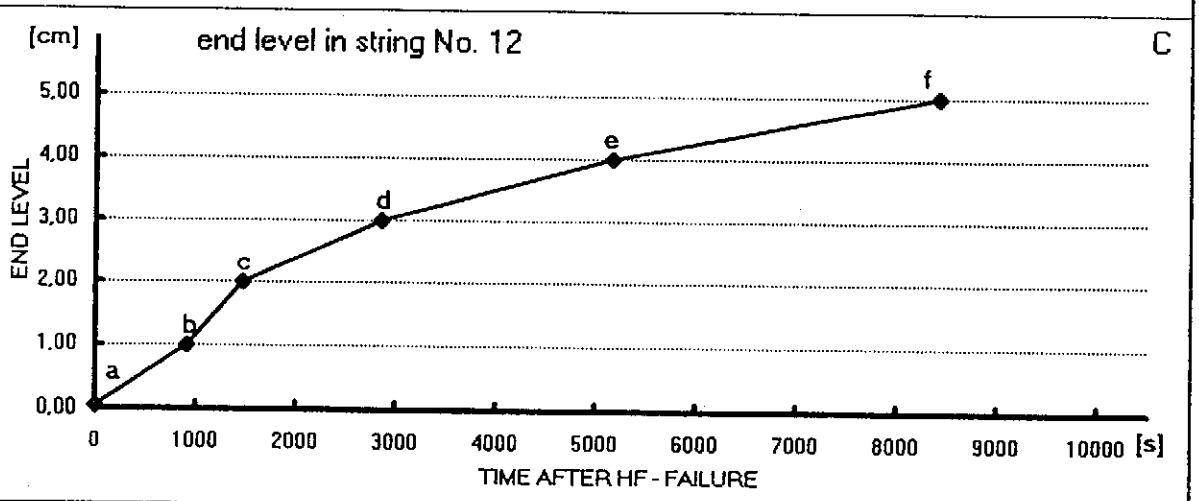

Dia.13

DIA13XLS
G.HORLITZ
30.11.1995

PRESSURES AND TEMPERATURES IN THE RETURN TUBE OF A 1830 m TESLA SUBUNIT FOR DIFFERENT OUTLET PRESSURES

heat load: 32.1 W/module (design)

outlet pressures : 'a' 5.92 'b' 10.00 'c' 12.80 'd' 15.82 [mbar]
'e' 20.00 'f' 25.00 'g' 27.25 [mbar]

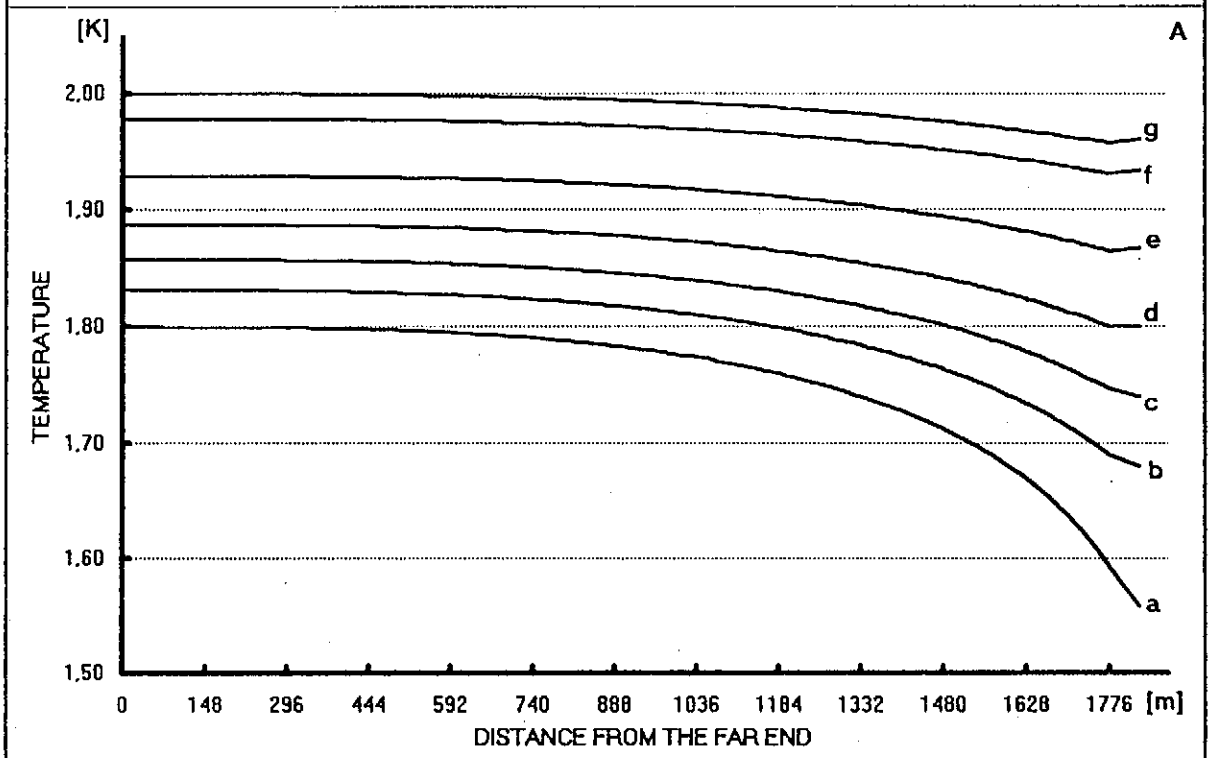

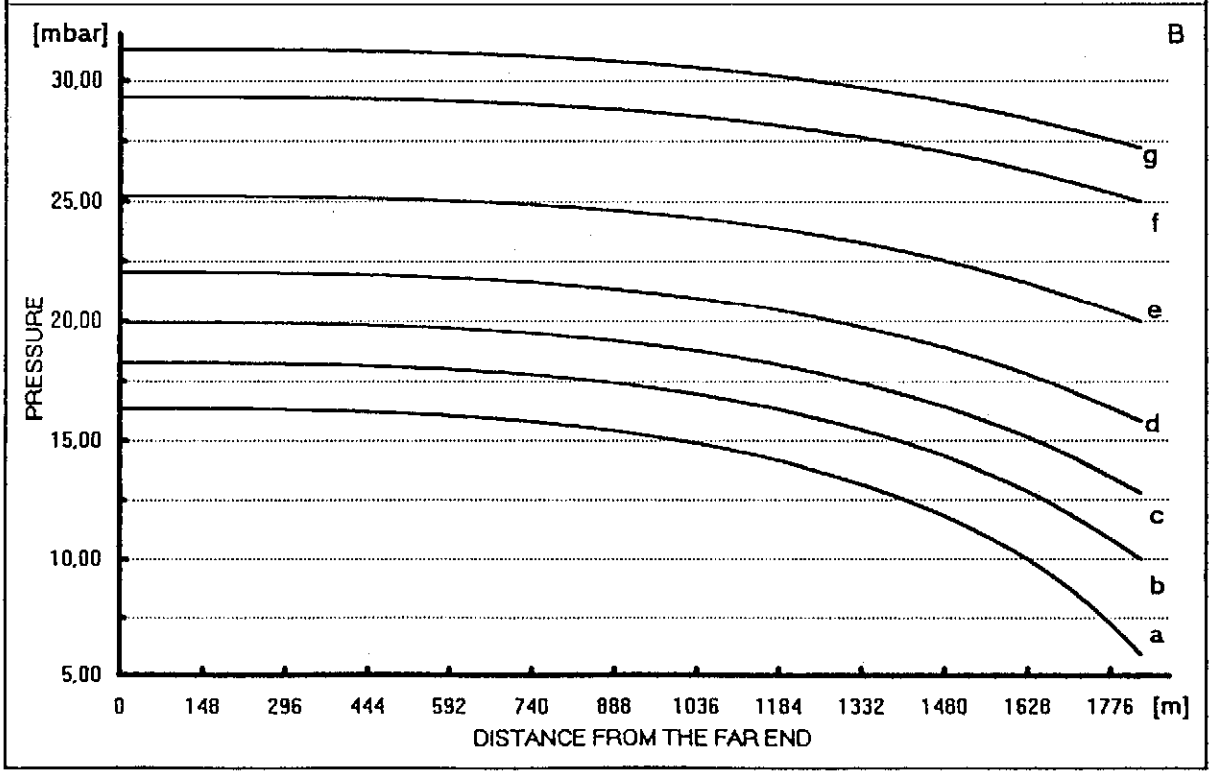

Dia.14

DIA14XLS
G.HORLITZ
30.11.1995

PRESSURES AND TEMPERATURES IN THE RETURN TUBE OF A 1830 m TESLA SUBUNIT FOR DIFFERENT OUTLET PRESSURES

heat load: 21.4 W/module (nominal)
outlet pressures : 'a' 12.81 'b' 16.11 'c' 20.00 [mbar]
'd' 25.00 'e' 27.25 'f' 29.60 [mbar]

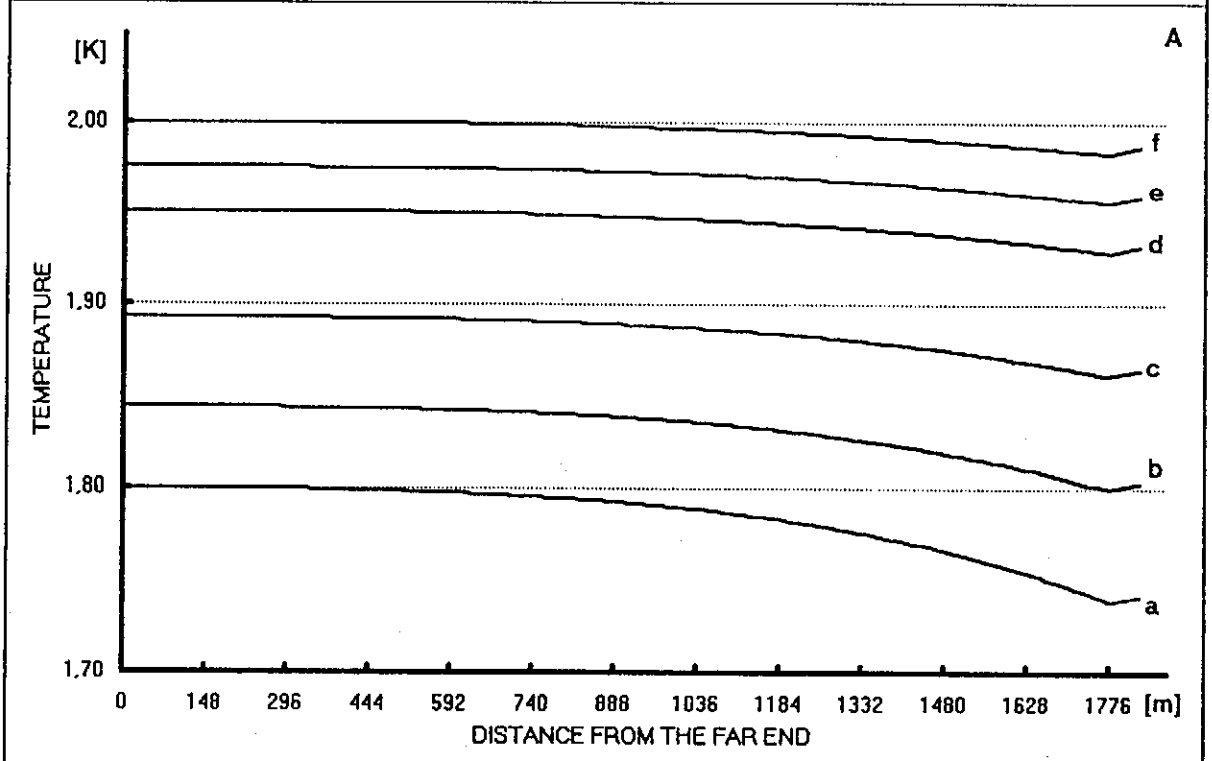

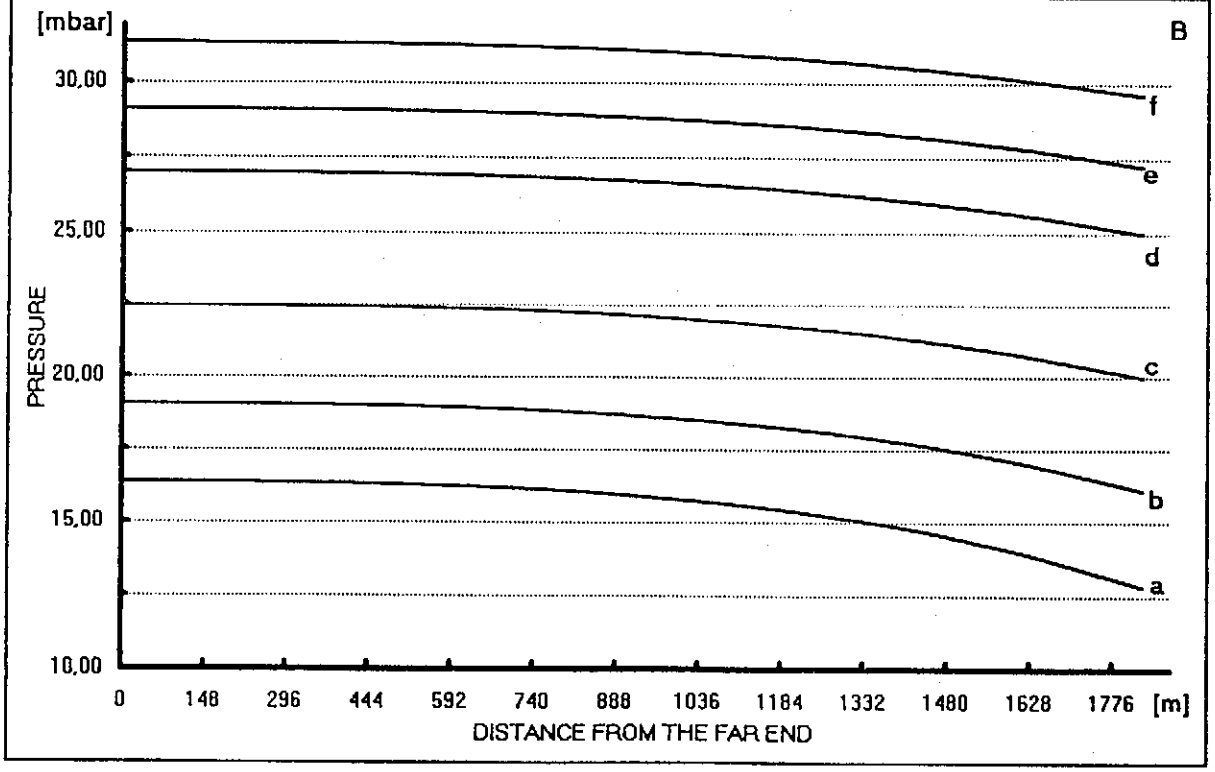

DIA. 15

DIA15.XLS
G.HORLITZ
30.11.1995

PRESSURE, TEMPERATURE, DENSITY AND FLOW SPEED AT THE END OF THE 0.3 m RETURN TUBE AS FUNCTION OF THE MAXIMUM CAVITY TEMPERATURE

heat loads : 'a' : 32.1 (design) ; 'b' : 21.4 (nominal) W/module

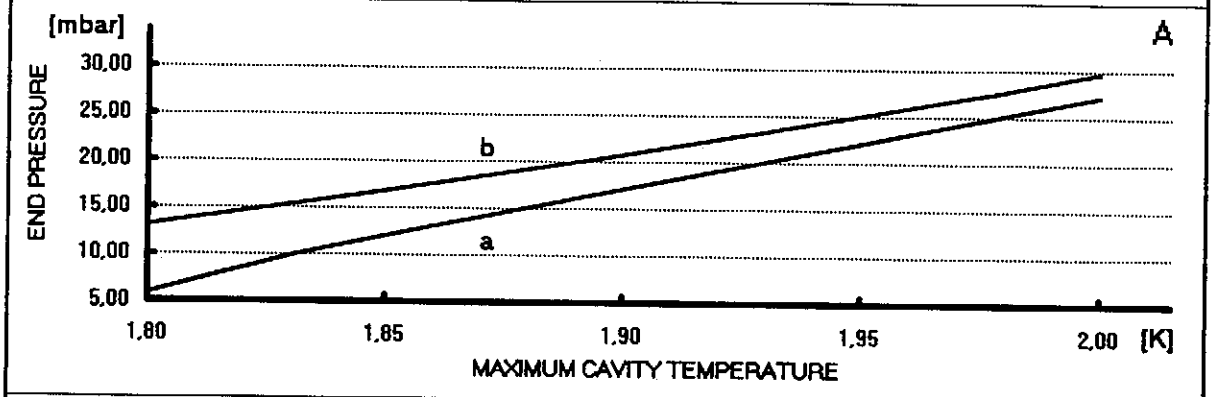

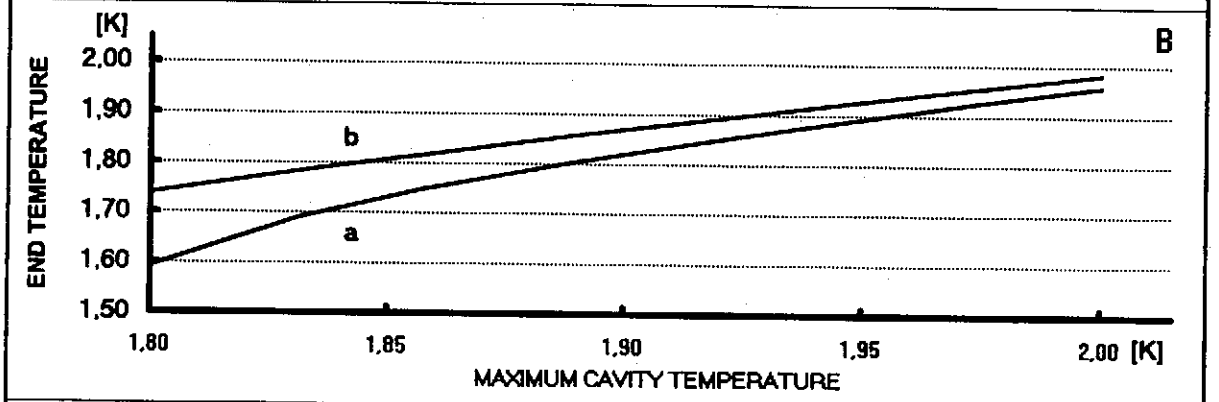

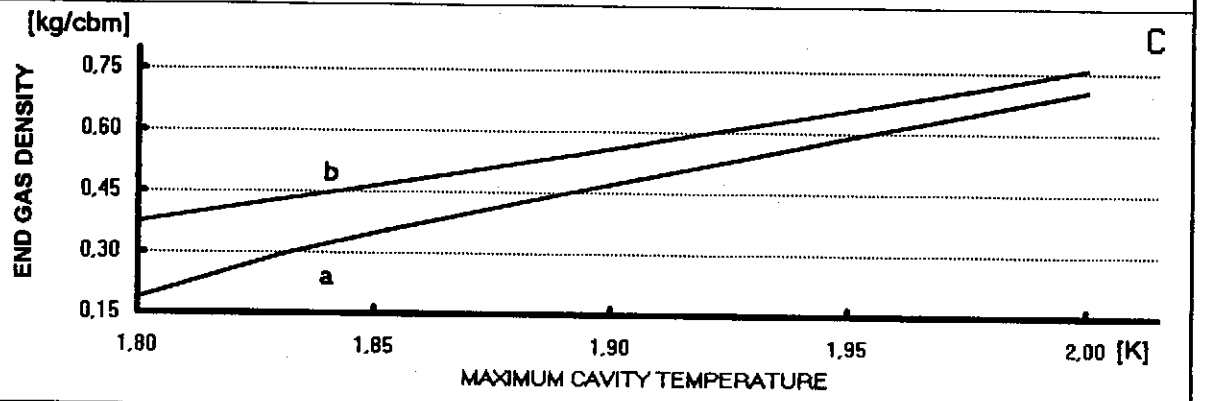

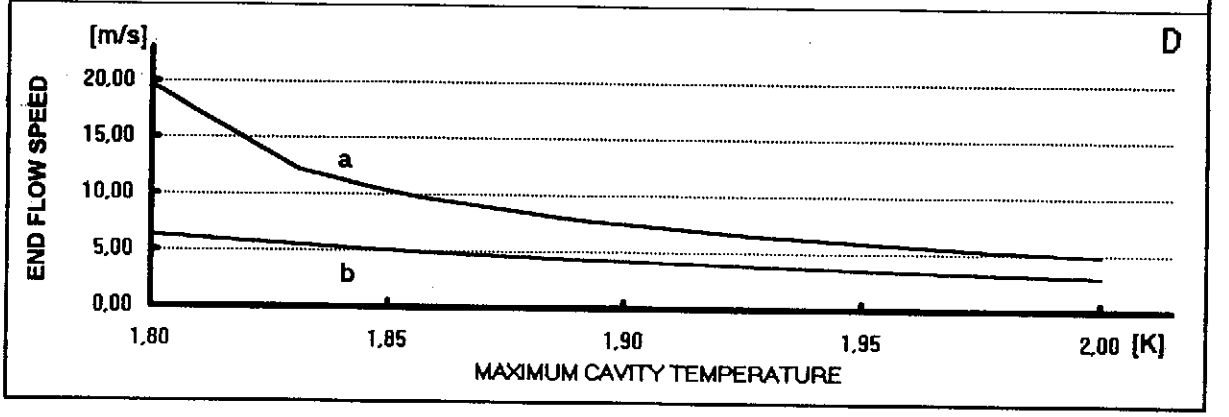

Dia. 16

PRESSURES AND TEMPERATURES FOR DIFFERENT SYSTEM LAYOUT CRITERIA

DIA16.XLS
G.HORLITZ
30.11.1995

criterion I : layout for maximum subunit temperature Tmax = 2.0 K
criterion II : layout for minimum subunit temperature Tmin = 1.8 K
heat loads: 'a' 32.1 (design); 'b' 21.4 (nominal) W/module

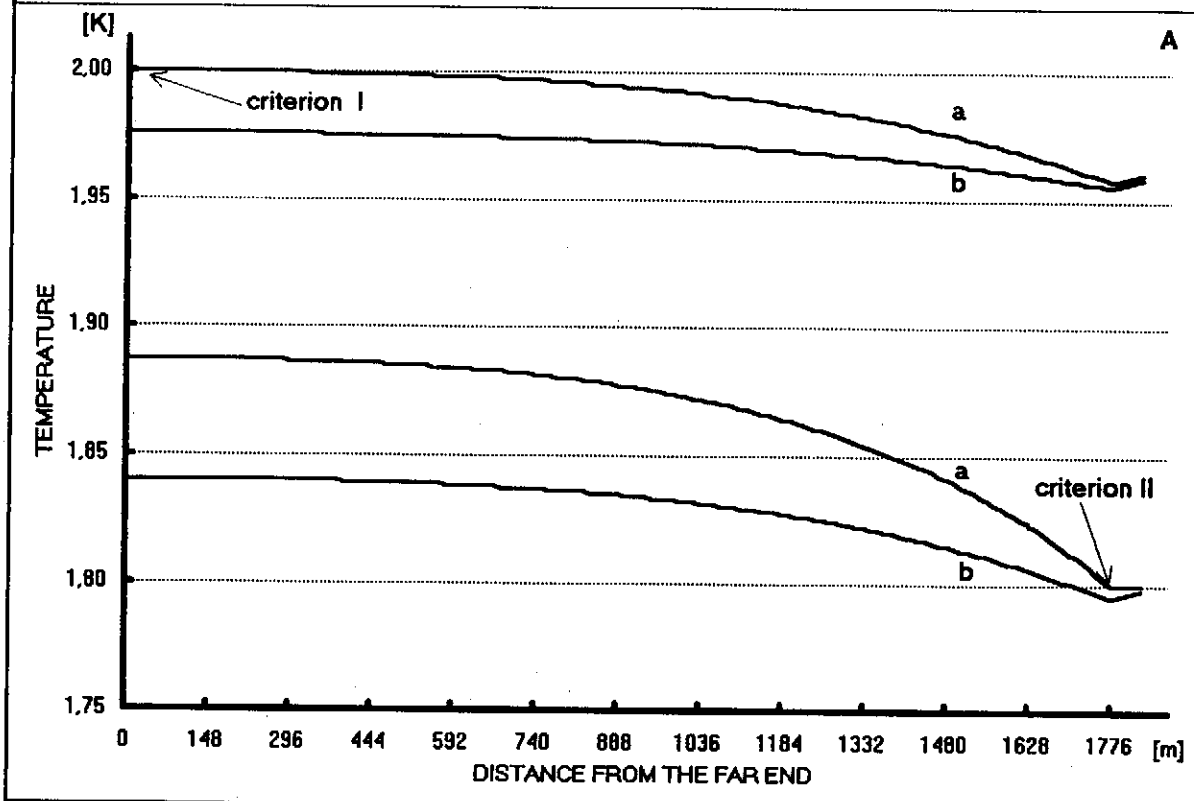

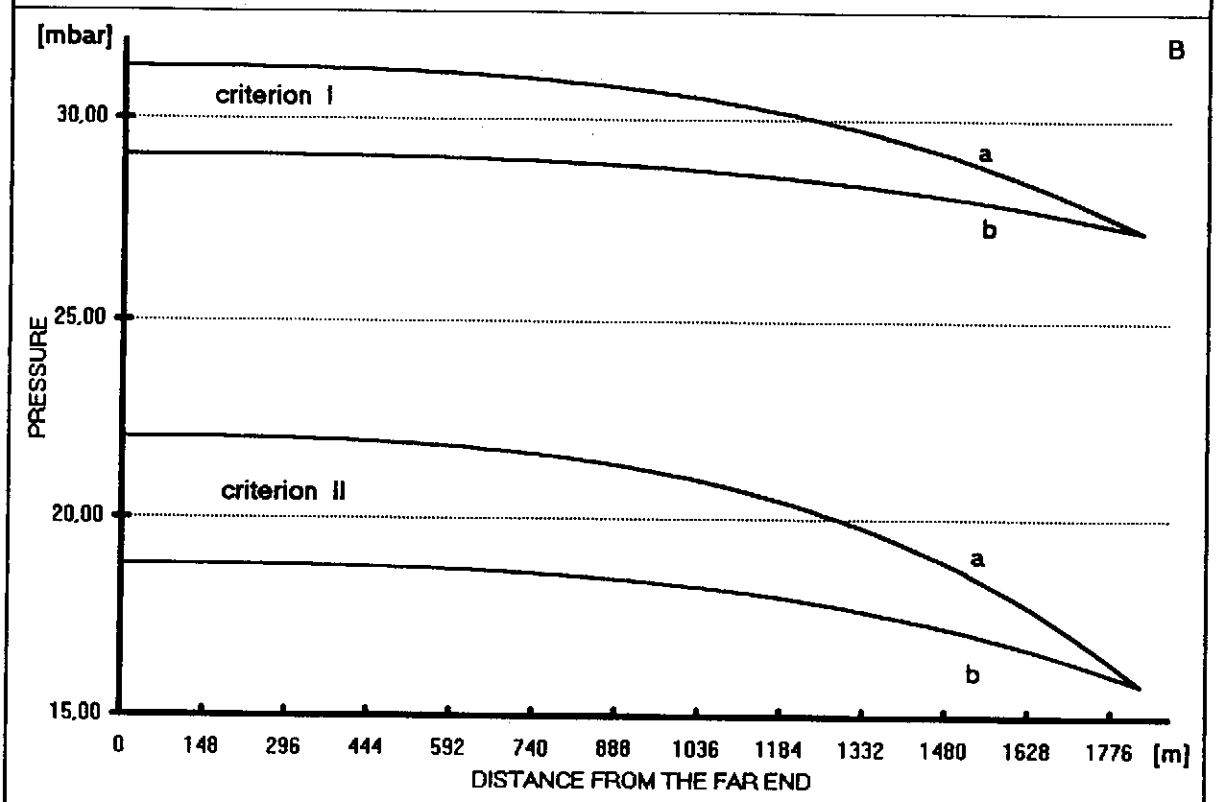

Dia. 17

TEMPERATURES, PRESSURES AND LIQUID LEVELS IN A SUBUNIT WITH ENLARGED RETURN TUBE DIAMETR

DIA17.XLS
G.HORLITZ
30.11.1995

return tube diameter: 0.4127 m

heat loads: 'a' 32.1 (design); 'b' 21.4 (nominal) W/module
return tube outlet pressure 15.0 mbar
maximum subunit temperature 1.8 K at design heat load

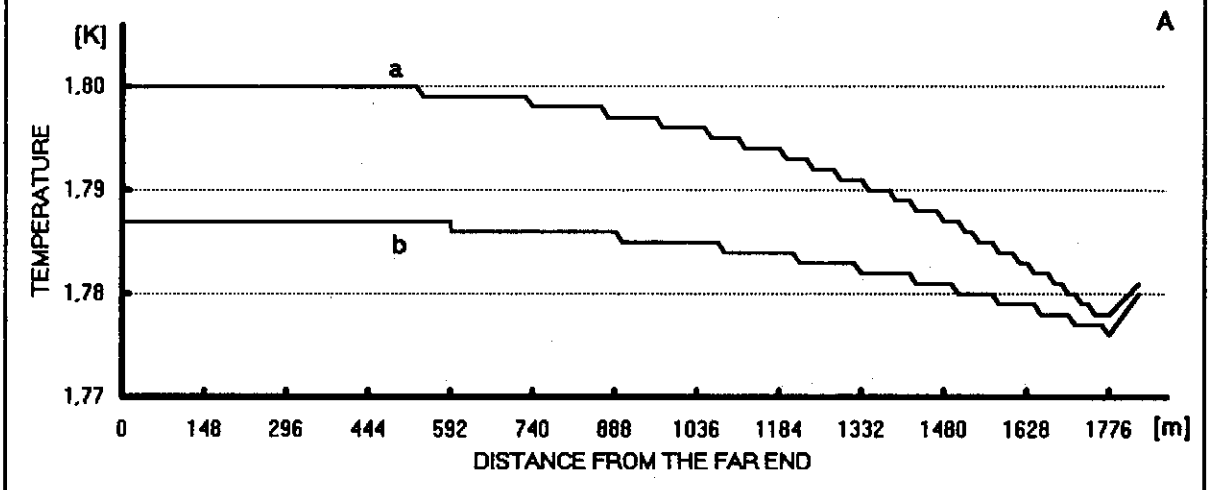

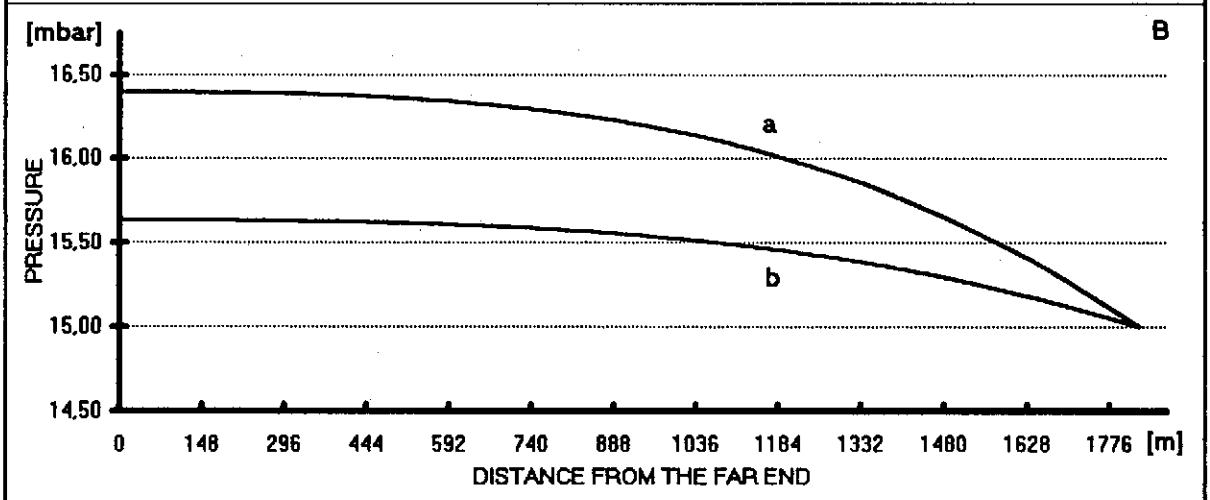

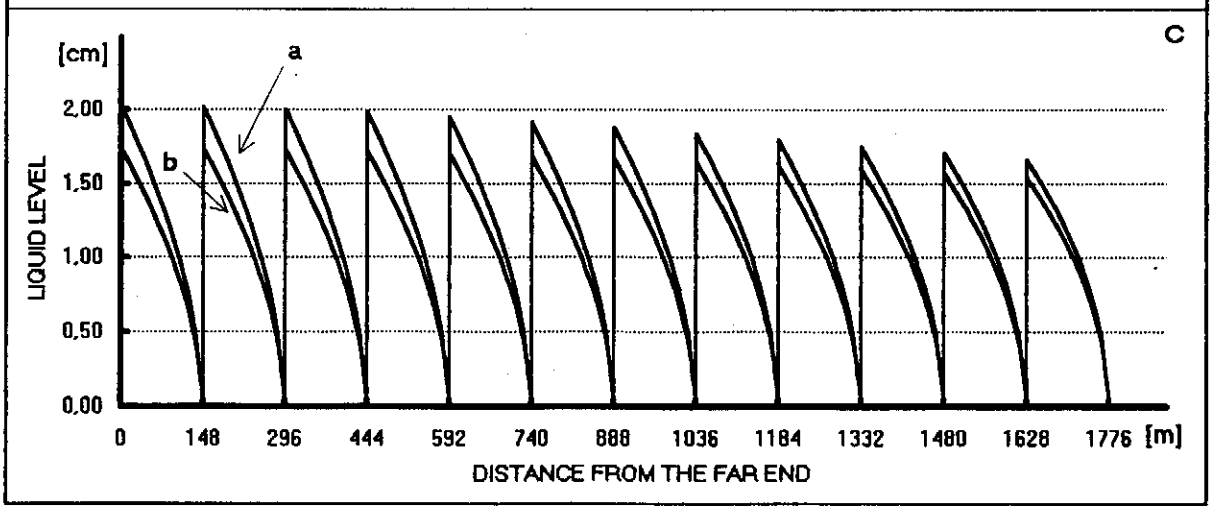

Dia.18

DIA18.XLS
G.HORLITZ
30.11.1995

FLOW DATA IN THE SUPPLY TUBE OF A 1812.4 m TESLA SUBUNIT WITH ONLY 1 JT-VALVE

heat loads: 'a' 32.1 (design); 'b' 21.4 (nominal); 'c' 2.8 (static) W/module

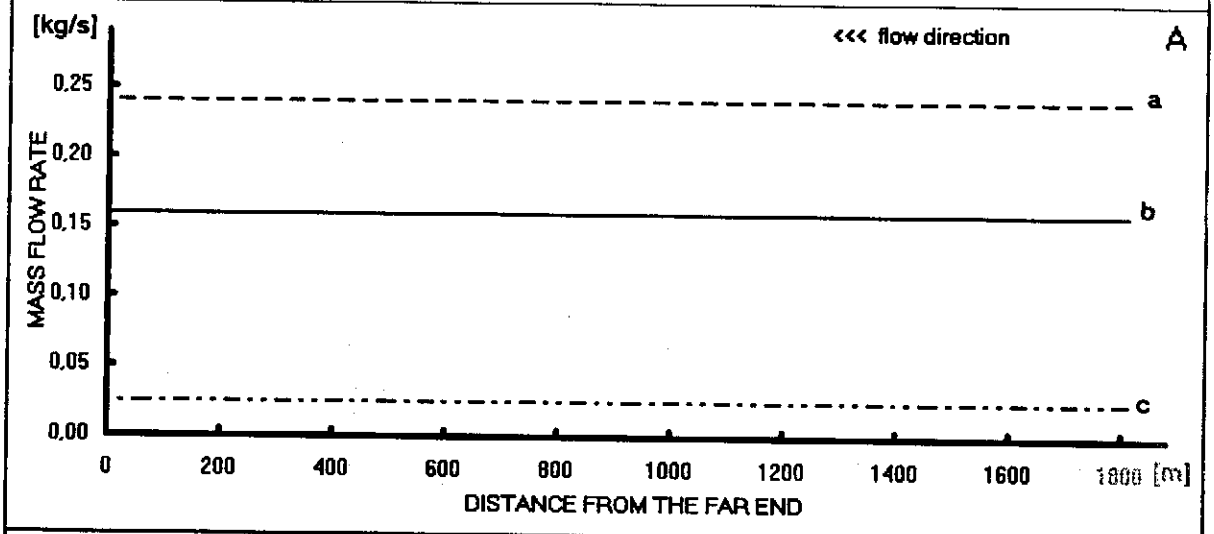

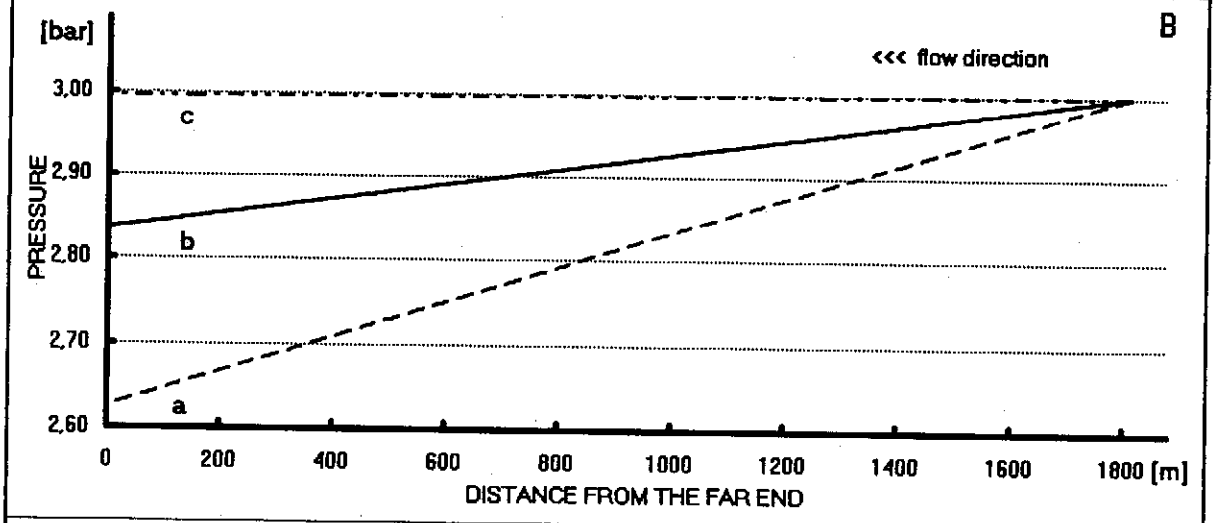

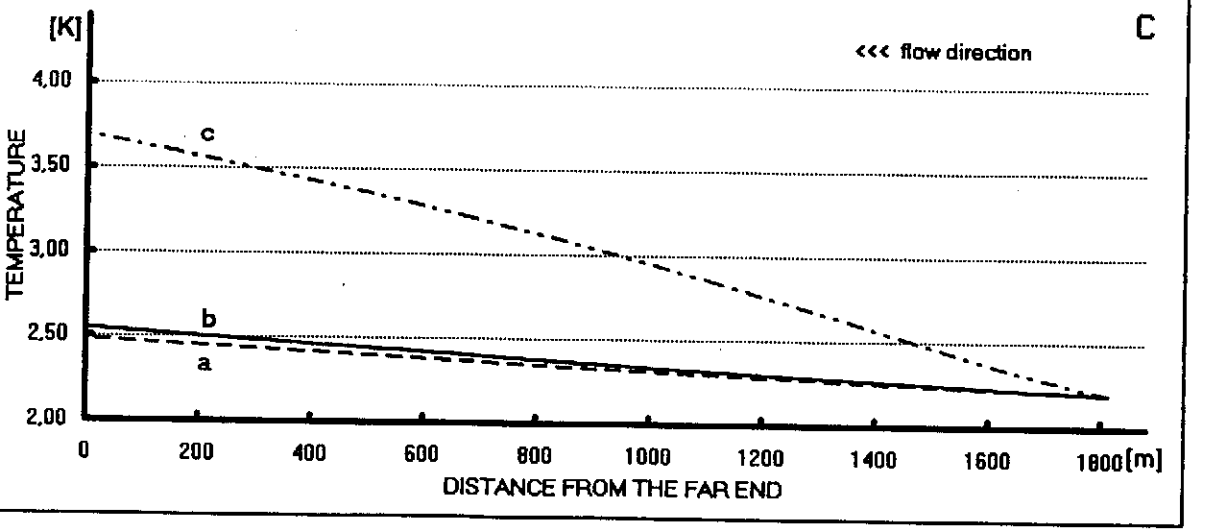

Dia. 19

DIA19.XLS
G.HORLITZ
30.11.1995

PRESSURES AND TEMPERATURES IN THE RETURN TUBE OF A 1812.4 m TESLA SUBUNIT WITH ONLY 1 JT-VALVE

heat loads: 'a' 32.1 (design); 'b' 21.4 (nominal); 'c' 2.8 (static) W/module

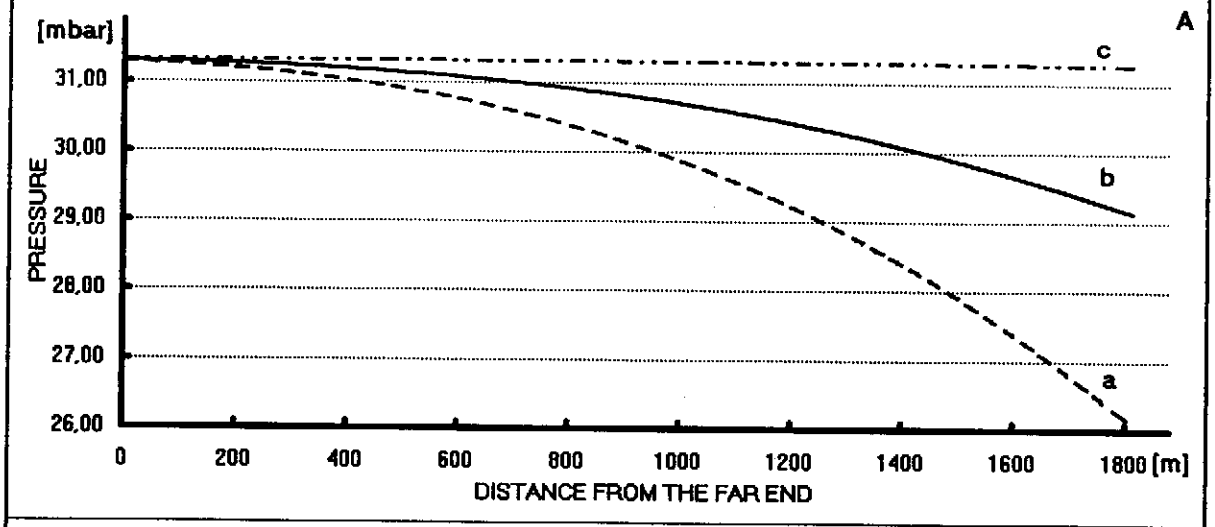

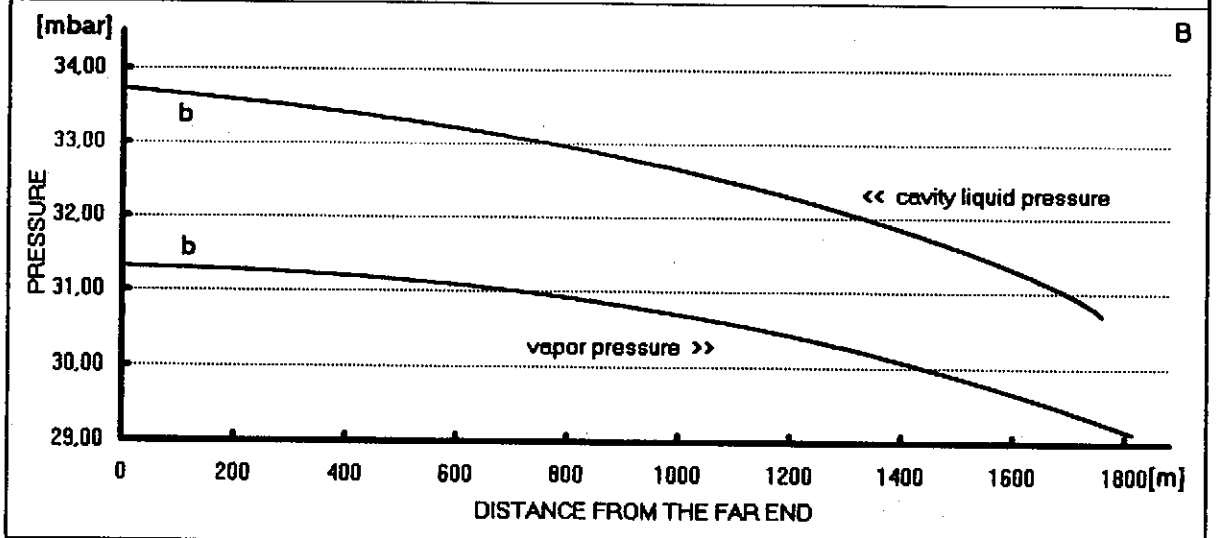

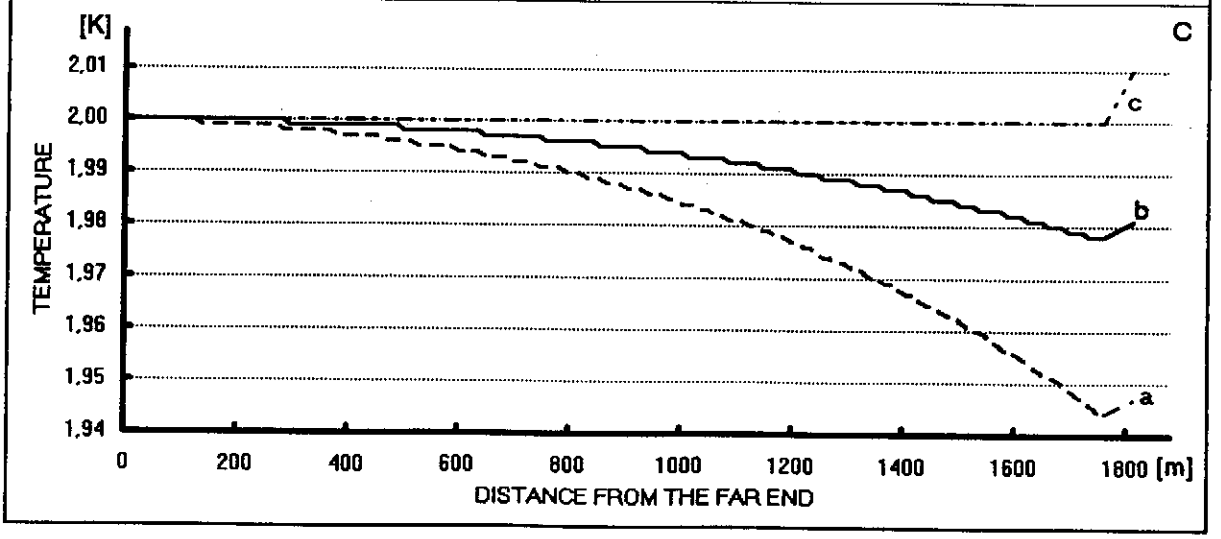

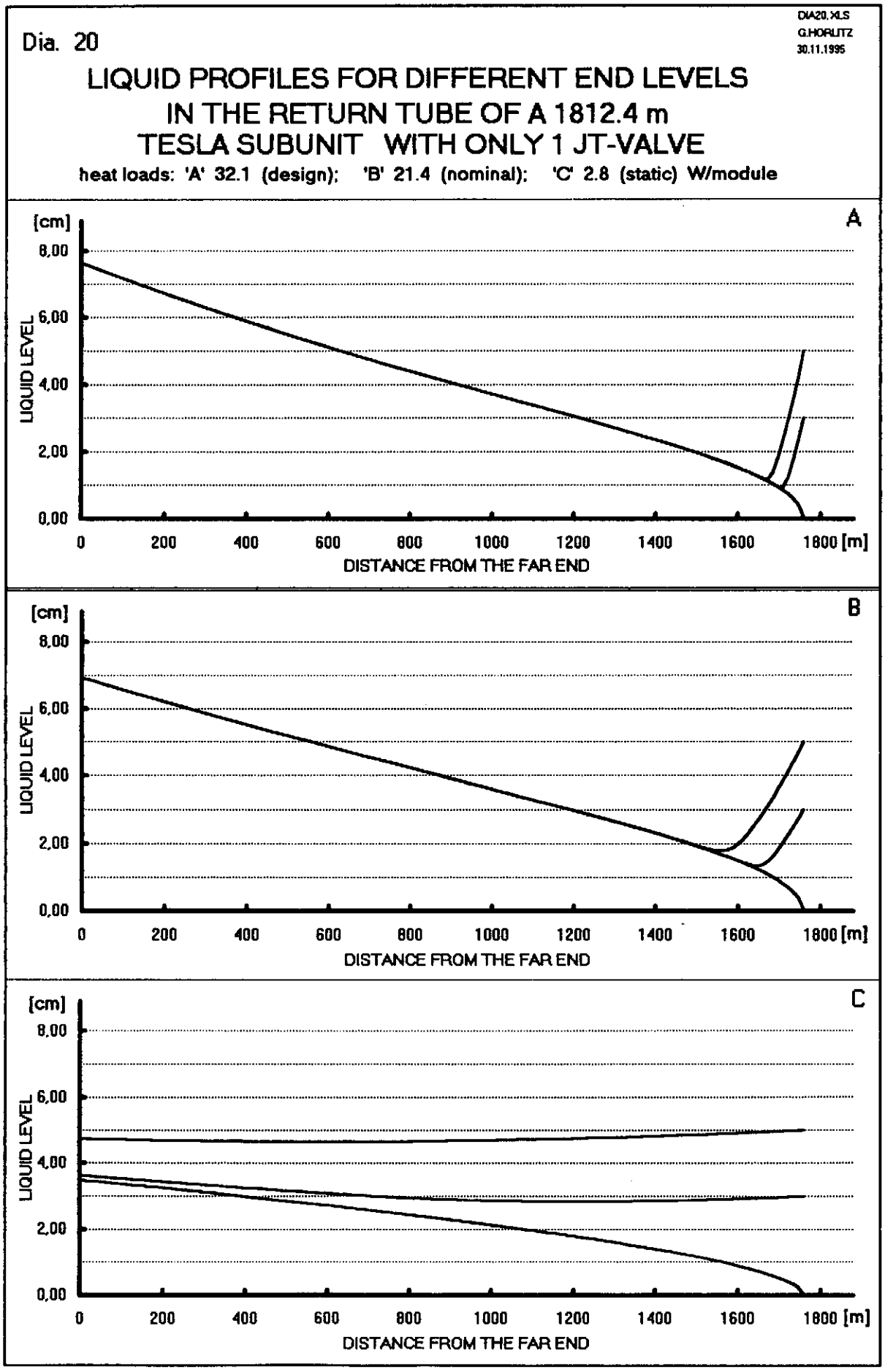
Dia. 20
DIA20.XLS
G.HORLITZ
30.11.1995
LIQUID PROFILES FOR DIFFERENT END LEVELS
IN THE RETURN TUBE OF A 1812.4 m
TESLA SUBUNIT WITH ONLY 1 JT-VALVE
heat loads: 'A' 32.1 (design); 'B' 21.4 (nominal); 'C' 2.8 (static) W/module
A
B
C
[cm]
8.00
6.00
4.00
2.00
0.00
LIQUID LEVEL
0
200
400
600
800
1000
1200
1400
1600
1800 [m]
DISTANCE FROM THE FAR END

Dia. 21

DIA21.XLS
G.HORLITZ
30.11.1995

MASSFLOW RATES AND FLOW SPEEDS IN THE RETURN TUBE OF A 1812.4 m TESLA SUBUNIT WITH ONLY 1 JT-VALVE

heat loads: 'a' 32.1 (design); 'b' 21.4 (nominal); 'c' 2.8 (static) W/module

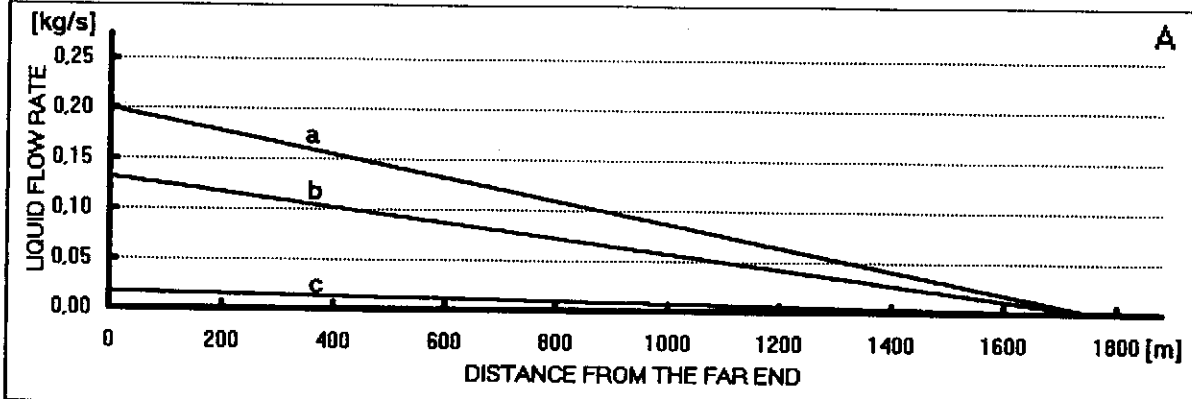

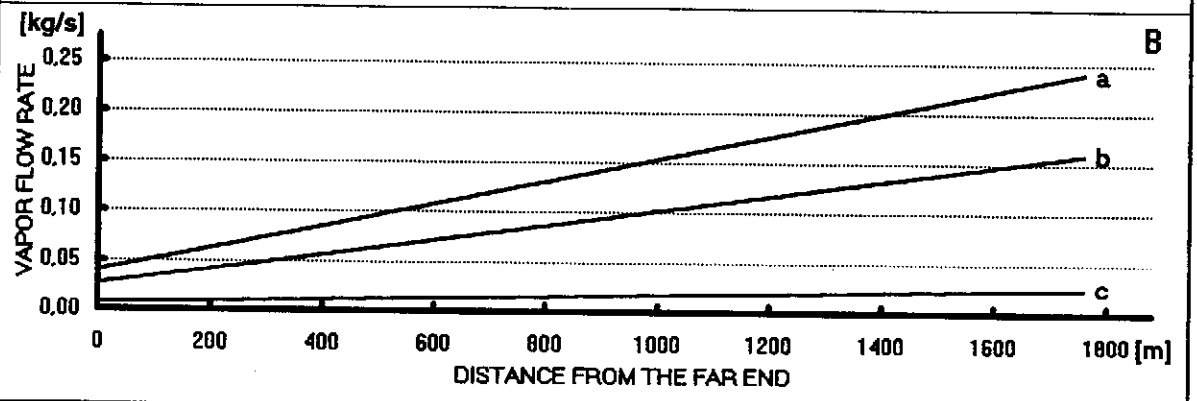

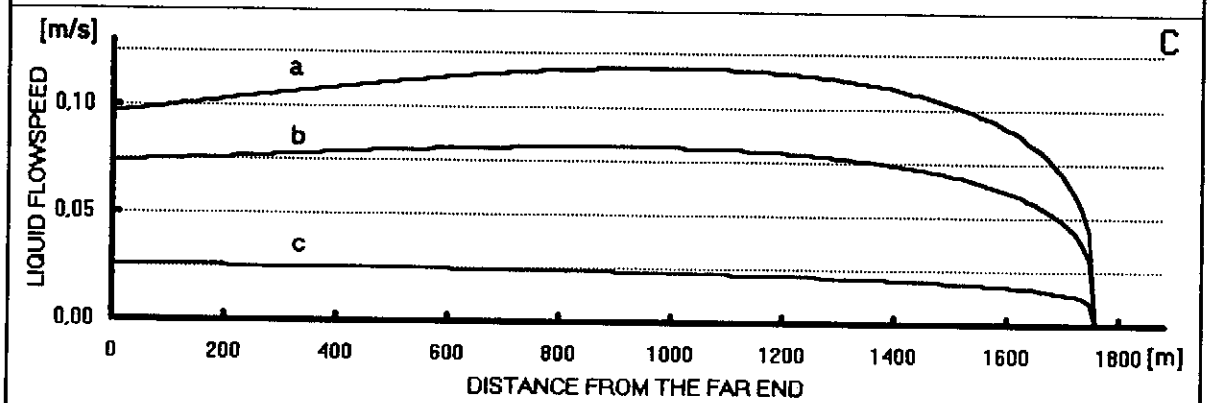

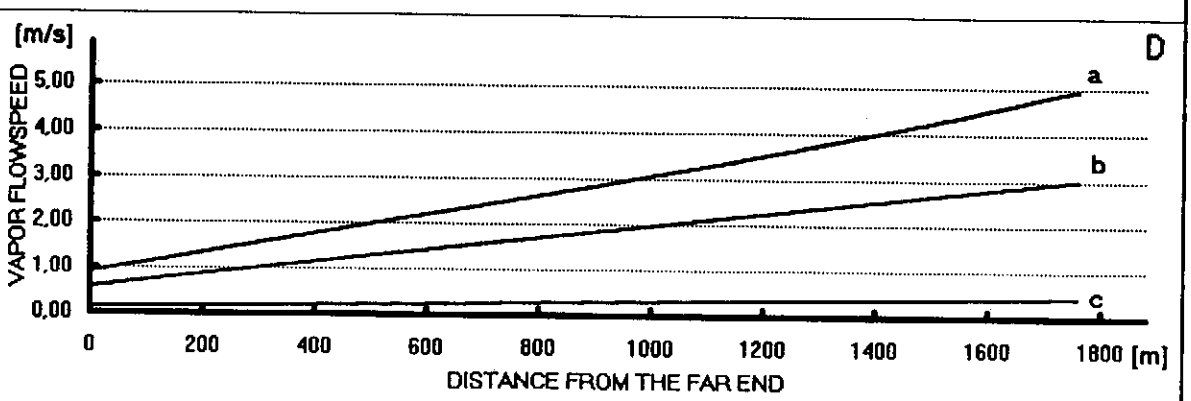

Dia. 22

DIA22.XLS
G.HORLITZ
30.11.1995

LONGITUDINAL HEAT FLOW IN THE LIQUID OF THE RETURN TUBE OF A 1812.4 m TESLA SUBUNIT WITH ONLY 1 JT-VALVE

heat loads: 'a' 32.1 (design); 'b' 21.4 (nominal); 'c' 2.8 (static) W/module

end levels: 'A' 0.0 cm 'B' 3.0 (cm 'C' 5.0 cm

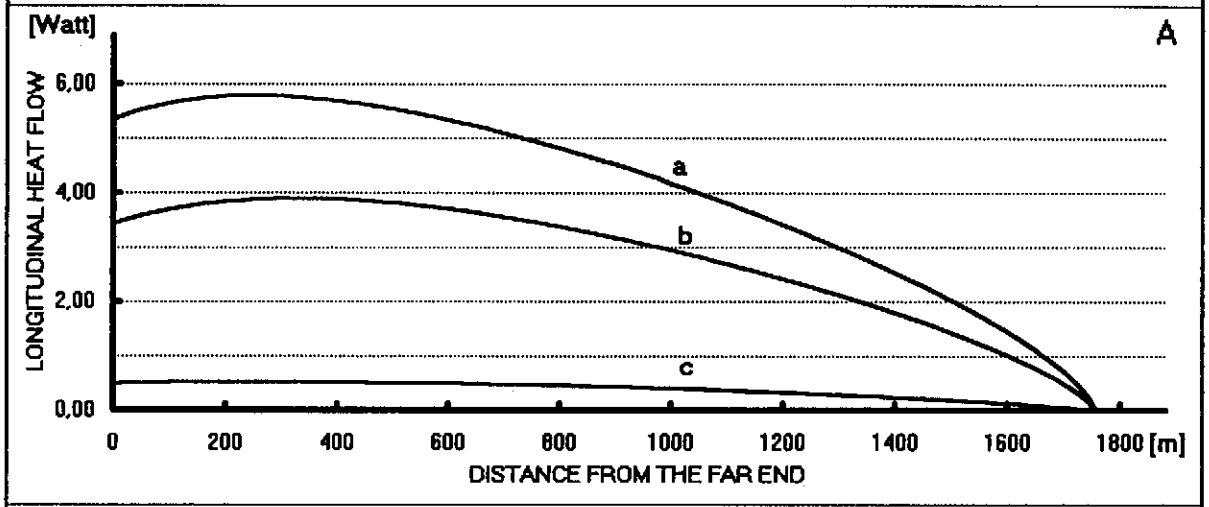

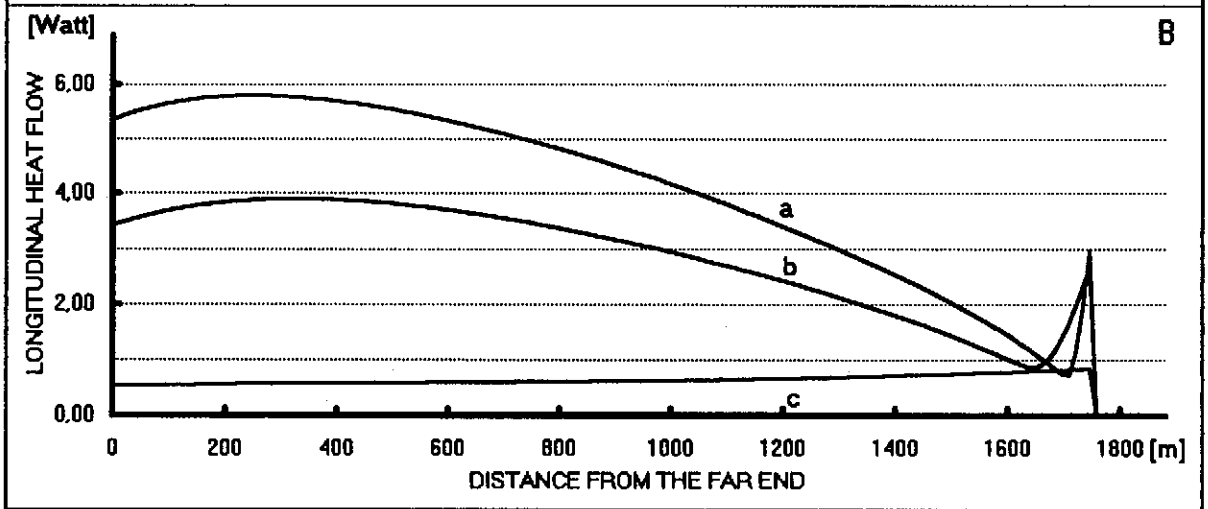

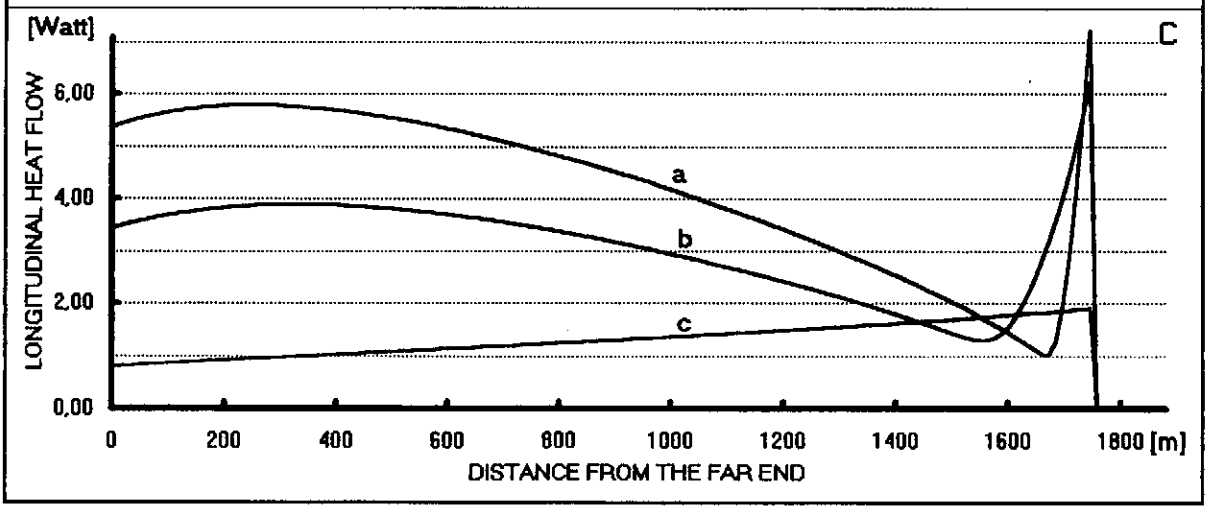

Dia. 23

DIA23.XLS
G.HORLITZ
30.11.1995

INFLUENCE OF HF- POWER FAILURES ON PRESSURE AND LIQUID LEVEL IN THE RETURN TUBE OF A 1812.4 m TESLA SUBUNIT WITH ONLY 1 JT-VALVE

heat loads: 32.1 W/module (design)

'a' all modules normally powered

'b' HF-power off in modules No. 137 t0 140

'c' heat load reduction compensated by endbox heater

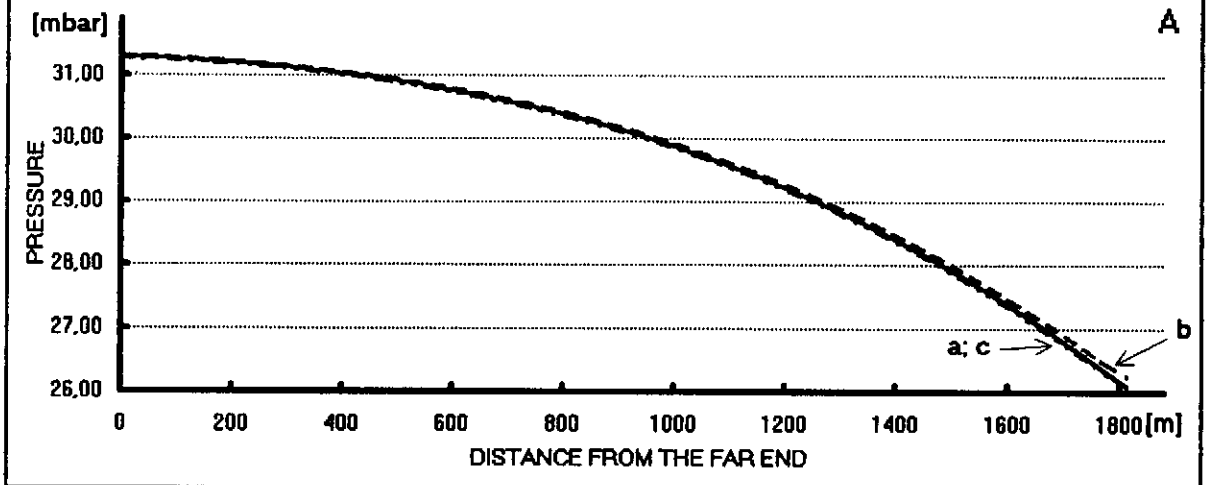

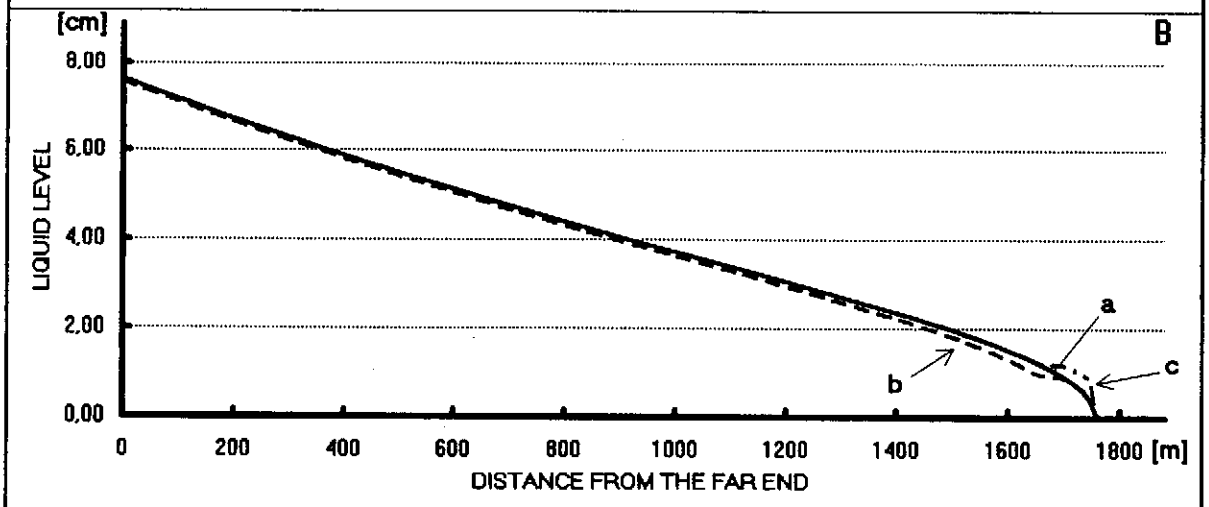

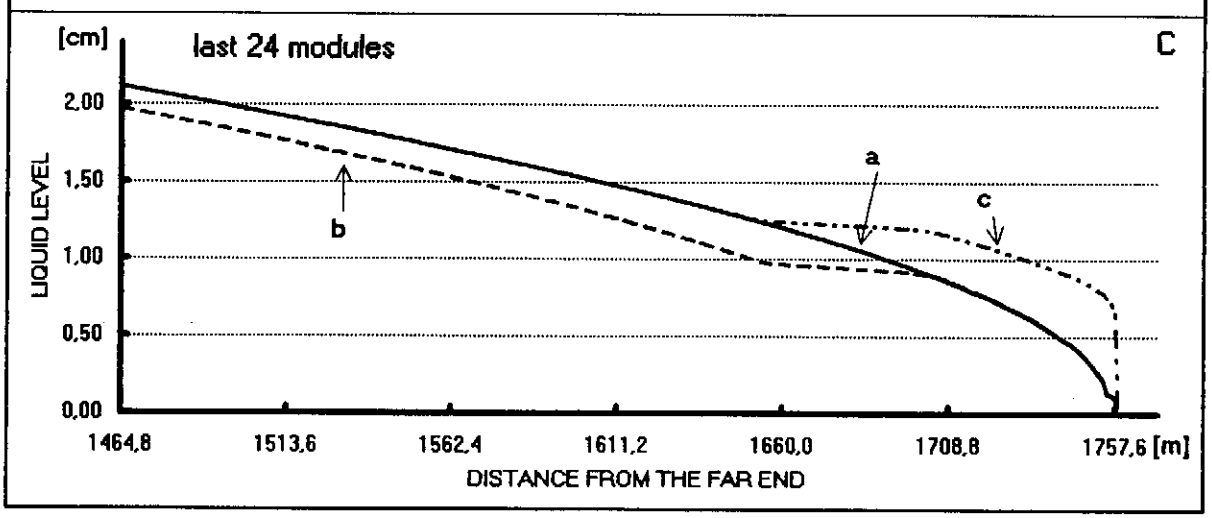

Dia. 24

DIA24XLS
G.HORLITZ
30.11.1995

CHANGE OF LIQUID LEVEL WITH TIME AFTER HF-POWER FAILURE IN A SUBUNIT WITH ONLY 1 JT-VALVE

heat loads: 32.1 W/module (design)

'a' : all modules normally powered

other curves: HF-power off in modules No. 137 to 140 at different times with unchanged flow rate as in 'a'

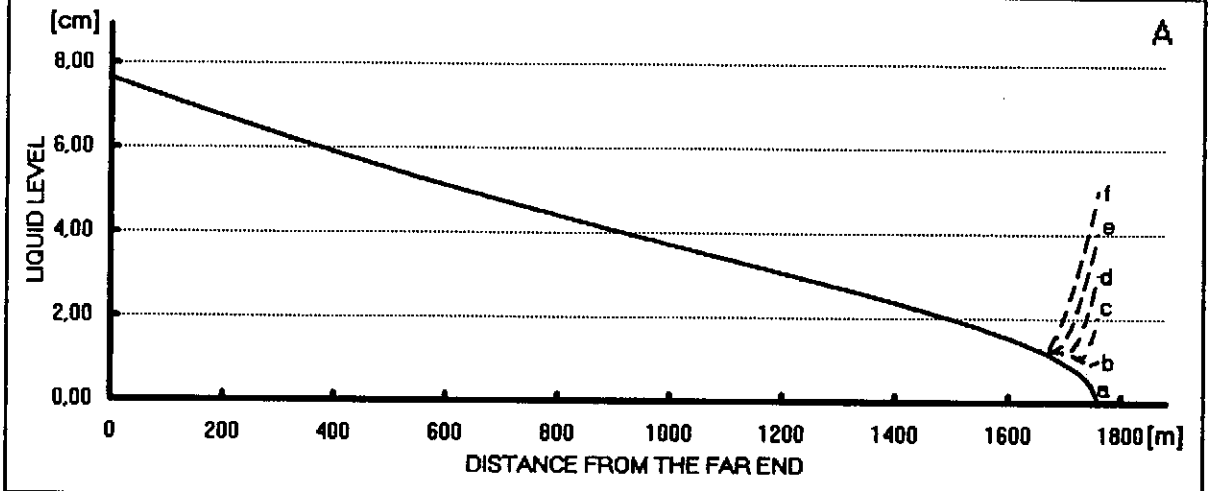

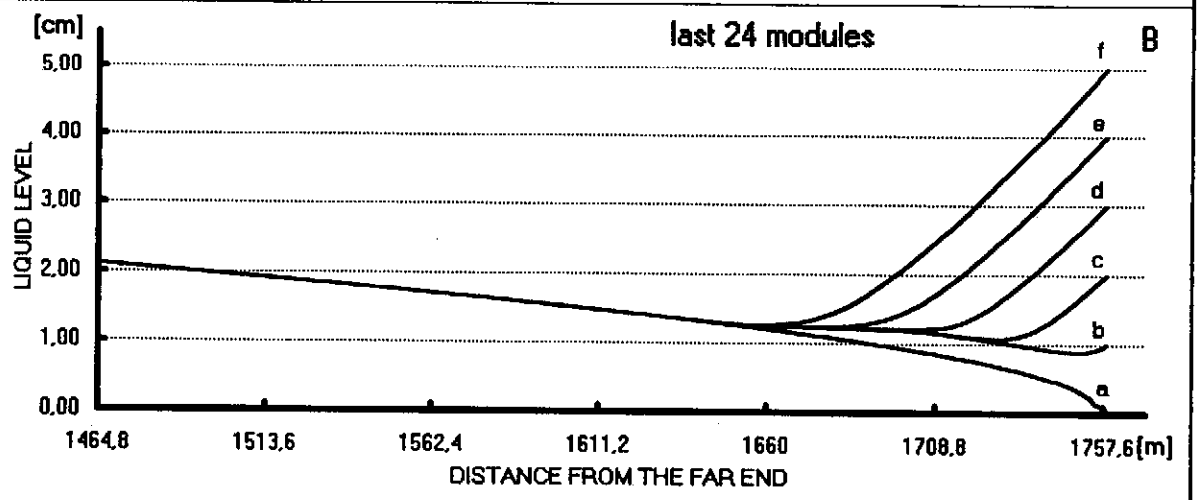

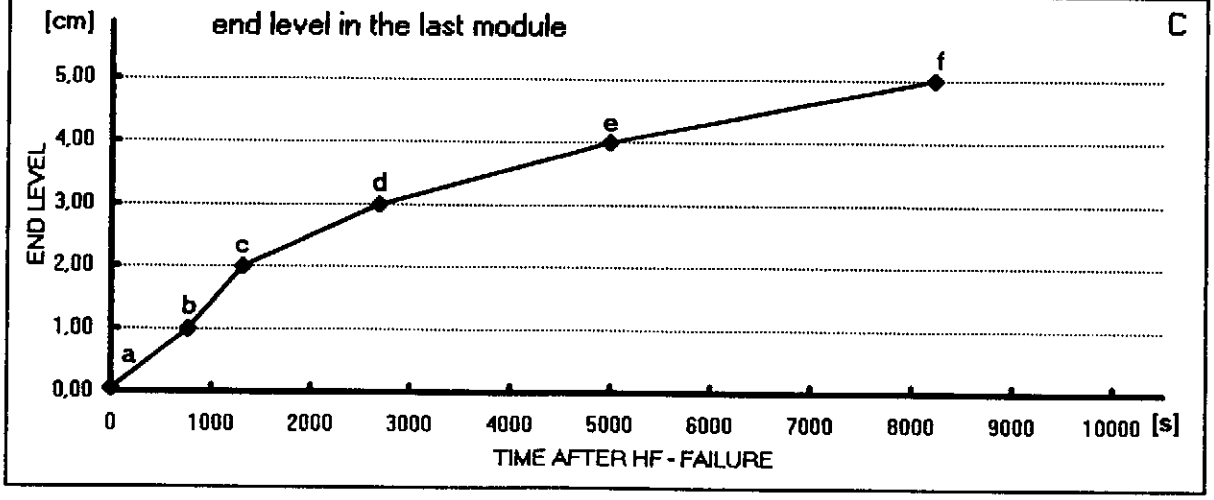

Dia. 25

DIA25.XLS
G.HORLITZ
30.11_09.1995

INFLUENCE OF HF- POWER FAILURES ON PRESSURE AND LIQUID LEVEL IN THE RETURN TUBE OF A 1812.4 m TESLA SUBUNIT WITH ONLY 1 JT-VALVE

heat loads: 32.1 W/module (design)
'a' all modules normally powered
'b' HF-power off in modules No. 65 t0 68
'c' heat load reduction compensated by endbox heater

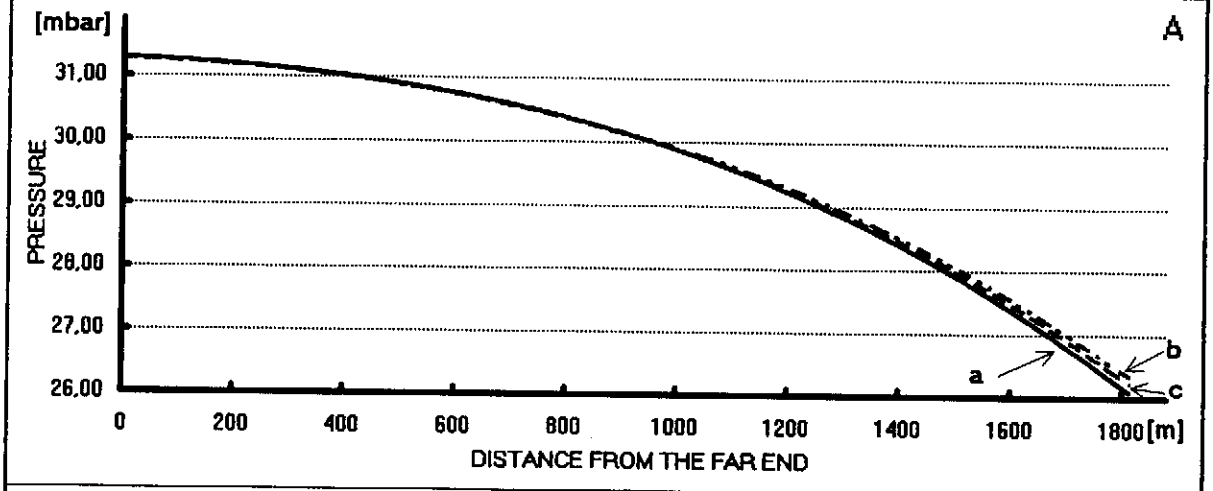

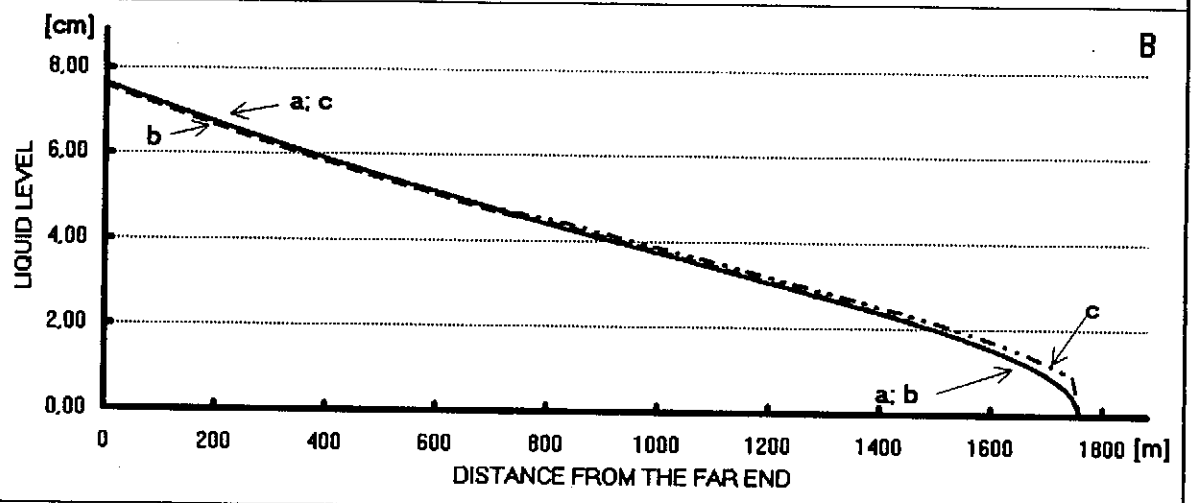

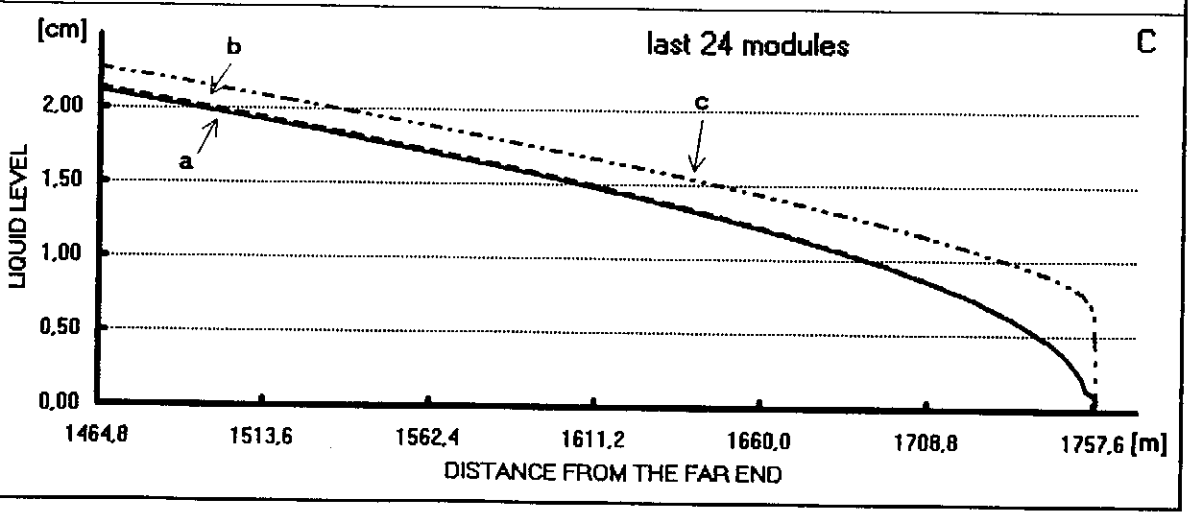

Dia. 26

DIA26.XLS
G.HORLITZ
30.11.1995

CHANGE OF LIQUID LEVEL WITH TIME AFTER HF-POWER FAILURE IN A SUBUNIT WITH ONLY 1 JT-VALVE

heat loads: 32.1 W/module (design)

'a' : all modules normally powered

other curves: HF-power off in modules No. 65 to 68
at different times with unchanged flow rate as in 'a'

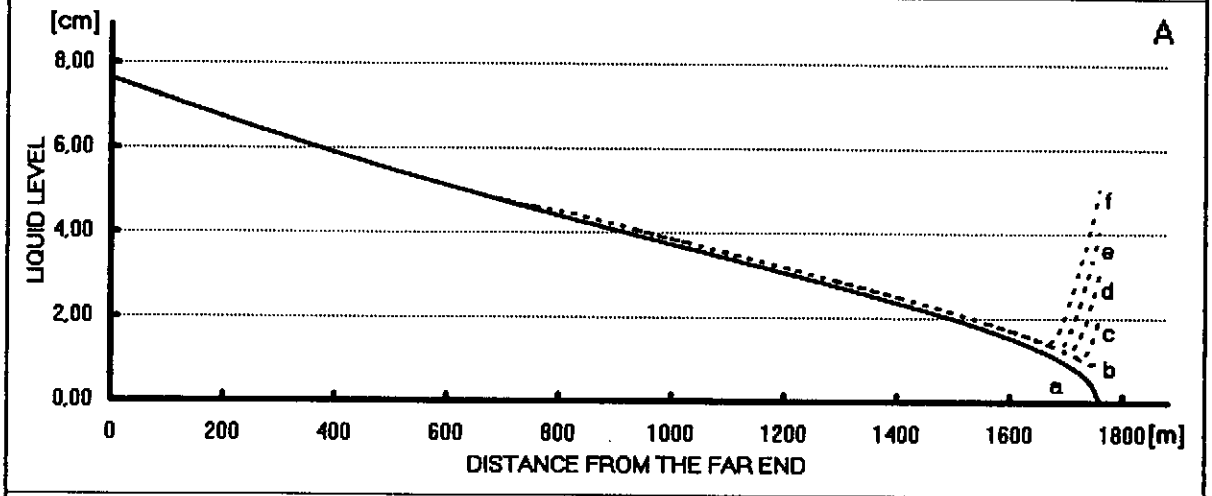

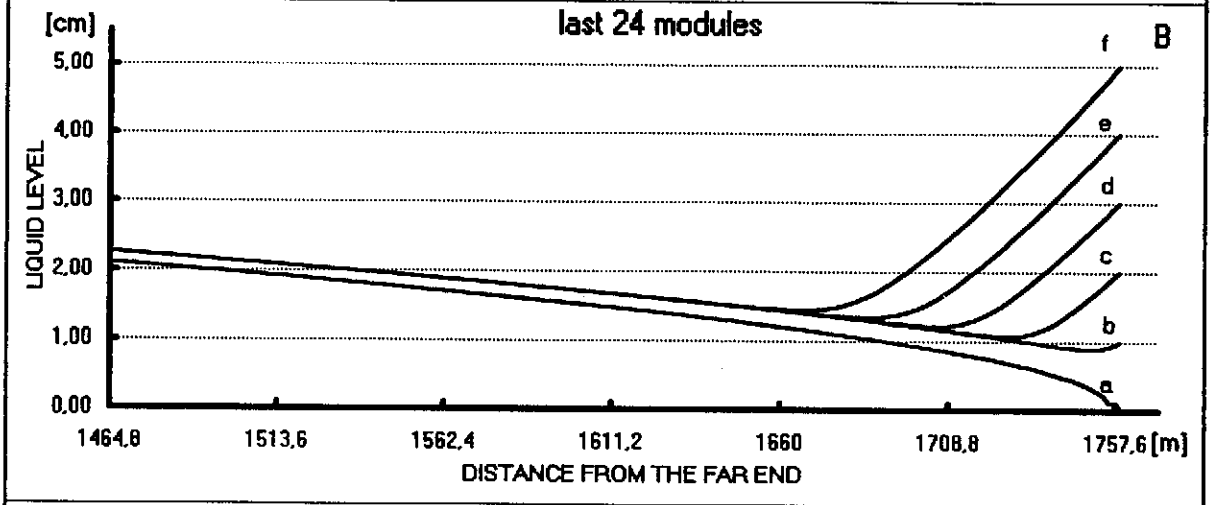

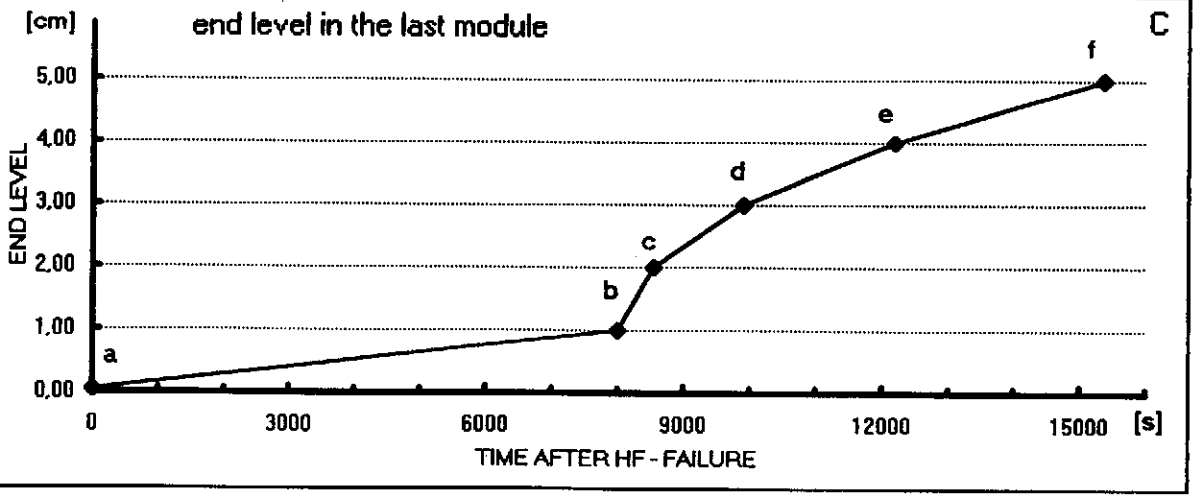

Dia. 27

DIA27.XLS
G.HORLITZ
30.11.1995

LIQUID LEVELS IN THE RETURN TUBE OF A 1830 m TESLA SUBUNIT UNDER DIFFERENT INCLINATION ANGLES 'W'

heat load: 32.1 W/module (design)
inclination angles [mrad] :
'A' : W= 0.0 (horizontal) ; 'B': W= - 1.0 (downwards); 'C' : W= +1.0 (upwards)

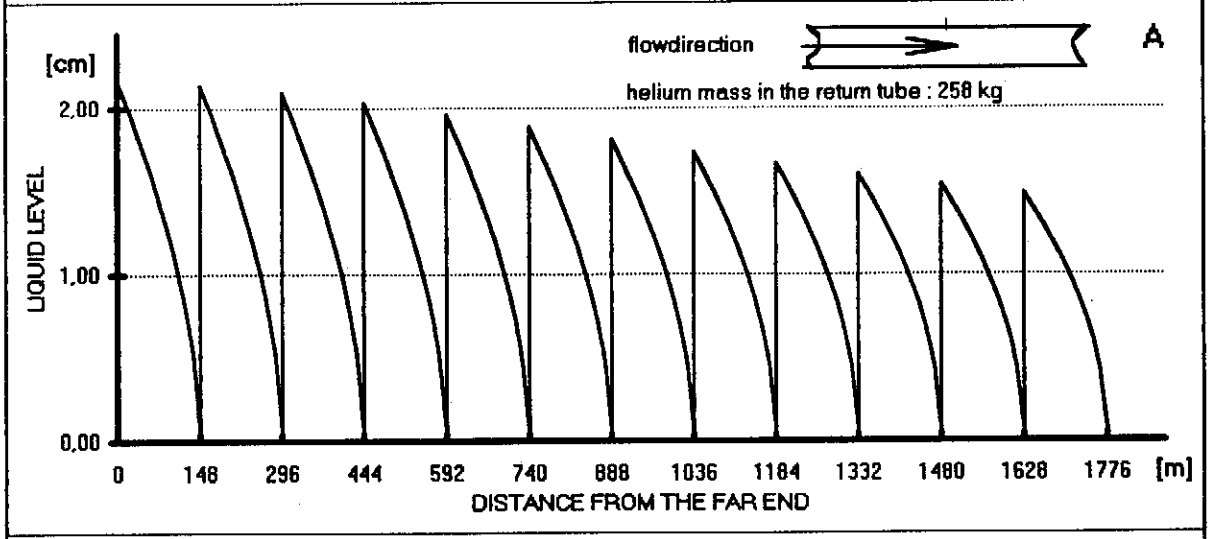

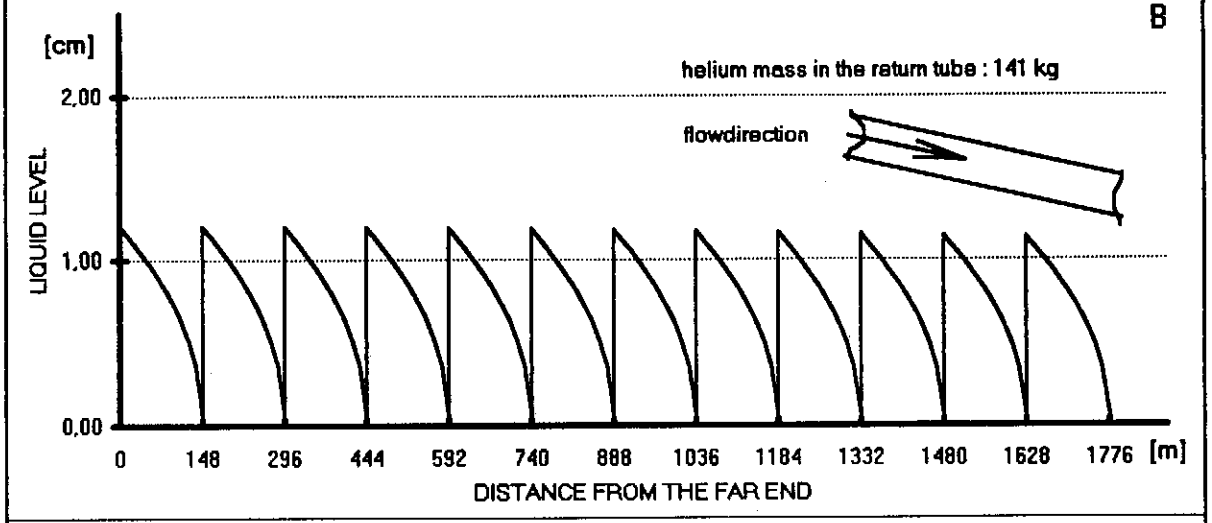

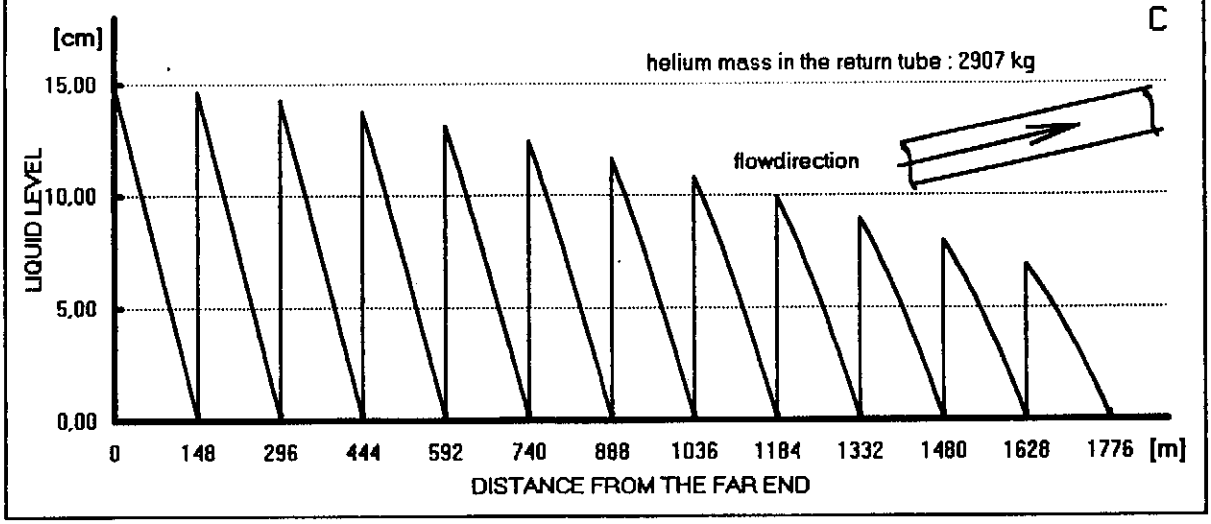

Dia. 28

DIA28.XLS
G.HORUTZ
30.11.1995

PRESSURES AND TEMPERATURES IN THE RETURN TUBE OF A 1830 m TESLA SUBUNIT OPERATED AT HALF OF THE HF-PULSE RATE

heat loads: 'a' 18.1 (design); 'b' 12.2 (nominal); 'c' 2.8 (static) W/module

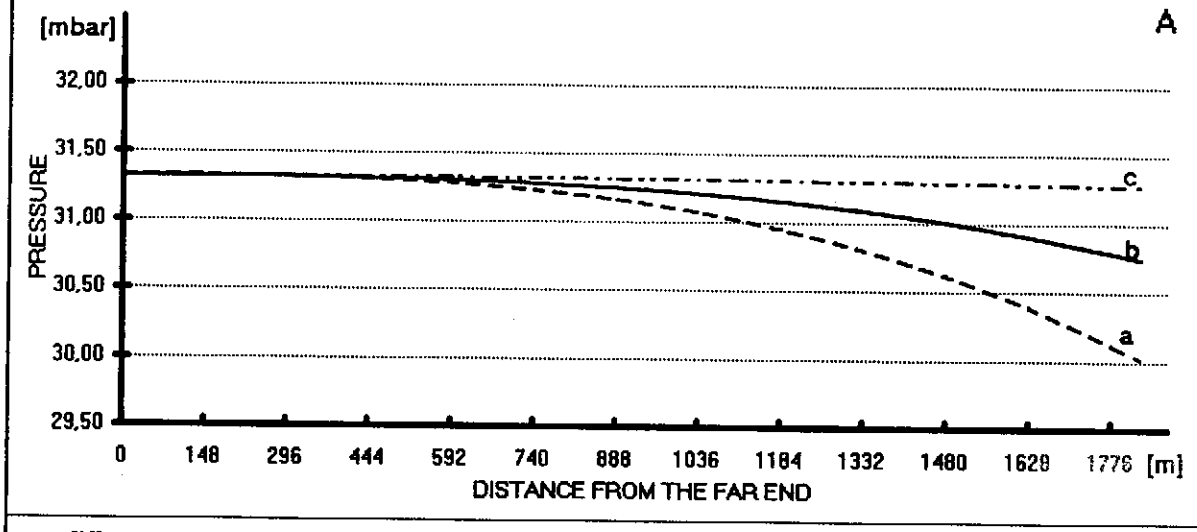

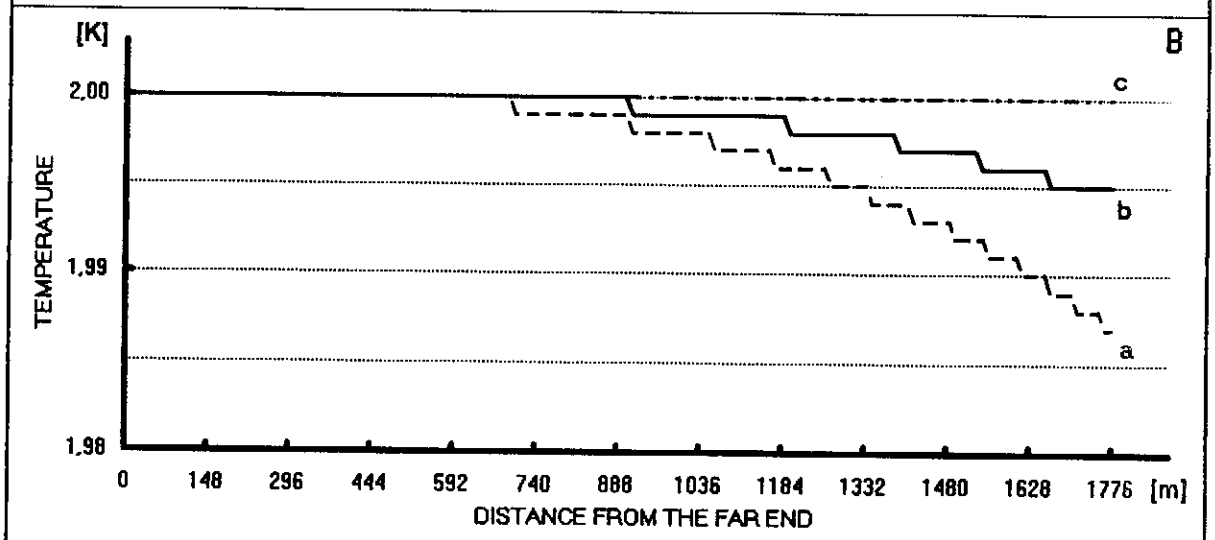

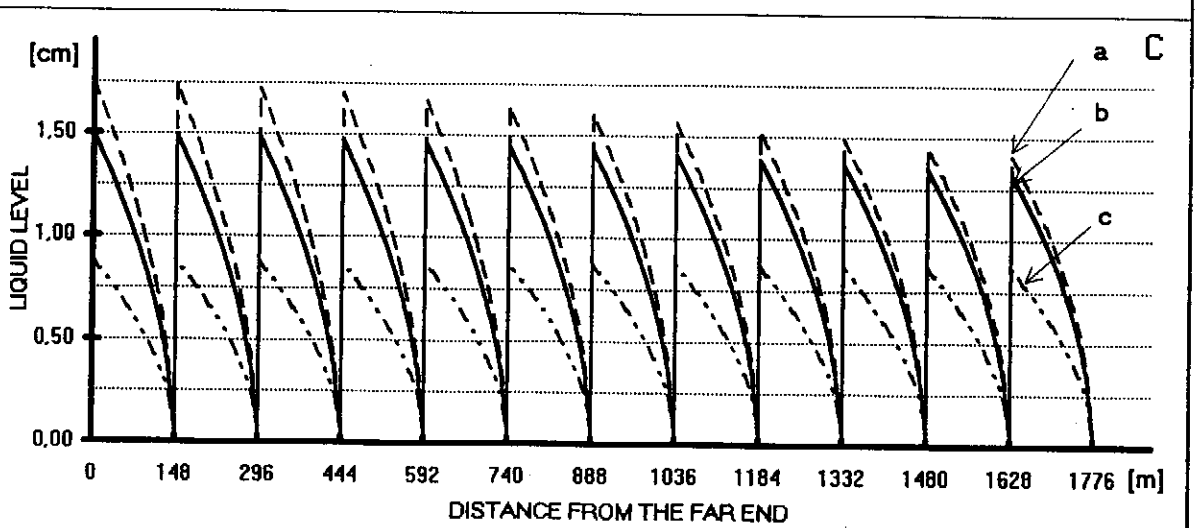

Dia. 29

DIA29.XLS
G.HORLITZ
30.11.95

PRESSURES AND TEMPERATURES IN THE RETURN TUBE OF A 1830 m TESLA SUBUNIT OPERATED AT HALF OF THE HF PULSE RATE FOR DIFFERENT SYSTEM LAYOUT CRITERIA

criterion I : layout for maximum subunit temperature Tmax = 2.0 K
criterion II : layout for minimum subunit temperature Tmin = 1.8 K
criterion III : layout for maximum subunit temperature Tmax = 1.8 K
heat loads: 'a' 18.1 (design); 'b' 12.2 (nominal) W/module